

NUMERICAL STUDY ON THE PIPE CONTAINING MULTIPLE ALIGNED AXIAL
CRACKS

MOHAMAD ZIKRIL HAKIM BIN MD SALEH

Report submitted in partial fulfillment of the requirements for the award of the degree of
Bachelor of Mechanical Engineering

Faculty of Mechanical Engineering
UNIVERSITI MALAYSIA PAHANG

JUNE 2013

UNIVERSITI MALAYSIA PAHANG

BORANG PENGESAHAN STATUS TESIS♦

JUDUL: **NUMERICAL STUDY ON THE PIPE CONTAINING
MULTIPLE ALIGNED AXIAL CRACKS**

SESI PENGAJIAN: 2009/2010

Saya MOHAMAD ZIKRIL HAKIM BIN MD SALEH (900125-06-5769)
(HURUF BESAR)

mengaku membenarkan tesis (Sarjana Muda/~~Sarjana~~ /~~Doktor Falsafah~~)* ini disimpan di Perpustakaan dengan syarat-syarat kegunaan seperti berikut:

1. Tesis adalah hakmilik Universiti Malaysia Pahang (UMP).
2. Perpustakaan dibenarkan membuat salinan untuk tujuan pengajian sahaja.
3. Perpustakaan dibenarkan membuat salinan tesis ini sebagai bahan pertukaran antara institusi pengajian tinggi.
4. **Sila tandakan (√)

SULIT

(Mengandungi maklumat yang berdarjah keselamatan atau kepentingan Malaysia seperti yang termaktub di dalam AKTA RAHSIA RASMI 1972)

TERHAD

(Mengandungi maklumat TERHAD yang telah ditentukan oleh organisasi/badan di mana penyelidikan dijalankan)

TIDAK TERHAD

Disahkan oleh:

(TANDATANGAN PENULIS)

(TANDATANGAN PENYELIA)

Alamat Tetap:

**NO B2 KAMPUNG BENTA LANGGAR
26620 PEKAN
PAHANG DARUL MAKMUR**

NORHAIDA BT AB RAZAK
(Nama Penyelia)

Tarikh: **26 JUNE 2013**

Tarikh: : **26 JUNE 2013**

- CATATAN:
- * Potong yang tidak berkenaan.
 - ** Jika tesis ini SULIT atau TERHAD, sila lampirkan surat daripada pihak berkuasa/organisasi berkenaan dengan menyatakan sekali tempoh tesis ini perlu dikelaskan sebagai atau TERHAD.
 - ♦ Tesis dimaksudkan sebagai tesis bagi Ijazah doktor Falsafah dan Sarjana secara Penyelidikan, atau disertasi bagi pengajian secara kerja kursus dan penyelidikan, atau Laporan Projek Sarjana Muda (PSM).

EXAMINER'S DECLARATION**UNIVERSITI MALAYSIA PAHANG****FACULTY OF MECHANICAL ENGINEERING**

I certify that the project entitled "*Numerical Study on the Pipe Containing Multiple Aligned Axial Cracks*" is written by *Mohamad Zikril Hakim bin Md Saleh*. I have examined the final copy of this report and in my opinion, it is fully adequate in terms of language standard, and report formatting requirement for the award of the degree of Bachelor Engineering. I herewith recommend that it be accepted in partial fulfillment of the requirements for the degree of Bachelor Mechanical Engineering.

(DR. YULI PANCA ASMARA)

Examiner

Signature

SUPERVISOR'S DECLARATION

I hereby declare that I have checked this project report and in my opinion this project report is sufficient in terms of scope and quality for the award of the Bachelor of Mechanical Engineering.

Signature:

Name of Supervisor: MDM. NORHAIDA BT AB. RAZAK

Position: LECTURER

Date: 26th JUNE 2013

STUDENT'S DECLARATION

I declare that this report titled "NUMERICAL STUDY ON THE PIPE CONTAINING MULTIPLE ALIGNED AXIAL CRACKS" is my result of my own research except as stated in the references. This report has not been accepted for any degree and is not concurrently submitted for award of another degree.

Signature:

Name: MOHAMAD ZIKRIL HAKIM BIN MD SALEH

Matrix Number: MA 09090

Date: 26th JUNE 2013

**IN THE NAME OF ALLAH,
THE MOST BENEFICENT, THE MOST MERCIFUL**

A special dedication of this grateful feeling in my beloved parents, Mr. Md. Saleh b. Ghani and Mrs. Rosna Bt. Ibrahim for giving me full of moral and financial support. It is very meaningful to me in order to finish up my degree's study. Not forgetting also to all my loving brothers and sisters. Last but not least to all my colleagues, my friends and those who involved in this project.

Thanks for all the support, wishes and love.

ACKNOWLEDGEMENT

Praise is to God for His help and guidance that finally I able to complete this undergraduate research project at one of my requirements to complete my study.

First and foremost I would like to express my gratitude to all the parties involved in this research. First of all, a special thanks to my supervisor Mdm. Norhaida Bt. AB. Razak for his willingness in overseeing the progress of my research work from its initial phases till the completion of it. I do believe that all his advice and comments are for the benefit of producing the best research work.

Secondly, I would like to extend my sincere appreciation to all staff in the laboratory especially all teaching engineers for their help and valuable advice during the experiment of this research. I do believe that all their advice, commitments and comments are for the benefit.

To all my friends and my entire course mates, thank you for believing in me and helping me to go through the difficult time. The experiences and knowledge I gained throughout the process of completing this undergraduate research project would prove invaluable to better equip me for the challenges which lay ahead. Last but definitely not least to my parent and family members, I can never thank you for love and for supporting me throughout my studies in Universiti Malaysia Pahang (UMP).

ABSTRACT

Failures due to the multiple cracks become a major concern in the pipeline industry and also in maintaining the pipeline integrity. The predictions of pipeline burst pressure in the early stage are very important in order to provide assessment for future inspection. The effects of the multiple aligned axial cracks on burst pressure of material Grade B was studied through an experimental and numerical simulation. The objectives of this research are to investigate the effects of multiple aligned axial cracks towards the burst pressure. This research focuses on two types of analysis which is experimental and simulations by using material Grade B pipe with outer diameter of 60.5mm, 600mm in length and thickness of 4mm. The burst test is done by applying internal pressure of hydraulic oil continuously at the pipe with artificially machined cracks until the pipe burst. MSC Marc Patran 2008r1 is used as a pre-processor and a solver in the analysis of material Grade B. A half of the pipe was modeled by considering the symmetrical conditions using the same parameter with a pipe that used in the burst test. In both analyses of experiment and simulation, the stress and strain are used as criteria for predicting the failure of the pipe. The result shows that as the length of the cracks increase, the burst pressure is decreased. The assessment method in predicting the burst pressure such as ASME B31G, Modified ASME B31G and DNV-RP-F-101 used as the comparison with the result taken from the analysis.

ABSTRAK

Kegagalan disebabkan oleh pelbagai jenis retak menjadi kebimbangan utama di dalam industri perpaipan dan juga dalam mengekalkan integriti perpaipan. Ramalan terhadap tekanan pecah didalam saluran paip pada peringkat awal adalah amat penting dalam usaha untuk menyediakan penilaian untuk pemeriksaan masa depan. Kesan tekanan pecah daripada pelbagai retak sejajar dengan paksi pada bahan Gred B telah dikaji melalui eksperimen dan kaedah unsur terhingga (FE). Objektif kajian ini adalah untuk menyiasat kesan pelbagai retak paksi sejajar terhadap tekanan pecah. Kajian ini memberi tumpuan kepada dua jenis analisis yang merupakan eksperimen dan simulasi dengan menggunakan bahan paip B Gred dengan diameter luar 60.5mm, 600mm panjang dan ketebalan 4mm. Ujian pecah dilakukan dengan mengenakan tekanan dalaman oleh minyak hidraulik dengan berterusan pada paip yang terdapat retak buatan mesin sehingga paip pecah. MSC Marc Patran 2008r1 digunakan sebagai pra-pemproses dan penyelesaian dalam menganalisis bahan Gred B. Separuh daripada paip dimodelkan dengan memandangkan keadaan simetri menggunakan parameter yang sama dengan paip yang digunakan dalam ujian pecah. Dalam kedua-dua analisis eksperimen dan simulasi, tekanan digunakan sebagai kriteria untuk meramalkan kegagalan paip. Hasil kajian menunjukkan bahawa semakin panjang kenaikan retak, tekanan pecah akan semakin berkurangan. Kaedah penilaian dalam meramalkan tekanan pecah seperti ASME B31G, Modified ASME B31G dan DNV-RP-F-101 digunakan sebagai perbandingan dengan keputusan yang diambil daripada analisis.

TABLE OF CONTENTS

	Page
EXAMINER’S DECLARATION	ii
SUPERVISOR’S DECLARATION	iii
STUDENT’ DECLARATION	iv
DEDICATION	v
ACKNOWLEDGEMENT	vi
ABSTRACT	vii
ABSTRAK	viii
TABLE OF CONTENTS	ix
LIST OF TABLES	xii
LIST OF FIGURES	xiii
LIST OF SYMBOLS	xvi
LIST OF ABBREVIATIONS	xvii
CHAPTER 1 INTRODUCTION	
1.1 Background of Research	1
1.2 Problems Statement	2
1.3 Research Objectives	3
1.4 Scopes of Research	3
1.5 Significant of the Research	3
CHAPTER 2 LITERATURE REVIEW	
2.1 Introduction	4
2.2 Usage of Pipe	4
2.3 Type of Pipe	5
2.3.1 Copper Pipe	5
2.3.2 Plastic Pipe	5

2.3.3	Steel Pipe	6
2.4	Defects in Pipe	6
2.4.1	Geometrical Defects	7
2.4.2	Defect resulting on Metal Lost	9
2.4.3	Planar Discontinuities	13
2.4.4	Change in Metal	14
2.5	Stress Based Failure Criterion	15
2.5.1	ASME B31G	16
2.5.2	Modified ASME B31G	18
2.5.3	DNV-RP-F-101	19
2.6	Corrosions Preventions	19
2.6.1	Corrosion Inhibitors	20
2.6.2	Material Selection	21
2.6.3	Cathodic Protection (CP)	21

CHAPTER 3 METHODOLOGY

3.1	Introduction	23
3.2	Flowcharts	23
3.3	Materials Used	26
3.4	Type of Tested Defects	28
3.5	Burst Test	29
3.5.1	Test Procedure	31
3.5.2	Precautions	34
3.6	Finite Element Analysis (FEA)	34
3.6.1	Simulation Procedure	35

CHAPTER 4 RESULT AND DISCUSSION

4.1	Introduction	55
4.2	Experiment Result	55
4.2.1	Burst Pressure	56
4.2.2	Cracks Behaviors	59
4.2.3	Cracks Interactions	60

4.3	Finite Element Analysis (FEA) Result	62
4.3.1	Burst Pressure	62
4.3.2	Comparison of Burst Pressure Based on the Cracks Length of d = 0.5mm	63
4.3.3	Comparison of Burst Pressure Based on the Cracks Length of d = 2.0mm	65
4.3.4	Comparison of Burst Pressure Based on the Distance between the cracks	67
4.3.5	Comparison of Burst Pressure between Assessment Method and Finite Element Analysis (FEA) at d = 0.5mm	70
4.3.6	Comparison of Burst Pressure between Assessment Method and Finite Element Analysis (FEA) at d = 2.0mm	73
4.3.7	Comparison of Burst Pressure of Assessment Method Based on Distance between Cracks	75
4.3.8	Displacement at the Distance between Cracks	79
4.3.9	Stress Distribution at the Between Cracks	83

CHAPTER 5 CONCLUSION AND RECOMMENDATION

5.1	Introduction	92
5.2	Conclusion	92
5.3	Recommendations	93

REFERENCES	94
-------------------	----

APPENDICES	96
-------------------	----

LIST OF TABLES

Table No:	Title	Pages
2.1	Mechanical properties of various grades of pipelines steel	6
3.1	Specification of the models	26
3.2	Chemical properties of the models	26
3.3	Comparison of chemical properties for material Grade B	27
3.4	Mechanical properties of the models	27
3.5	Cracks dimension	29
3.6	Burst test cracks	30
3.7	Specification of the models	37
3.8	Cracks dimension	37
4.1	Burst pressure result from the experiment	56
4.2	Result comparison	57
4.3	Simulation result	63
4.4	Burst pressure for assessment method and finite element analysis for d = 0.5mm	71
4.5	Burst pressure for assessment method and finite element analysis for d = 2.0mm	73

LIST OF FIGURES

Figure No:	Title	Page
2.1	Regular buckle	7
2.2	Ovality	8
2.3	Wrinkle	8
2.4	Knob	9
2.5	General corrosions	10
2.6	Longitudinal corrosions	10
2.7	Circumferential corrosions	11
2.8	Spiral corrosions	12
2.9	Rupture	12
2.10	Fatigue cracks	13
2.11	Stress corrosions cracks	14
2.12	Lapped grinding	14
2.13	Longitudinal extent of the corrosions area	16
2.14	Assumed parabolic corroded area for short corrosions defects	17
2.15	Assumed rectangle corroded area for long corrosion defects	17
2.16	Volatile corrosion coatings	20
3.1	Overall flowchart	24
3.2	Methodology flowchart	25
3.3	True stress strain graph from tensile test	27
3.4	Pipe design modeling	28
3.5	Cracks on pipe	28
3.6	Pipe clamper	31
3.7	Hydraulic pump	32
3.8	Seal at the end of the pipe	32
3.9	Complete installation	33
3.10	Example of the burst of the pipe	34
3.11	Configuration before starting the MSC Patran	36

3.12	Simulation sequences	36
3.13	Geometry setup a) Point setup b) Line setup c) Curve line setup	38
3.14	Full sketch of pipe	39
3.15	Surface setup	39
3.16	Solid setup a) Solid creating b) Extrude method c) Translation vector	40
3.17	Surface transform setup	41
3.18	Full solid generated model	41
3.19	Mesh seed for uniform and one way bias setup	42
3.20	Fully mesh seeded model	43
3.21	Meshing process a) Element shape b) Material properties	44
3.22	Equivalent	44
3.23	Meshed model	45
3.24	Focused mesh at the crack and distance between the cracks	45
3.25	Boundary condition setup a) Displacement setting b) Condition c) Surface selected	46
3.26	Fixed area setup	47
3.27	Fixed area selected	47
3.28	Pressure setting a) Pressure and name set b) Pressure value	48
3.29	CSV data	49
3.30	Field setting	49
3.31	Material selection for elastic region	50
3.32	Material properties setup	51
3.33	Analysis setup a) Follower forces b) Non-positive definite c) Relative residual force	52
3.34	Command prompt setup	53
3.35	Result data taken	54
3.36	Quick plot	54
4.1	Cracks configuration	57
4.2	Graph of burst pressure against cracks length	58
4.3	Crack part of the pipe after the burst test	59
4.4	Bulging or knob defect	60

4.5	Crack interaction	61
4.6	Comparison graph of burst pressure versus cracks length, $2c_2$ for all value of $2c_1$ at $d = 0.5\text{mm}$	65
4.7	Comparison graph of burst pressure versus cracks length, $2c_2$ for all value of $2c_1$ at $d = 2.0\text{mm}$	66
4.8	Graph of burst pressure according to the distance between the cracks at $2c_1 = 25\text{mm}$	67
4.9	Graph of burst pressure according to the distance between the cracks at $2c_1 = 50\text{mm}$	68
4.10	Graph of burst pressure according to the distance between the cracks at $2c_1 = 75\text{mm}$	69
4.11	Graph of burst pressure according to the distance between the cracks at $2c_1 = 100\text{mm}$	70
4.12	Graph of comparison for assessment method and FEA for burst pressure	72
4.13	Graph of comparison for assessment method and FEA for burst pressure	75
4.14	Graph of burst pressure for ASME B31G according to the distance between the cracks	76
4.15	Graph of burst pressure for Modified ASME B31G according to the distance between the cracks	77
4.16	Graph of burst pressure for DNV-RP-F-101 according to the distance between the cracks	78
4.17	Graph of burst pressure for FEA according to the distance between the cracks	78
4.18	Comparison of the displacement by the different combination of length	80
4.19	Bar chart for the percentage of the displacement and remaining distance	82
4.20	(a-d) Vin Misses Stress contour for $2c_1 = 25\text{mm}$ and $2c_2 = 50\text{mm}$	85
4.21	(a-d) Vin Misses Stress contour for $2c_1 = 25\text{mm}$ and $2c_2 = 75\text{mm}$	88
4.22	(a-d) Vin Misses Stress contour for $2c_1 = 25\text{mm}$ and $2c_2 = 100\text{mm}$	90

LIST OF SYMBOLS

$2c_1$	Crack length
$2c_2$	Crack length
d	Distance between the cracks
OD	Outer diameter
t	Crack thickness

LIST OF ABBREVIATIONS

3D	Three Dimensions
ASTM	American Society for Testing and Material
ASME	American Society for Mechanical Engineer
API	American Petroleum Institute
DNV	Det Norske Veritas
RP	Recommended Practice
FEA	Finite Element Analysis
FEM	Finite Element Method

CHAPTER 1

INTRODUCTION

1.1 BACKGROUND OF RESEARCH

Oil and gas are also called hydrocarbon or petroleum. They come from the underground and provide fuel for machines and vehicles, heating and energy for industries. Hydrocarbons are taken from the ground are a mixture of gases, liquids, semi-solids like waxes and also solids like asphalt, tar and pitch. The oil often been used to provide petrol, diesel, activation fuel and fuel oil. The gas was used to generate electricity, widely used in the industry, and some were converted into synthetic petrol. Oil and gas rise to the earth's surface through the gaps in the rock. But where they cannot seep through or around the rock, they become trapped. Hence, the oil and gas located only several kilometers below the surface, so it just needs to be drilled to retrieve the petroleum [1].

The main problems lie after this process where the transportation of the petroleum. Mostly the drilling process happens at the offshore which is quite far from the land. So in order to make a transfer, the pipe is used as a transfer medium instead of a ship. Basically the pipe had their limit and durability.

So for a long usage, the pipe will get some crack from the corrosion and other effects. Hence, the pipe will not safe enough to transport the petroleum. The pipe might have a leak or may be burst up [2].

In order to overcome the problems, an investigation was made where some research will be conducted as a guideline. The main focus of the research is about the relationship between the length of cracks and the burst pressure. For the pipe properties, it only uses one type of pipe which is pipe with material Grade B as a model to complete the experiment and also as a reference. There are 20 types of cracks that be examined in this research. Then the result that founds from the experiment will be compared with the result from the research.

1.2 PROBLEM STATEMENT

Piping system might have a crack after being used for a long time. It will bring trouble to the industry that used the cracked pipe and also might become dangerous if the pipe fail. This will result in a leaky and also bust up on the pipe. If this happens, not only the industry will suffer from the failure, but also the safety of the workers. The environment around it will be affected too. So it is really important to avoid this happening. One of the options is by using the piping inspection. By using the piping inspection, the inspector will inspect the pipe and search for any cracks and defects or failure. Then the life estimation of the pipe can be defined. So, the pipe can be changed when the life estimation almost expired. This can avoid any failure happen to the pipe during it being used.

There are lots of defects during the service's inspection such as corrosion, single defects, parallel defects and so on. But some of them come in the form of multiple cracks where there are no reliable criteria to predict the failure. The validation of this model also has not been done yet. So it is crucial to validate them and also determine this type of defect [3-4]. Thus, the pipe that contain with several types of multiple aligned axial crack will be tested.

1.3 RESEARCH OBJECTIVES

The aim of this research is about the numerical study on the pipe containing multiple aligned axial cracks. Hence, the objectives of this research are:

1. To analyze the interaction between different cracks length.
2. To predict the failure pressure of different cracks length.
3. To investigate the effect of the distance between the cracks toward the failure pressure.
4. To determine the relationship between the length and the distance between the cracks towards the failure pressure of the pipe.

1.4 SCOPES OF THE RESEARCH

The scopes of the research are as follows:

1. Material used is piped with material Grade B
2. Focusing on different combination of crack length
3. Use MSC Marc Patran 2008r1 for the finite element analysis

1.5 SIGNIFICANT OF THE RESEARCH

The multiple cracks happen in the pipe are really serious agenda. By doing this research, it is hoped that the failure pressure for multiple crack especially the aligned axial crack can be determined. Thus, there is more pipe leakage and also blown up pipe can be reduced since the pipe is already known when it needs to be replaced. The people and also environment as well, will be safer from the danger and also pollutant.

CHAPTER 2

LITERATURE REVIEW

2.1 INTRODUCTION

Nowadays, a pipe is a common medium that widely been used all around the world in order to transfer fluid [1]. By using these kind of medium, fluid can be easily transferred and also can save a lot of money and time. There are many industries that using a pipe to transfer fluid such as oil and gas industries and also chemical based industries. Because of there are so many properties of pipe, each of the industries only used the most suitable pipe according to the material that the industry used. This is to ensure the pipe is good enough and also can withstand the fluid that flow through it. As for the pipe itself, it can be used in a period without any problems [1-2].

2.2 USAGE OF THE PIPE

In general, pipe has been used as a medium to transfer fluid from a place to another. This fluid includes water, oil, chemical, steam, smoke and also gas. By using a pipe, the transferring job becomes easier. In the factory, they use pipe to transfer the waste product into a waste tank and also use a pipe to transfer steam, gas and also heat from the boiler to the machine. The pipe also used in transfer oil from the oil rig at the offshore to the base at the land [4]. Usage of pipe is not limited to only transfer fluid but they also can be used as the cooling system like in a radiator and others.

2.3 TYPES OF THE PIPES

There is a lot of pipe that used by the company in all around the world. Each pipe is used based on their mechanical properties which are the better properties means better performance of the pipe and it can be used for a long time.

2.3.1 Copper pipe

Copper pipe is resisting corrosion, so it is commonly used pipe in water supply lines. It costs more than plastic but it lasts. There are two common types of copper pipe. The first one is rigid copper, which is coming in three thicknesses. Type M is the thinnest but is strong enough for most uses. Types L and Type K are thicker and used in outdoor and drain applications. Pipes are usually connected with soldered (sweat) fittings and compression fittings can connect the pipe to shut-off valves. The other one is flexible copper, which is often used for dishwashers, refrigerator icemakers, and other appliances that need a water supply. It is easy to bend. Sections of flexible copper pipe are joined using either soldered or compression fittings [5-6].

2.3.2 Plastic pipe

Plastic pipe comes as either ABS (acrylonitrile-butadiene-styrene) or PVC (polyvinyl-chloride). Most homes and small industries have plastic pipes and fittings because it's inexpensive and easy to use. ABS, which is this black pipe, was the first plastic pipe to be used in residential plumbing. Today, many areas do not allow ABS in new construction because joints can come loose. Another is PVC, where this white or cream colored pipe is the most commonly used pipe. It's strong, untouchable by chemicals, and seems to last forever. The rating and diameter is stamped right on the pipe. Schedule 40 PVC is strong enough for residential drain lines. CPVC (chlorinated polyvinyl chloride) pipe has the strength of PVC but is heat-resistant, which makes it acceptable in many regions for use on interior supply lines.

Schedule 80 PVC is sometimes used for cold-water supply lines, but it is not allowed in some regions because it is not suitable for hot water [5-6].

2.3.3 Steel pipe

Steel pipe is the most common pipe that has been used in global industries. This is because the material properties of the steel pipe itself. Steel is among the best material in the aspect of durability and long life lasting compared to the other material. This kind of pipe normally used in many industries to transfer fluid such as oil, gas, water, chemical, smoke and others. In steel pipe itself, there are certain levels or grades for differentiating the steel pipe durability. There are various grades of steel, but the common used by industries is X42, X52, X65, X80 and X100 steels [7]. The higher grades mean the high durability of the steel. Table 2.1 shows the mechanical properties of the pipeline steel.

Table 2.1: Mechanical properties of various grades of pipelines steel [7-9]

Mechanical properties (steel)	X42	X52	X65	X80	X100
Young's modulus (MPa)	20700	20700	20700	20700	20700
Poisson's ratio	0.3	0.3	0.3	0.3	0.3
Yield Strength (MPa)	285	358	456	646	802
Tensile Strength (MPa)	464	551	570	760	891

2.4 DEFECTS IN PIPE

The pipes itself have their own life expectancy. When being installed in a long period at a certain place, the pipe will undergo a process called defects. This defect will make the pipe become unusable and need to be changed to a new one. There are many defects that can be occurring in the piping system. Since this study involves the pipe that being used in the offshore, so the defects are focused on the steel pipe only. The defects can be categorized as follows.

2.4.1 Geometrical Defects

Geometrical defects involve a smaller change in wall thickness than the allowable wall thickness tolerance and result in stress accumulation and concentration [10]. There are many types of geometrical defect such as regular buckle, ovality, wrinkle, and knob. The details of these defects will be explained in the next subsection.

Regular buckle

This is a residual deformation of the pipe wall inside the pipe without sharp edges extending over an area. The possible cause of the origin is commonly external mechanical impact in the pipe [10]. Figure 2.1 shows the condition of the regular buckle.

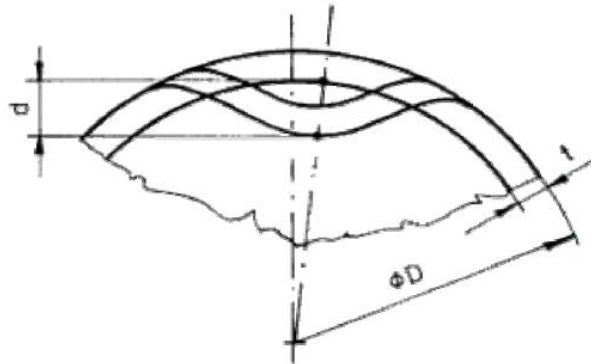


Figure 2.1: Regular buckle [10]

Ovality

This type of defect is a nearly symmetric deviation of the pipe cross-section from the circular shape resulting in elliptical cross-section without sharp break points. The possible cause of these defects is on the pipe manufacturing and also external mechanical impact on the pipe [10]. Figure 2.2 shows the Ovality configuration.

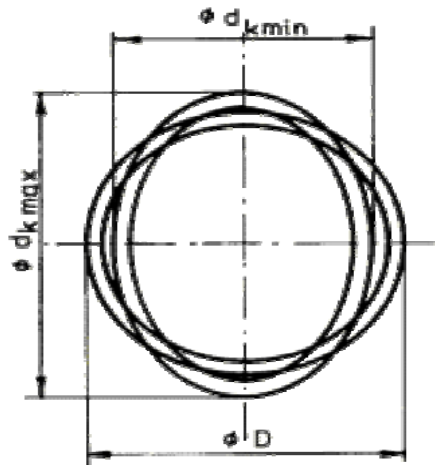


Figure 2.2: Ovality [10]

Wrinkle

From the characteristic of the rippled side of the pipe (number and shape of ripples) the extent of deformation of the opposite side if the pipe can be concluded. The normal cause of this kind of defect is external mechanical impact and also soil movement [10]. Figure 2.3 shows how the wrinkle happens.

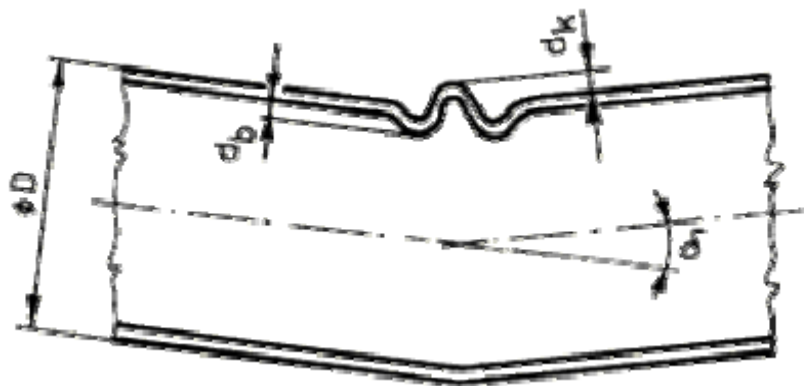


Figure 2.3: Wrinkle [10]

Knob

This is defined as residual deformation of the pipe wall outside the pipe without any sharp edge extending over an area. Possible cause of origin is changed in internal pressure interacting with another defect [10]. Figure 2.4 shows the knob defects.

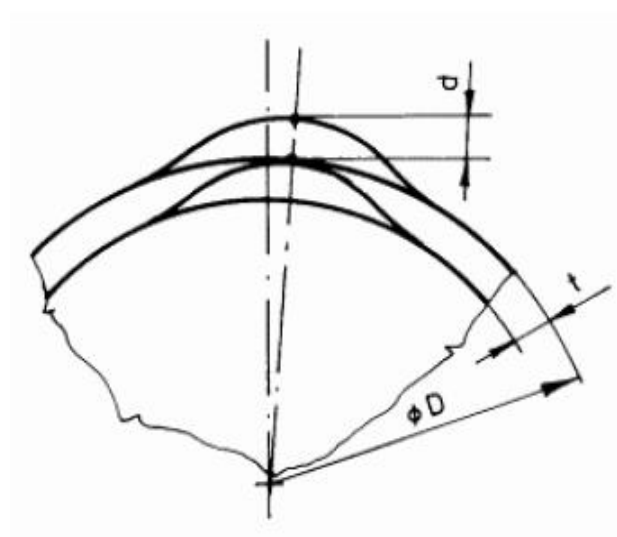


Figure 2.4: Knob [10]

2.4.2 Defects resulting in metal loss

Refer to the greater change in the wall thickness compare to the allowable wall thickness tolerance. This will result in the stress concentration [10]. This also called as corrosion. There are many types of corrosion such as general corrosion, longitudinal corrosion, circumferential corrosion, and spiral corrosion. The description will be stated in the next subsection.

General Corrosion

This is referring to the metal loss extending over a significant area of the pipe resulting in wall thickness decrease. The possible cause of origin is effect of the transported

medium, inappropriate material selection, imperfect coating, damaging coating, and inadequate cathodic protection [10]. Figure 2.5 shows the general corrosion configuration.

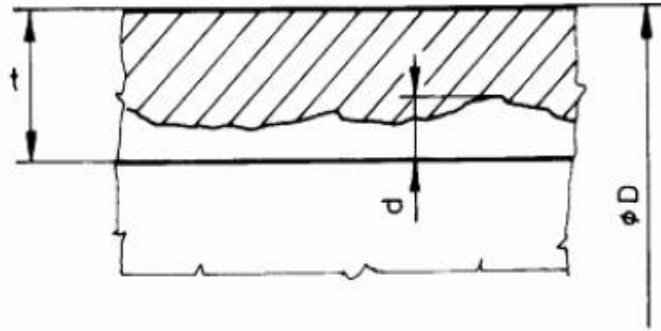


Figure 2.5: General Corrosion [10]

Longitudinal Corrosion

The metal loss parallel with the center line of the pipe resulting in wall thickness decrease having an axial length which exceeds the nominal outside diameter of the pipe and its circumferential size is significantly smaller. Possible cause of origin is an improper welding technology, damaged coating, installation and short circuited structure [10]. Figure 2.6 shows the longitudinal corrosion happen.

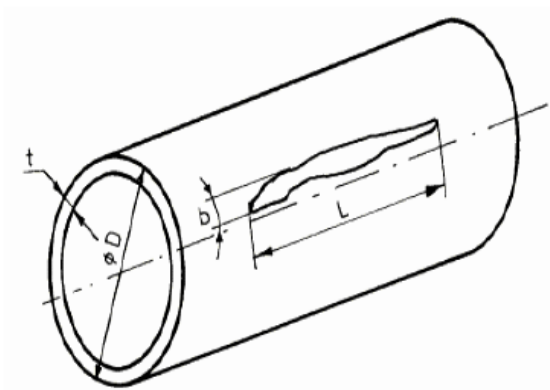


Figure 2.6: Longitudinal corrosion [10]

Circumferential Corrosion

This referring to metal loss perpendicular to the center line of the pipe resulting in wall thickness decrease having a circumferential length which is significantly greater than the width. The possible cause of this origin is like improper welding technology, imperfect coating, damaged coating and also installation. The figure 2.7 shows the configuration for the defects [10].

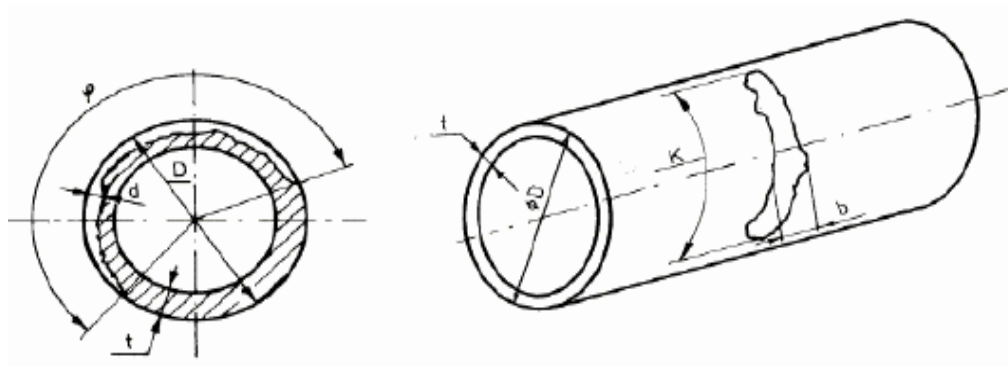


Figure 2.7: Circumferential corrosion [10]

Spiral Corrosion

This is metal loss subtending nearly constant angle to the center line of the pipe, forming a continuous strip or repeating periodically resulting in wall thickness decrease. The possible cause of origin is imperfect coating. Figure 2.8 shows the spiral corrosion defects [10].

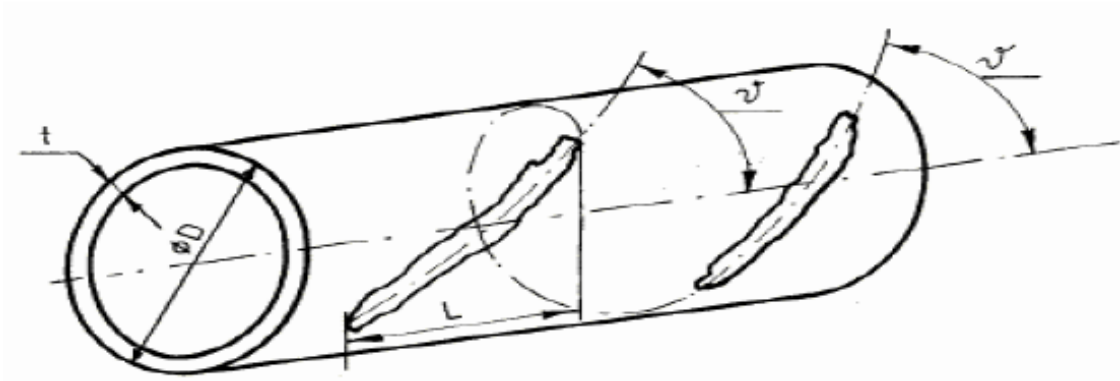


Figure 2.8: Spiral corrosion [10]

Rupture

This defect generally longitudinal discontinuity caused by superficial or near superficial manufacturing defect. The possible cause of origin is at the pipe manufacturing. Figure 2.9 shows the rupture configuration [10].

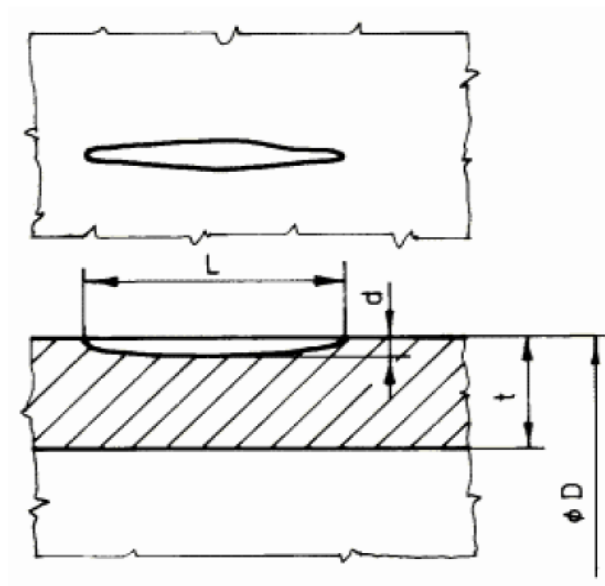


Figure 2.9: Rupture [10]

2.4.3 Planner discontinuities

Planner discontinuities are conditions where two dimensions are significantly greater than the third one [10]. This refers to the cracks like defects. There are several types of planned discontinuities which are fatigue crack, stress corrosion cracks and lapped grinding. The details are explained in the next subsections.

Fatigue Crack

It is generally growing crack originated due to constant or variable amplitudes cyclic load at a stress level under yield strength. The possible cause of origin is cyclic load caused by operation conditions like low-cycle fatigue, high-cycle fatigue, and fatigue crack propagation. The figure 2.10 shows the fatigue crack sample [10].

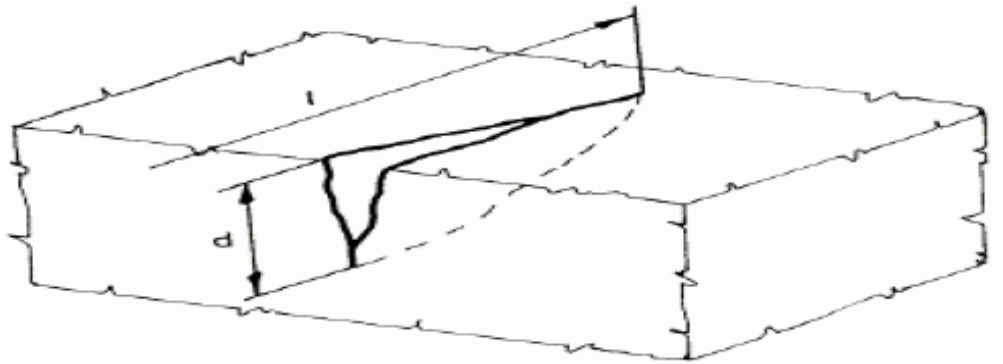


Figure 2.10: Fatigue crack [10]

Stress Corrosion Crack

The crack originated due to common action of sufficient tensile stress and medium having critical electrochemical potential. The possible cause of origin is it can be concluded from the above crack. The figure 2.11 shows the stress corrosion crack [10].



Figure 2.11: Stress corrosion crack [10]

Lapped Grinding

One or multi-part material discontinuity which makes the pipe wall multi-layer and the possible cause of origin is the pipe manufacturing. Figure 2.12 shows the lapped grinding defects [10].

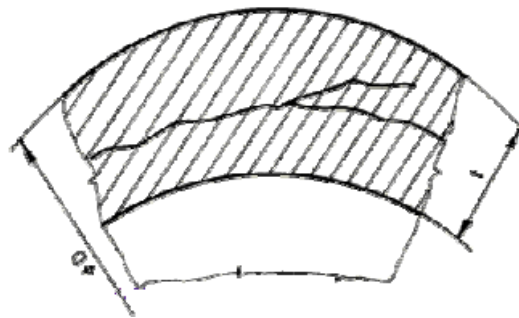


Figure 2.12: Lapped grinding [10]

2.4.4 Change in metal

Usually, the change in the metal does not cause change in dimension or shape of the pipe geometry. This is because the change does not exceed the allowable limit of the metal.

But they result in a disadvantageous change in the material structure and by this way in material characteristics [10].

Arc Drawing

Refer to the burned surface of the pipe wall extending over a relative small area caused by the any part of the electric circuit of the welding apparatus due to improperly applied welding technology. Possible cause of origin is improperly applied welding technology [10].

Strain Ageing

This refers to the application of such steel which became brittle due to the dislocation of blocking effect of its nitrogen content. It is also from the improper material selection. The possible cause of this origin is improperly material selection [10].

In this research, the main possibilities that contributed in the non-aligned axial cracks are due to the corrosion which is in the metal loss type. The thickness of the pipe will be reduced due to the corrosion and the cracks will be created. Thus this research is focusing on the corrosion defects in the pipe. The other defects also will result in the same cracks, but corrosion gives the more effect in these cracks [10-11].

2.5 STRESS BASED FAILURE CRITERION

There are lots of corrosion assessment codes available to estimate the burst pressure of corroded pipeline depending on loading and the scopes. Examples of codes are ASME B31G, modified ASME B31G, DNV RP-F101, and some others. The details of the method will be discussed in the preceding sections.

2.5.1 ASME B31G

American Society of Mechanical Engineers (ASME) B31G originally developed and published in 1984 where it is used for the determination of the remaining strength of the externally corroded pipe subjected to internal pressure loading.

The ASME B31G criterion [9] is developed based on full scale tests of pressured to failure corroded pipes. It allows determination of the remaining strength of the corroded pipes and estimating of the maximum allowable operating pressure (MAOP). However, the B31G criterion contains some simplifications. Another shortage, is the possibility of only proving the pipe integrity under internal pressure, other stresses are not taken into account. There is also restricted in assessable defects, which is the corroded area depth between 10% and 80% [7].

This method is based on the measurement of the longitudinal extent of the corroded area as shown in Figure 2.13. It considers the depth and longitudinal extent of corrosion, but ignores its circumferential extent.

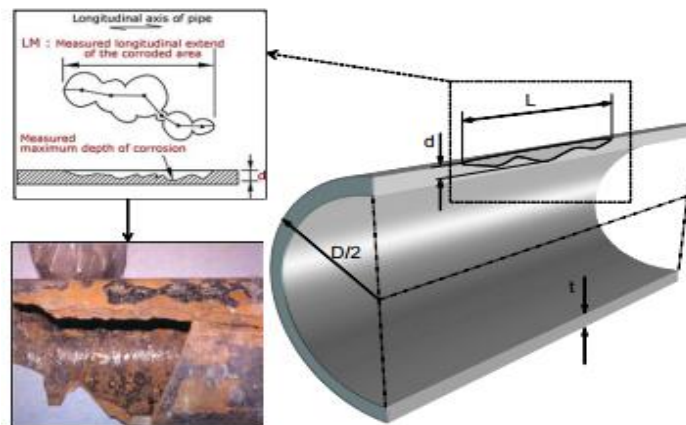


Figure 2.13: Longitudinal extent of the corrosion area [9]

The corroded area is approximated depending on the defect length as parabolic or rectangular shape. Short longitudinal extent of corrosion areas is approximated by the parabolic shape and long longitudinal extent of corrosion areas is approximated by the rectangular shape, as shown in Figure 2.14 and Figure 2.15, respectively [9].



Figure 2.14: Assumed parabolic corroded area for short corrosion defect [9]

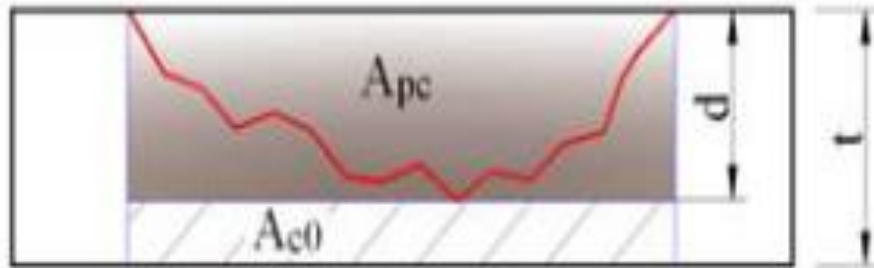


Figure 2.15: Assumed rectangular corroded area for longer corrosion defect [9]

The predicted failure pressure can be estimated by Equation (2.3) and Equation (2.4) for short and long defect respectively [7].

$$S_{flow} = 1.1 \times SMYS \quad (2.1)$$

$$M = \sqrt{1 + 0.8z}, \quad z = \frac{L^2}{Dt} \quad (2.2)$$

For short defect, $z \leq 20$

$$P_f = S_{flow} \frac{2t}{D} \left[\frac{1 - \frac{2}{3} \left(\frac{d}{t} \right)}{1 - \frac{2}{3} \left(\frac{d}{t} \right) \frac{1}{M}} \right] \quad (2.3)$$

For long defect, $z > 20$

$$P_f = S_F \frac{2t}{D} \left(1 - \frac{d}{t} \right) \quad (2.4)$$

2.5.2 Modified ASME B31G Criterion

The B31G method was found to be too conservative and has been modified, the new method is called Modified B31G or 0.85-area Method. This method removes some conservatism by changing the flow stress limit to SMYS+ 69MPa. This is very close to the conventional fracture mechanism definition of the flow stress: the average of the yield and ultimate strength. This modification results in the change of the failure equation, which is also dependent on the limit on defect length. The equation to calculate the failure pressure is modified as follows [7, 9].

$$S_{flow} = SMYS + 69MPa \quad (2.5)$$

$$P_f = S_{flow} \frac{2t}{D} \left[\frac{1 - 0.85 \left(\frac{d}{t} \right)}{1 - 0.85 \left[\left(\frac{d}{t} \right) / M \right]} \right] \quad (2.6)$$

The short longitudinal extent of corrosion areas and long longitudinal extent of corrosion areas shown in equation (2.8) and equation (2.9) [7]

$$z = \frac{L^2}{Dt} \quad (2.7)$$

For short defect, $z \leq 50$,

$$M = \sqrt{1 + 0.6275z - 0.003375z^2} \quad (2.8)$$

For long defect, $z > 50$,

$$M = 0.032z + 3.3 \quad (2.9)$$

2.5.3 DNV RP-F-101 Criterion

DNV RP-F-101 provides guidance on single and interacting defects under pressure only and combined loading. It is a method to evaluate corroded pipelines under complex condition such as internal pressure, corrosion induce defect and longitudinal compressive and bending loads due to soil movement. The allowable corroded pipe pressure of a single metal loss defect subjected to internal pressure loading with defect depth not exceeding 85% of wall thickness is given by the following acceptable equation [7].

$$P_f = \frac{2t}{D-t} SMTS \left[\frac{1 - \left(\frac{d}{t}\right)}{1 - \left(\frac{d_1}{tQ}\right)} \right] \quad (2.10)$$

Where the factor Q is given as:

$$Q = \left(1 + 0.31 \frac{L^2}{Dt} \right)^{\frac{1}{2}} \quad (2.11)$$

2.6 CORROSION PREVENTION

There are no ends to produce a corrosion control program. Now, a successful corrosion control program is easy to find and also to perform it. Started with the design that really effectively and can reduce the percentage of corrosion, perfect installation where the

installation of the piping systems also includes the installation for non-corrosion piping systems, corrosion control method and lastly maintaining and observation. Those steps are crucial in the part of executing the corrosion. There is lots of the method that really recommended as a part of the successful corrosion control program that used by most oil and gas pipeline company [12].

2.6.1 Corrosion inhibitors

Corrosion inhibitors are compounds which when added to the upstream pipeline can inhibit the corrosion of carbon and low-alloy steels which are commonly used because of their cost effectiveness [13].

As an example is a volatile corrosion inhibitor coating. It is quite unique where they are organic compound that protect metal surfaces by emitting a vapor such as an amine base compound. The nitrogen on the amine will attracted to the polar metal surface, thus the rest molecule is very hydrophobic and repels water to retard corrosion [13]. Figure 2.16 shows how the VCI works.

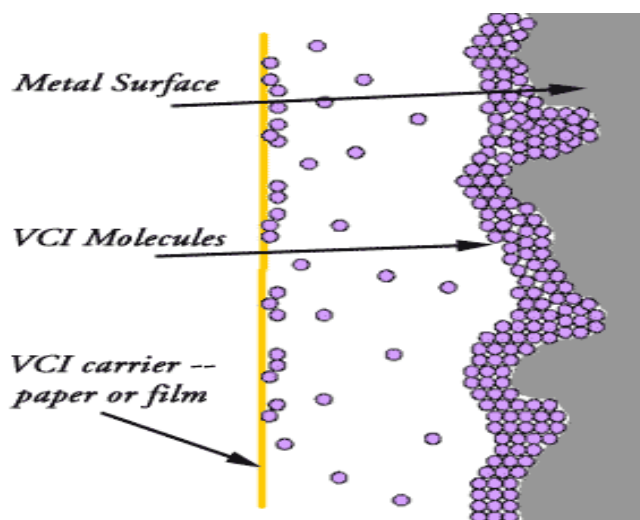


Figure 2.16: Volatile Corrosion Inhibitor Coating [13]

2.6.2 Material Selection

From a purely technical standpoint, an obvious answer to corrosion problems would be to use more corrosion resistant materials. In many cases, this approach is an economical alternative to other corrosion control methods. Corrosion resistance is not the only property to be considered in making materials selection but it is of major importance in the chemical process industries. The choice of a material is the result of several compromises. For example, the technical appraisal of an alloy will generally be a compromise between corrosion resistance and some other properties such as strength and weldability [14].

And the final selection will be a compromise between technical competence and economic factors. In specifying a material, the task usually requires three stages:

- Listing the requirements
- Selecting and evaluating the candidate material
- Choosing the most economical material

The materials selection process is also influenced by the fact that the materials are either considered for the construction of a new system, or for the modification or repairs in an existing facility. For the construction of new equipment, the selection procedure should begin as soon as possible and before the design is finalized. The optimum design for corrosion resistance will often vary with the material used. In a repair application, there is usually less opportunity to redesign, and the principal decision factors will be centered on delivery time and ease of fabrication in the field. It is also advisable to estimate the remaining life of the equipment so that the repair is not over-designed in terms of the corrosion allowance [14].

2.6.3 Cathodic protection (CP)

From that beginning, CP has grown to have many uses in marine and underground structures, water storage tanks, gas pipelines, oil platform supports, and many other

facilities exposed to a corrosive environment. Recently, it has proven to be an effective method for protecting reinforcing steel from chloride-induced corrosion.

Cathodic protection has become a widely used method for controlling the corrosion deterioration of metallic structures in contact with most forms of electrolytically conducting environments such as the environments that containing enough ions to conduct electricity such as soils, seawater and basically all natural waters. Cathodic protection basically reduces the corrosion rate of a metallic structure by reducing its corrosion potential, bringing the metal closer to an immune state. From a thermodynamics point of view, the application of a CP current basically reduces the corrosion rate of a metallic structure by reducing its corrosion potential towards its immune state as shown here for iron and steel or here for aluminum and its alloys [15].

CHAPTER 3

METHODOLOGY

3.1 INTRODUCTION

In this chapter, all the process from the beginning of the research until the end has been stated. Methodology is crucial to make sure the research is running smoothly, based on the objectives and also make it easy to refer. By using the flow chart, the research can be done easily because it shows step by step of the process in this research.

In order to achieve the smooth and clear research, the method that's been used must be accurate and clear. So the methodology will include and describe all about the process that involve in this research. With this also, the arrangement of this report will become more structured and easier to understand.

3.2 FLOW CHART

Flow chart really helped in order to make the research methodology will remain on the right path. This is because the methodology was created based on the objectives and scopes. So, this flow chart will guide the flow of the methodology. The overall flow chart is presented in the figure 3.1 while the methodology flowchart is in the figure 3.2.

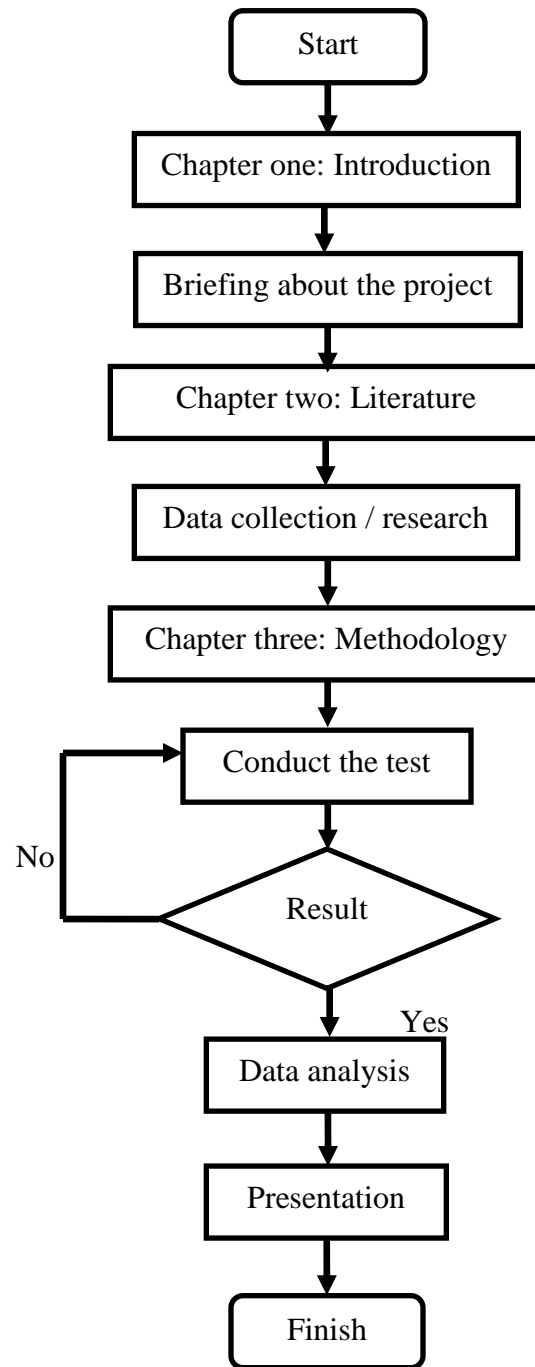


Figure 3.1: Overall Flowchart

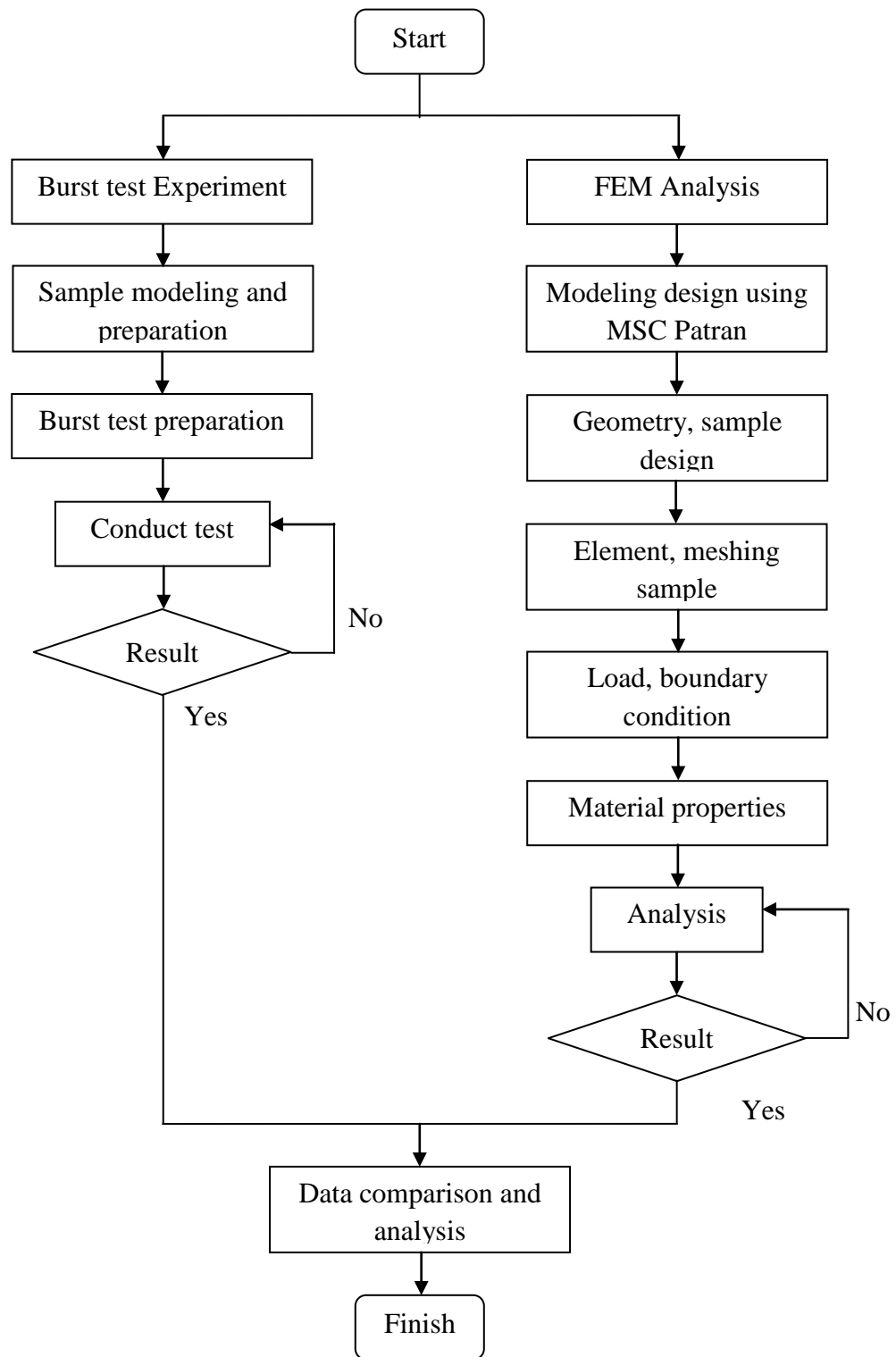


Figure 3.2: Methodology Flowchart

3.3 MATERIAL USED

Pipe with material Grade B is the one that has been chosen to perform the test. Table 3.1 shows the specification that the pipe that's been used in the test.

Table 3.1: Specification of material Grade B steel pipe

Type	Material Grade B
Length (mm)	600
Thickness (mm)	4
Outer diameter, OD (mm)	60.5

The data for the chemical properties is taken from the composition analysis that's been done using a specimen of material Grade B. The data for the chemical properties is on the table 3.2.

Table 3.2: Chemical properties of material Grade B steel pipe (%)

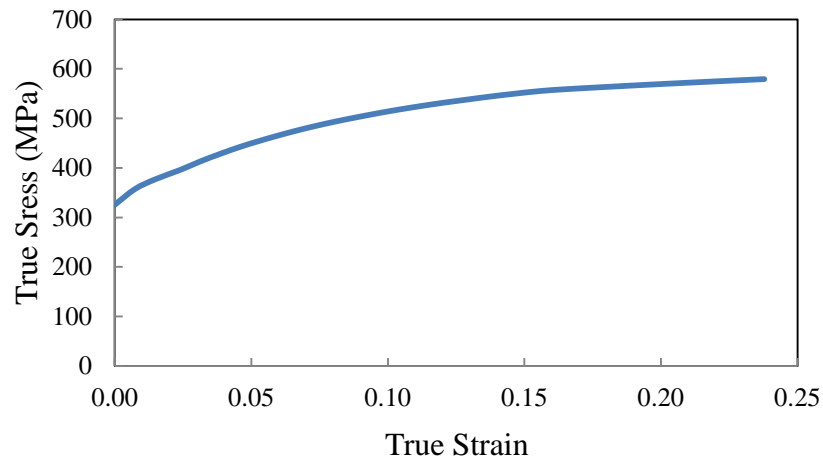
	C	Mn	P	S
Material Grade B	0.258	0.559	0.001	0.001

By using the data from the composition analysis, the chemical composition of pipe with material Grade B have been compared to the other material chemical composition in order to search the similar type of pipe. This is because to make sure whether there are other pipe that have the similar chemical composition with material Grade B. The comparison table is on the table 3.3. From the table, the chemical properties material Grade B is lower than the API 5L L245 which is using the maximum value. Since this data is more similar than the others and also the data are no exceeding the maximum value, material Grade B can be considered as the pipe API 5L L245.

Table 3.3: Comparison between material Grade B with API 5L L245 (%) [16]

	C	Mn	P	S
Material Grade B	0.258	0.559	0.001	0.001
API 5L L245 (max value)	0.26	1.20	0.003	0.003

The mechanical properties of the API 5L L245 pipe is determined by using the tensile test. The data of the stress strain will be converted to the true stress strain to be used in the field section in the finite element analysis for the plastic region data. Figure 3.3 shows the graph of true stress strain from the tensile test.

**Figure 3.3:** True stress strain graph from tensile test**Table 3.4:** Mechanical properties of API 5L L245 pipe

Mechanical properties	API 5L L245 pipe
Young's modulus (MPa)	207000
Poisson's ratio	0.3
Yield Strength (MPa)	326
Tensile Strength (MPa)	466

3.4 TYPE OF TESTED DEFECTS

In this research of multiple aligned axial cracks, there are four major lengths of defects that will be tested. There are 25, 50, 75 and 100mm in length. Each of the length will be paired with the other length of defects. Then for each combination of defect length will have two different widths within those two defects. Each combination with the width will named as case 1 until 20. The depth of the defect is about 50% of the wall thickness which is about 2 mm. Figure 3.4 and 3.5 shows the crack modeling design. $2c_1$ is the first length and the $2c_2$ is the second length. While d is the distance between both cracks. Table 3.5 shows the cracks dimension.

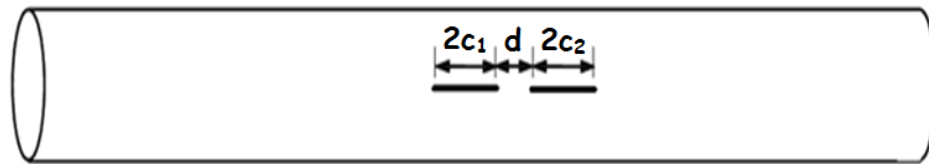


Figure 3.4: Pipe design modeling

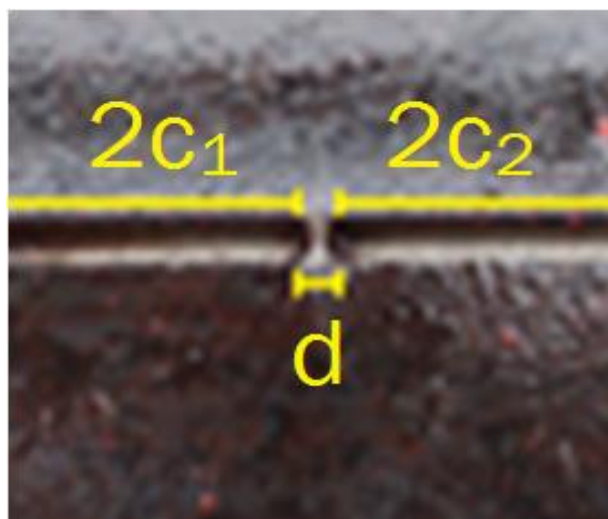


Figure 3.5: Cracks on pipe

Table 3.5: Cracks dimension

Defect configuration	defect size		
	$2c_1$ (mm)	$2c_2$ (mm)	d (mm)
Case 1	25	25	0.5
Case 2	25	25	2.0
Case 3	25	50	0.5
Case 4	25	50	2.0
Case 5	25	75	0.5
Case 6	25	75	2.0
Case 7	25	100	0.5
Case 8	25	100	2.0
Case 9	50	50	0.5
Case 10	50	50	2.0
Case 11	50	75	0.5
Case 12	50	75	2.0
Case 13	50	100	0.5
Case 14	50	100	2.0
Case 15	75	75	0.5
Case 16	75	75	2.0
Case 17	75	100	0.5
Case 18	75	100	2.0
Case 19	100	100	0.5
Case 20	100	100	2.0

3.5 BURST TEST

The burst pressure test had been used in this research. This type of test is a quite common test that had been used for most problems involved with piping systems. The purpose of the burst test is used to determine the failure pressure of the cracked pipe.

During the test, hydraulic oil will be pumped into a cracked pipe until the pipe will burst up. Then the maximum pressure will be recorded. This maximum pressure is read as the failure pressure for the cracked pipe based on the ultimate tensile stress.

To run the burst test, there are several tools required and equipment that need to be installed with the pipe. There are:

- Hydraulic pump and oil
- Connector host
- Pipe clamper
- Pipe wrench

There are only two experiments that conducted in this research. This is because of there are some problems that cannot be avoided. The first problem is lack of materials. The material properties of the pipe that used to do the burst test is API 5L L245 pipe. This kind of pipe is quite hard to find. The other problem is the cost of the material. Since the pipe is rare, so the cost of the pipe is becoming quite high. So, only two pipes that can be afforded in order to do the burst test.

Since there are only two pipes that can be tested but there are 20 cases to be researched, only two cases have been selected due to several parameters taken. The parameter taken is about the length of cracks and the distance between the cracks. Table 3.6 shows the two cases that have been selected.

Table 3.6: Burst test crack

Crack configuration	defect size		
	$2c_1$ (mm)	$2c_2$ (mm)	d (mm)
Experiment 1	100	100	0.5
Experiment 2	100	100	2.0

The two cases selected to become the burst test specimen because there are so many cracks lengths. So with many cracks lengths, the variable is too many. So the only one cracks length will be selected which is 100mm for both cracks. For the distance between the cracks, both 0.5 and 2.0mm is used as the variable of the burst test. The crack length is taken for 100mm because from this theory, this will result in the lowest burst pressure. Since the burst test is quite dangerous, the minimum burst pressure will be taken which is from the longest cracks length.

3.5.1 TEST PROCEDURE

The burst test had been conducted under a lecturer and several staff observations. This is to ensure the test will go on smoothly and without any injuries occur. The burst test will be conducted as follows.

The apparatus and tools such as pipe, hydraulic pump and the oil, spanner, funnel, pipe wrench, pipe clammer and host connector are in a good condition as in the figure 3.6 and 3.7. The both ends of the pipe were capped by circumferential welding to seal the end of the pipe as in figure 3.8.



Figure 3.6: Pipe clammer



Figure 3.7: Hydraulic pump



Figure 3.8: Seal at the end of the pipe.

The connecting host was warped before connect it together with the pipe using threaded-pipe tape and tightly installed. This is to ensure there are no leakage at the thread of the pipe and the host connector. The pipe was placed in the pipe clammer and tightly

clamped. The cracks was faced towards upwards direction to make the crack easier to observe. Figure 3.9 shows the complete installation of the pipe with the camper.



Figure 3.9: Complete installation

After that the host was connected to the hydraulic pump and the hydraulic oil was poured into the pump using the funnel. The hydraulic pump was simultaneously pumped with the air hole was opened to remove any air that trapped. After all the air is removed, the hydraulic oil was kept pouring and also at the same time the hydraulic pump was pumped. The pumping rate must be almost constant to receive the most accurate readings. The pumping process was continued until the pipe burst and the maximum pressure was recorded. After the pipe burst up, the pipe clammer and the host was loosen.

If necessary, the oil that remained in the pipe was saved to be used in the next test. The test place was cleaned and all the apparatus and the tools have been safely stored. Figure 3.10 shows how the burst happens in the pipe.



Figure 3.10: Example of the burst of the pipe.

3.5.2 PRECAUTION

Burst test is considered as a quite dangerous test where it requires a pressure and also a burst from the crack that cannot be determined the type of burst of it. So it is more safety if stays far away from the pipe. In this test, it requires a full concentration and also caution to ensure the safety is protected. Also please make sure to wear all the safety equipment such as safety boots, glove and goggles to avoid any damage to self. Note that, the test will be conducted in the wide area such as in a parking lot without any car. This is to make sure that the wider area will create more space for the pipe to burst. This also can reduce the percentage of persons in charge will involve in any injuries.

3.6 FINITE ELEMENT ANALYSIS (FEA)

The next step is to do an analysis using finite element analysis to obtain the real data and lastly find the result for this research. In this FEA, MSC Marc Patran 2008r1 has been used for pre-processing and post-processing. It also used as a solvent in this research. This software, MSC Marc Patran 2008r1 is the quite famous where it's been used widely for Finite Element Analysis (FEA). It can be used to make a meshing on the surface and also

solid meshing. It also supports the modeling and analysis setup for other simulation processes such as MSC Nastran, ANSYS and others.

Using MSC Marc Patran 2008r1, almost all of the finite element solvent such as linear, non-linear and also thermal solvent is easier because it provides quite many tools that streamline the analysis setup. The meshing also is quite easy to create on the surface and also at the solid because it gives a lot of options on the meshing type that need to be included such as hex and tetra. The mesh also really easy to control using the mesh seed before the meshing is applied.

Also for the other constrain such as boundary conditions, loads applied and analysis setup, all of it is easy to understand and use. The data from the result also come with a lot of options such as displacement, stress and strain, pressure and also forces.

3.6.1 SIMULATION PROCEDURE

Before started, a new file was created in order to save all the data and file of the simulation from the MSC Marc Patran 2008r1. The application was started in from the file that already created. This can be done by right click on the application and find the start in column. The directory of the folder that already created before was inserted.

After the application was opened, the analysis code for MSC Marc Patran 2008r1 was changed. Then the geometry scales was stated in millimeters. This can be done by clicking on the preference button on the taskbar and choose the geometry scale factor. Change it to “1000.0 (millimeters) as shown in the figure 3.11. Then the project can be started.

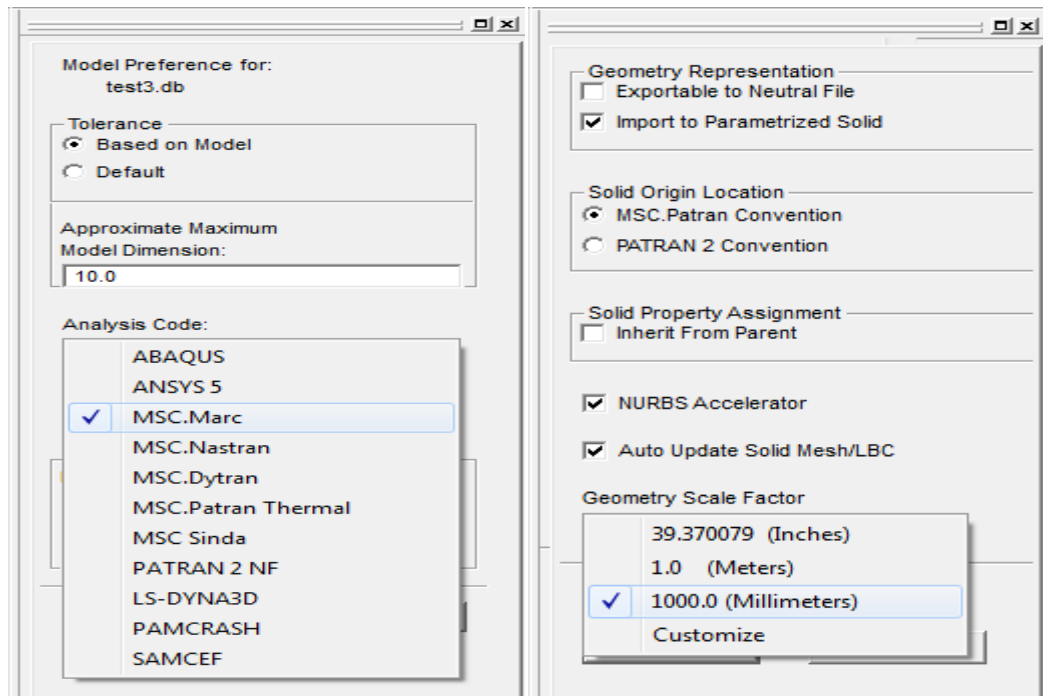


Figure 3.11: Configuration before starting the MSC Patran

For starting the analysis, the design was created first. MSC Marc Patran 2008r1 already has the flow from the beginning to the end on how doing it. Figure 3.12 shows the sequence on flow how doing the simulation.



Figure 3.12: Simulation sequences

For the design modeling, only half of the pipe was modeled. This is because of the symmetrical shape of the pipe and this option can be stated in the following steps. The model was created according to the data for the analysis such as in table 3.7 and 3.8.

Table 3.7: Specification of the models

Length, L (mm)	600
Thickness, t (mm)	4
Outer diameter, OD (mm)	60.5

Table 3.8: Cracks dimension

Configuration	defect size		
	$2c_1$ (mm)	$2c_2$ (mm)	d (mm)
Case 1	25	25	0.5
Case 2	25	25	2.0
Case 3	25	50	0.5
Case 4	25	50	2.0
Case 5	25	75	0.5
Case 6	25	75	2.0
Case 7	25	100	0.5
Case 8	25	100	2.0
Case 9	50	50	0.5
Case 10	50	50	2.0
Case 11	50	75	0.5
Case 12	50	75	2.0
Case 13	50	100	0.5
Case 14	50	100	2.0
Case 15	75	75	0.5
Case 16	75	75	2.0
Case 17	75	100	0.5
Case 18	75	100	2.0
Case 19	100	100	0.5
Case 20	100	100	2.0

Geometry

For sketching the models, the geometry button was clicked first. This button enables to create the pipe sample to be tested. Using the create button, point as the object and the XYZ as the method, the point was created using coordinates. By using the curve as the object and the point as the method, the line was created. All the point of the pipe was lined up as the pipe is in a half design. Then using 2D Arc2point, the circle was created. The circle line was created to complete the half pipe design. For the cracks, there are small curve that inside the crack. So also using this option, the curve at the situated point was created and all the point was been connected to make the half pipe sketch with cracks. Figure 3.13 shows the point, line and curve line setup while figure 3.14 shows the full sketch of the half pipe.

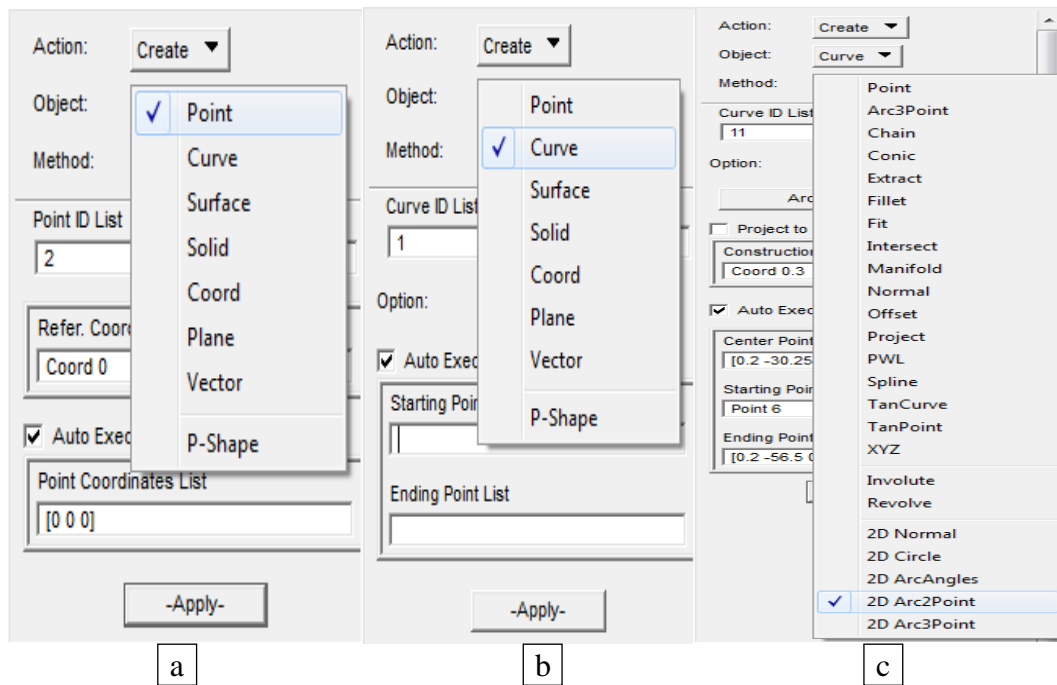


Figure 3.13: Geometry setup a) Point setup b) Line setup c) Curve line setup

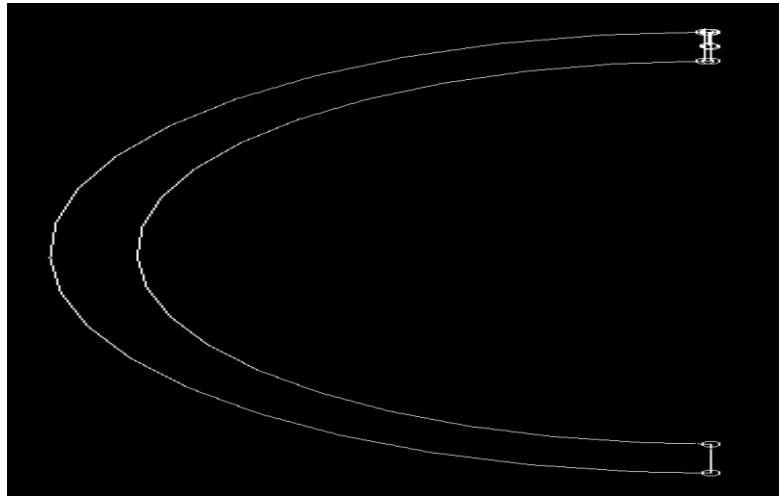


Figure 3.14: Full sketch pipe

After that, the surface at the pipe's sketching was created by selecting create a surface. The surface is created by selecting two curves that are in the opposite direction of each other. The surface is crucial to do the next steps which is to make the models become in 3 dimensions. Figure 3.15 shows the surface setup.

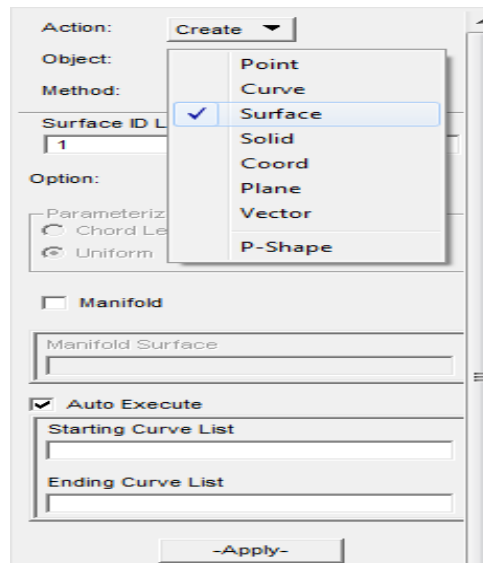


Figure 3.15: Surface setup

Then the models was solid generated. To do so, create solid was selected by using a method of the extrude. The solid type was changed to the full type from the hollow type. The surface was selected to be extruded and the solid was generated. The value for the extruded solid was inputed at the translation vector. Figure 3.16 shows the full setup for solid extruding.

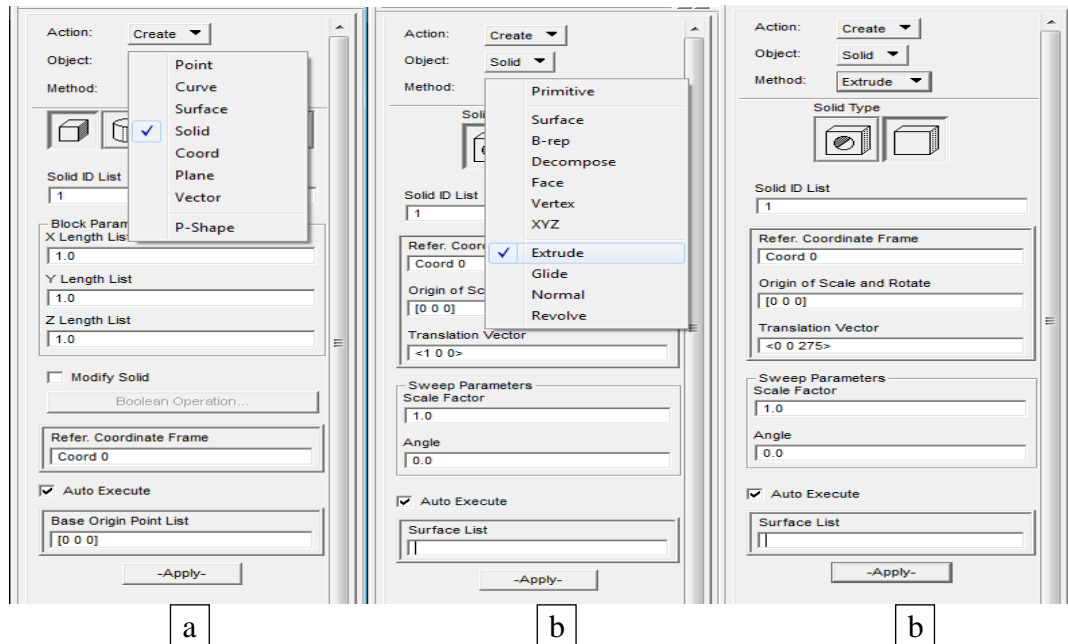


Figure 3.16: Solid setup a) Solid creating b) Extrude method c) Translation vector

The next steps is the cracks at the pipe was created. Since the extrude can only generate the solid, the cracks parts was left unextruded to make it as a cracks. Then the transform option was selected to transform the surface of the cracks to the other side. This was needed to be done for the solid extrude since the extrude is only can be done by selecting the surface. The value for the transform is according to the length of the cracks. The value was inputed in the direction of vector section. Figure 3.17 shows the surface transform setup.

The image shows a software dialog box for setting up surface transforms. The fields are as follows:

- Action: Transform
- Object: Surface
- Method: Translate
- Surface ID List: 6
- Type of Transformation: Cartesian in Refer. CF, Curvilinear in Refer. CF
- Refer. Coordinate Frame: Coord 0
- Translation Vector: Reverse Direction, Auto Update Magnitude, Direction Vector: <0 0 100>, Vector Magnitude: 100.0
- Translation Parameters: Repeat Count: 1
- Delete Original Surfaces
- Auto Execute
- Surface List: Solid 3.6
- Button: -Apply-

Figure 3.17: Surface transforms setup

After that, the solid parts of the pipe was continued to extrude. The solid in between two cracks was created according to the data. Then the same setup was continued to make the other cracks. Finally, the pipe was extruded to the end of the pipe. The full models was finished designs as in figure 3.18.



Figure 3.18: Full solid generated models

Elements

The simulation was continued to the next parts which the element for the models was created. The element button in the simulation sequence was clicked followed by a mesh seed with uniform type. Mesh seed is very important in order to control the value of the elements that have in the parts of the models. For the uniform type, the mesh was divided equal in numbers for the selected parts. This setting was used to create the mesh at the crack width, length and also depth. This setting also was used at the pipe diameter, thickness and the distance between the cracks.

Then the one way bias type of mesh seed was selected. This setting made the mesh is more concentrated on the one side only. This setting used the ratio of the length between the concentrate mesh over the unconcentrated mesh. This setting was used at the both ends of the pipe. The mesh was focused more on the side which is next to the cracks. The setup is shown in figure 3.19 and figure 3.20 shows the fully meshed seed models.

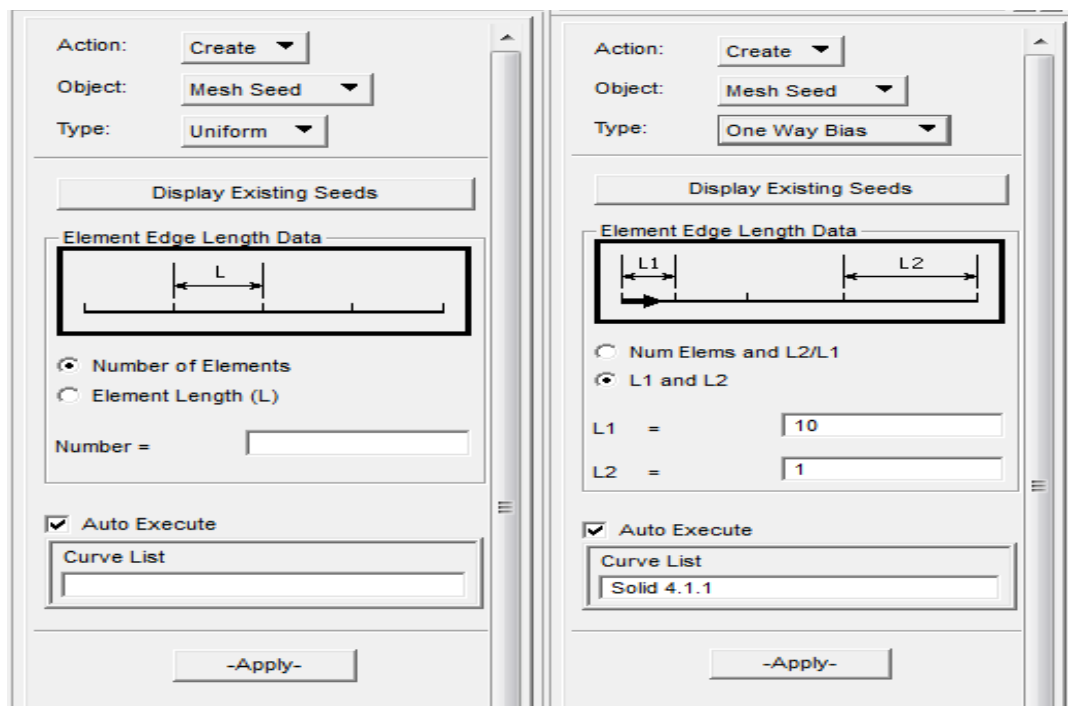


Figure 3.19: Mesh seed for uniform and one way bias setup

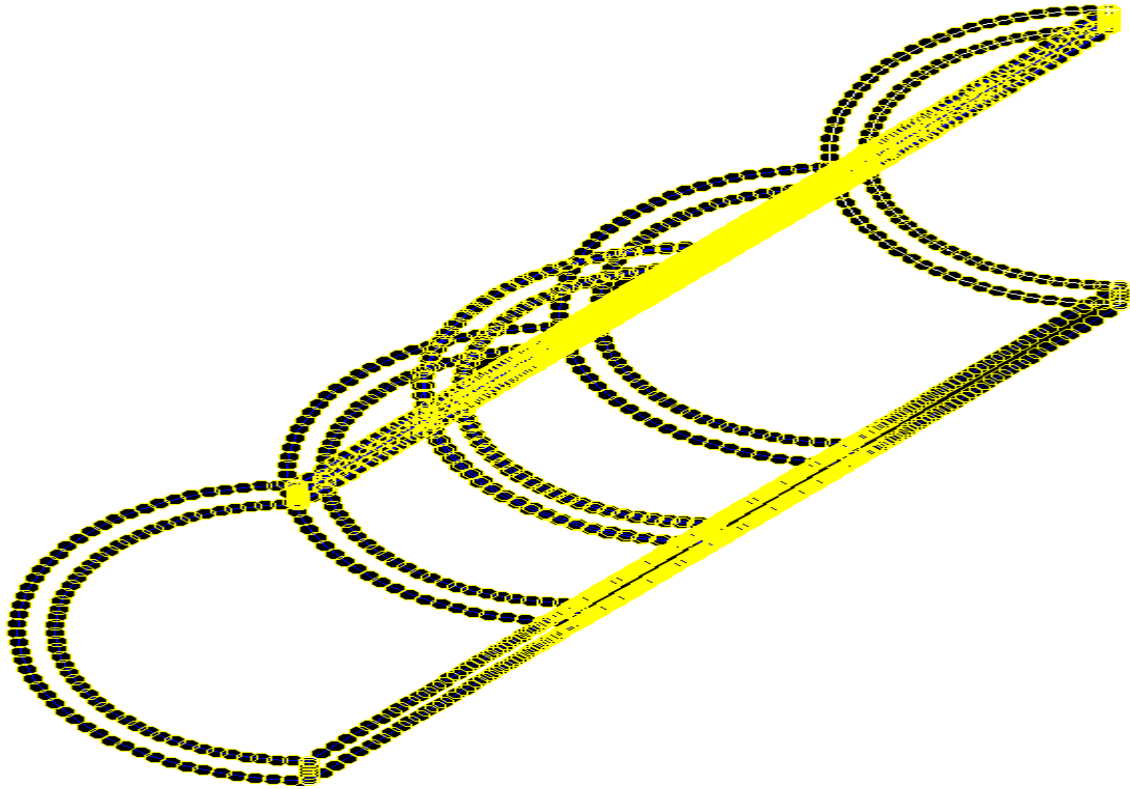


Figure 3.20: Fully mesh seeded models

After all the mesh seed was finished, the mesh was created using the Mesh geometry. Solid type was selected and also the entire models was selected for the meshing. Hex element shape was used and Solid was selected to be meshed in a Solid List column. When creating the new property, 3D solid was used and the property name was named as steel. Standard geometry and reduce integration option was selected before input the properties. Figure 3.21 shows the meshing process. After the meshing process, equivalent option was selected to connect all the mesh in the solid parts. This process will reduce all nodes and also remove the duplicate and excess nodes. Figure 3.22 shows the equivalent setup.

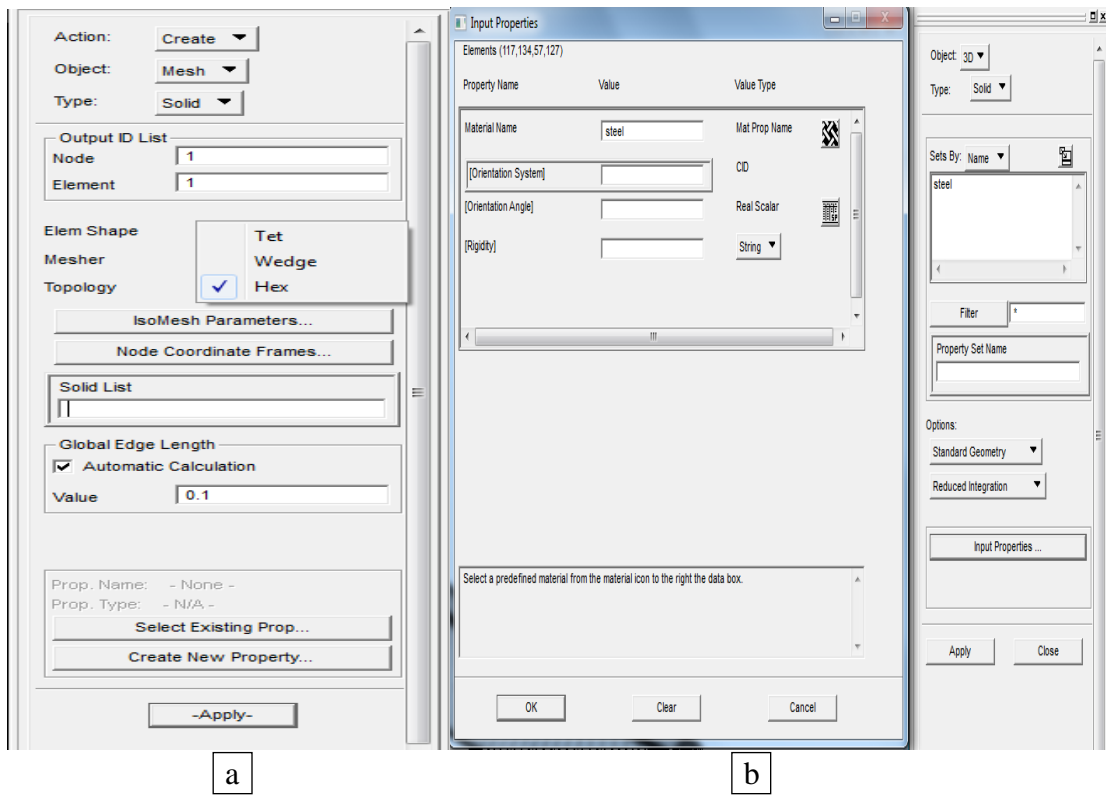


Figure 3.21: Meshing process a) Element shape b) Material properties

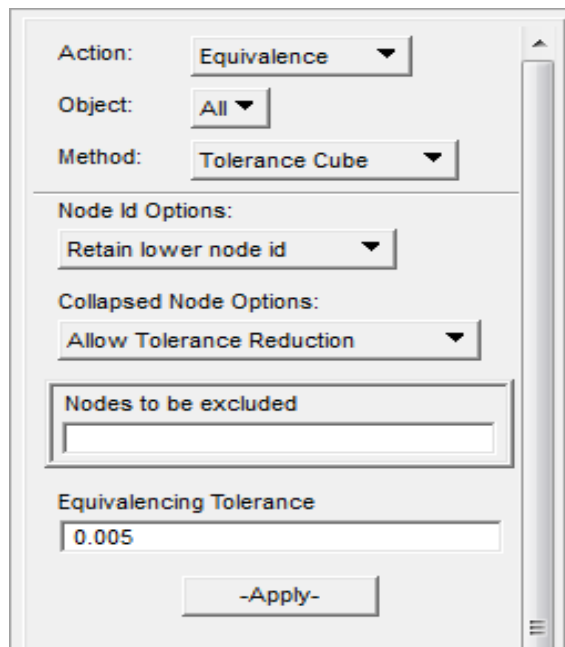


Figure 3.22: Equivalent

After all the process of element which is meshing was finished, the models was having the solid meshed as in figure 3.23. The mesh at the distance between cracks was more focused as at the both sides of the pipe that is nearest to the cracks. The focused mesh is shown in the figure 3.24.

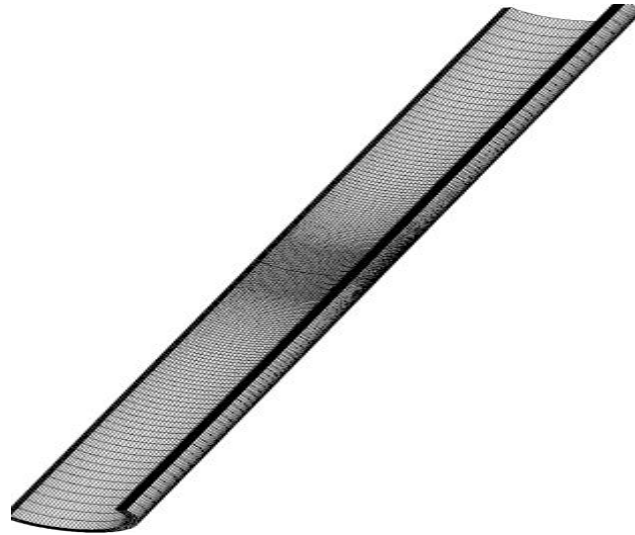


Figure 3.23: Meshed model

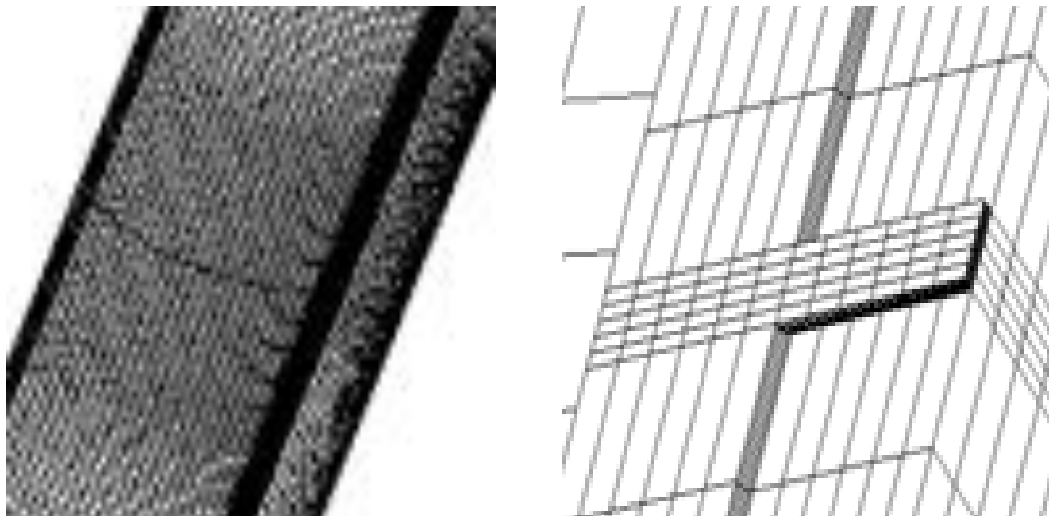


Figure 3.24: Focused mesh at the cracks and distance between cracks

Loads and boundary conditions

The third step was to specify the loads and boundary conditions. This function is used to set the limitation and condition of the models. This is the part where the symmetry of the pipe was created. The Load/Boundary Conditions button was clicked. Here, all the load and boundary condition was named. For the fixed boundary condition, the displacement setting was selected and the name of Fixed was named. At the input data, $\langle 0,0,0 \rangle$ was entered for both translational and rotational value. This was functioned as there are no translation and rotation of the x, y and z axis, $\langle X, Y, Z \rangle$. As for the symmetry, the axis of the symmetry was determined first. In this case, the symmetry was the x symmetry. Hence the value for the x-symmetry was $\langle 0, , \rangle$ for translational and $\langle , 0,0 \rangle$ for the rotation. This means that on the x-axis have the rotational only and have translated in the y and z axis. Figure 3.25 shows the setup for boundary conditions.

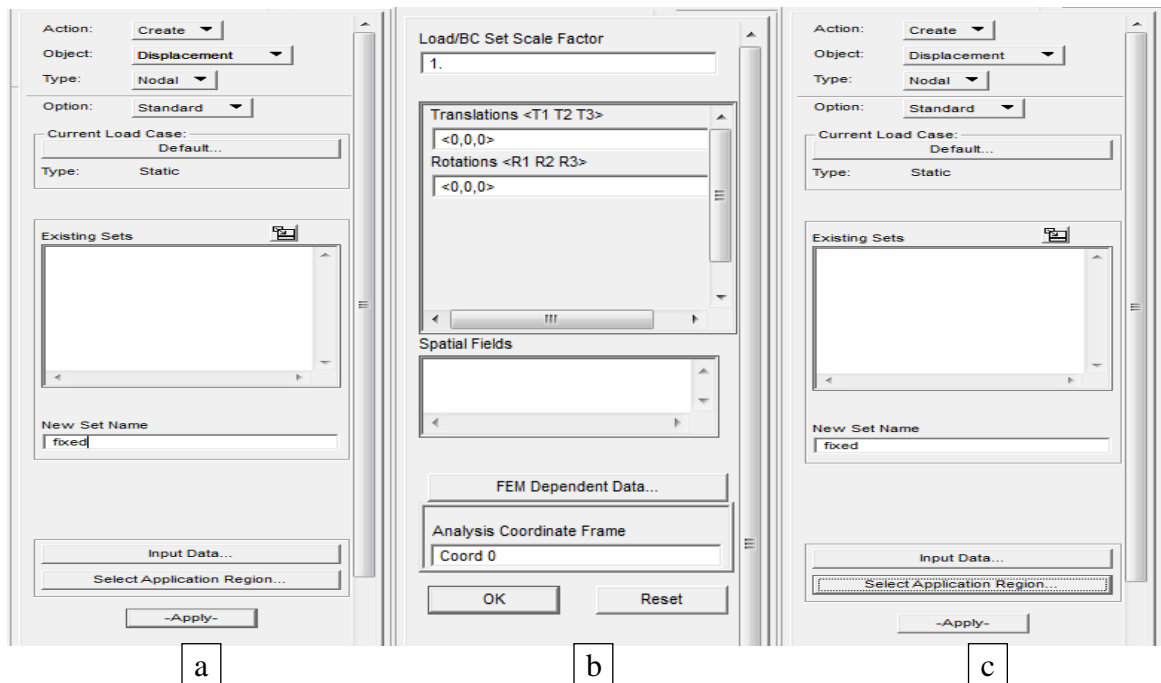


Figure 3.25: Boundary condition setup a) Displacement setting b) Conditions c) Surface selected

The selection of region was selected according to the area that need to be described. As for example, the fixed area was situated at the both ends of the pipe, so the fixed area was taken at the both end sides of the pipe. Figure 3.26 shows the fixed setup and figure 3.27 show the fixed area.

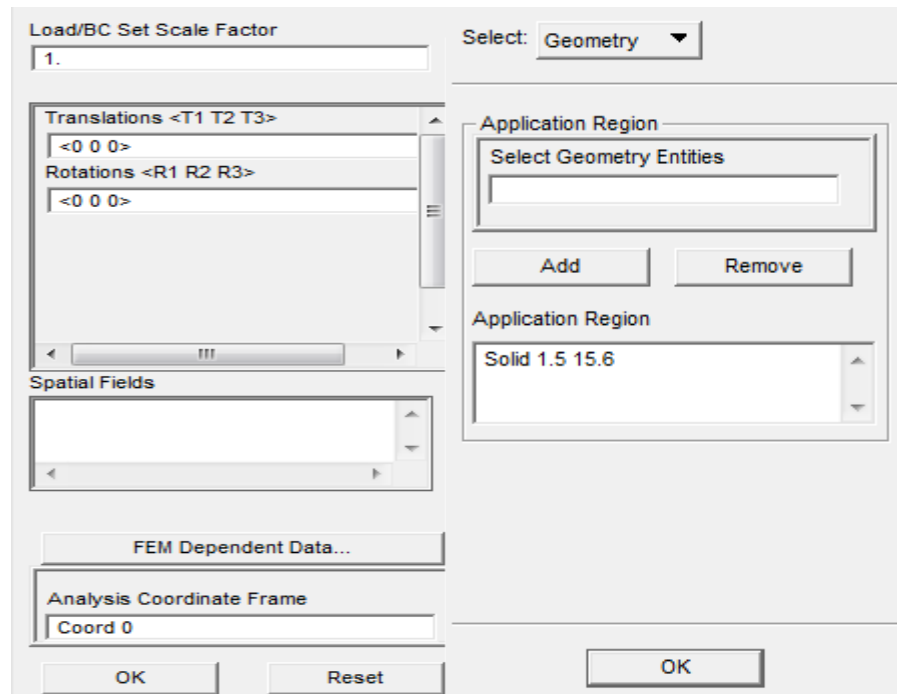


Figure 3.26: Fixed area setup

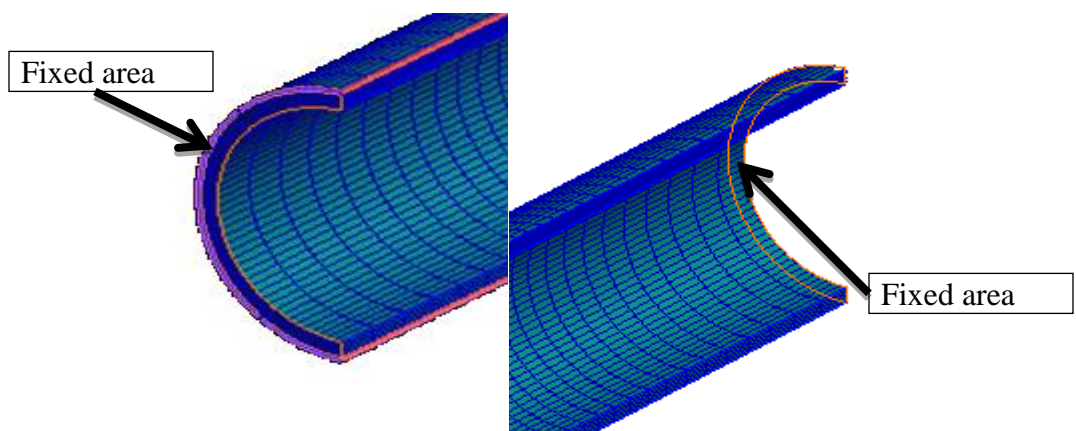


Figure 3.27: Fixed area selected

Next is for the pressure exerted to the models. Here the pressure was internal pressure. So the pressure setting was selected and also gave the named as Pressure. After that, the value of the pressure was inserted. The value was read in pressure (MPa) and the surface was selected at the application region. All the inner surface of the pipe was selected and then the pressure was applied. The load and displacement was checked so that the load and displacement created was correct. Figure 3.28 shows the pressure setting.

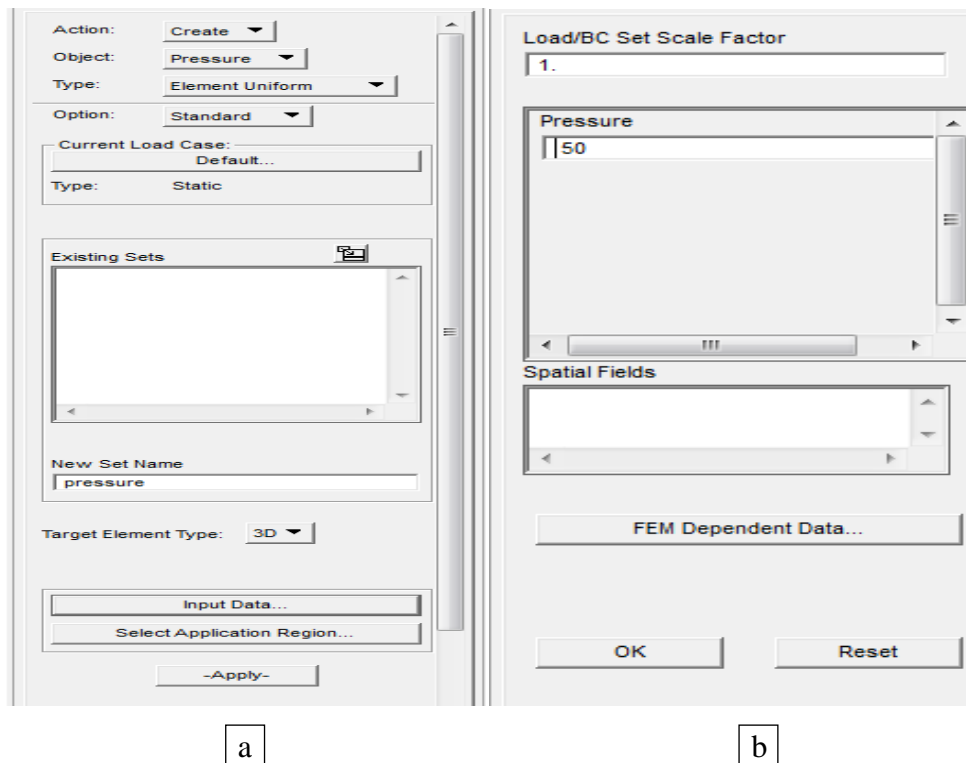


Figure 3.28: Pressure setting a) Pressure selected and name set b) value for the pressure

Field

For the next step was the field setting. The field parts were done to enter the true plastic stress-strain data. The field button was clicked and the name of the file that needs to be read in the material section was named. The strain section was been ticked. Then the data from the CSV file of the stress-strain data was loaded. The data will be loaded into the field setting by clicking input data. The data is shown in figure 3.29. After that, the load data of the stress-strain in the material was enabled. Figure 3.30 shows the field settings.

1D Material Scalar Table Data

Input Data Auto Highlight Import/Export...

Data

	e	Data
e-1	0.0000000E+000	3.2581000E+002
e-2	7.4000000E-003	3.5742999E+002
e-3	1.4700000E-002	3.7685001E+002
e-4	2.4100000E-002	3.9623999E+002
e-5	3.1300001E-002	4.1312000E+002
e-6	3.8400002E-002	4.2812000E+002
e-7	4.5600001E-002	4.4194000E+002
e-8	5.2600000E-002	4.5404001E+002
e-9	5.9599999E-002	4.6514001E+002

OK Undo

Figure 3.29: CSV data

Action: Create

Object: Material Property

Method: Tabular Input

Existing Fields 📄

Field Name material gred b

Table Definition

Active Independent Variables

Temperature (T)

Strain (e)

Strain Rate (er)

Time (t)

Frequency (f)

Magnetic Induction (B)

Magnetic Field Intensity (H)

Input Data ...

[Options...]

Figure 3.30: Field settings

Materials

The next steps was the material parts. The material properties of the models was stated. The data was consisted of two parts which is plastic and elastic region. The value of the young modulus and the poisons ratio of the material used was inserted at the elastic parts. While the elastic parts was selected to be loaded by the field section. Figure 3.31 shows the material setting for elastic region.

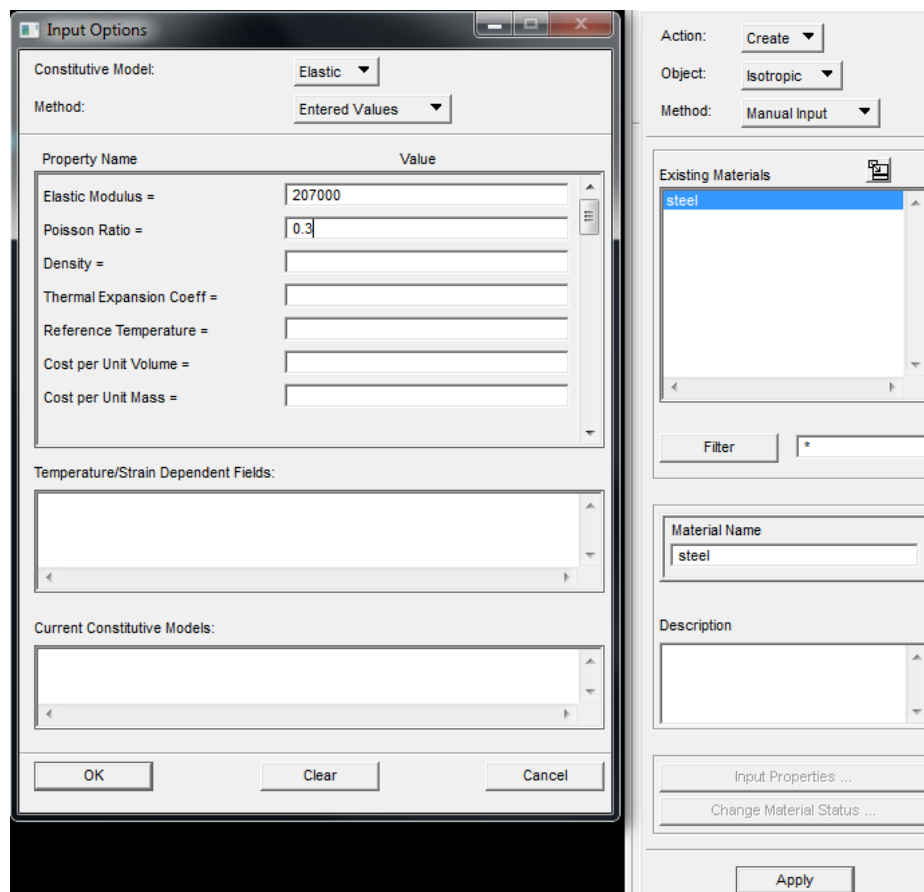


Figure 3.31: Material selection for elastic region

Properties

Before the analysis, the last steps was defining the properties of the models. The properties section was selected and the object part was changed to become a 3D as our project was in the 3 dimensions. Then the name for the properties was named and the reduce integration was selected at the option setting. Then the properties of the models was inserted and the whole models was selected as the application region. Figure 3.32 shows the materials properties setup.

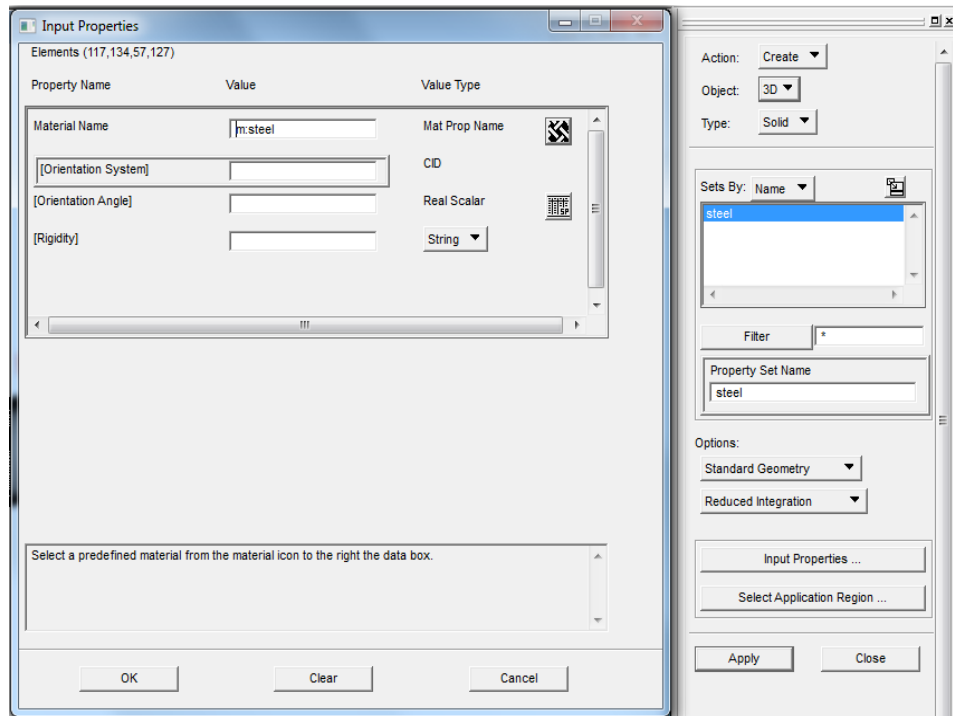


Figure 3.32: Materials properties setup

Analysis

The setting was in entire models and analysis deck for this option. The non-positive define in solver option at job parameter was enabled. At the load step creation, solution parameter was clicked and the follower force was enabled. Then, the Load Increment

Parameter was selected and value of 50 was entered for the step of the output. On the iteration parameter, the residual force was changed to 0.001 to have more accuracy and also better result. Figure 3.33 shows the setting for the analysis setup.

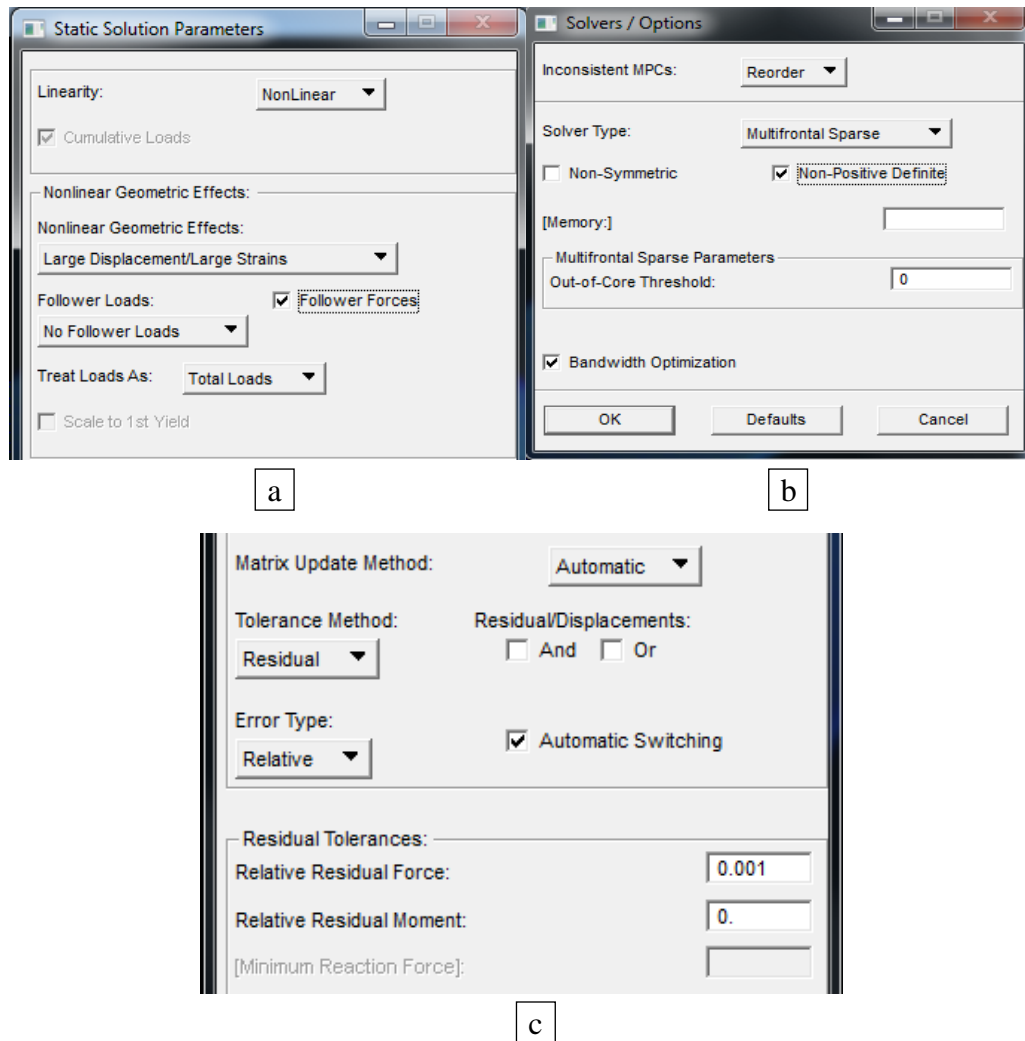
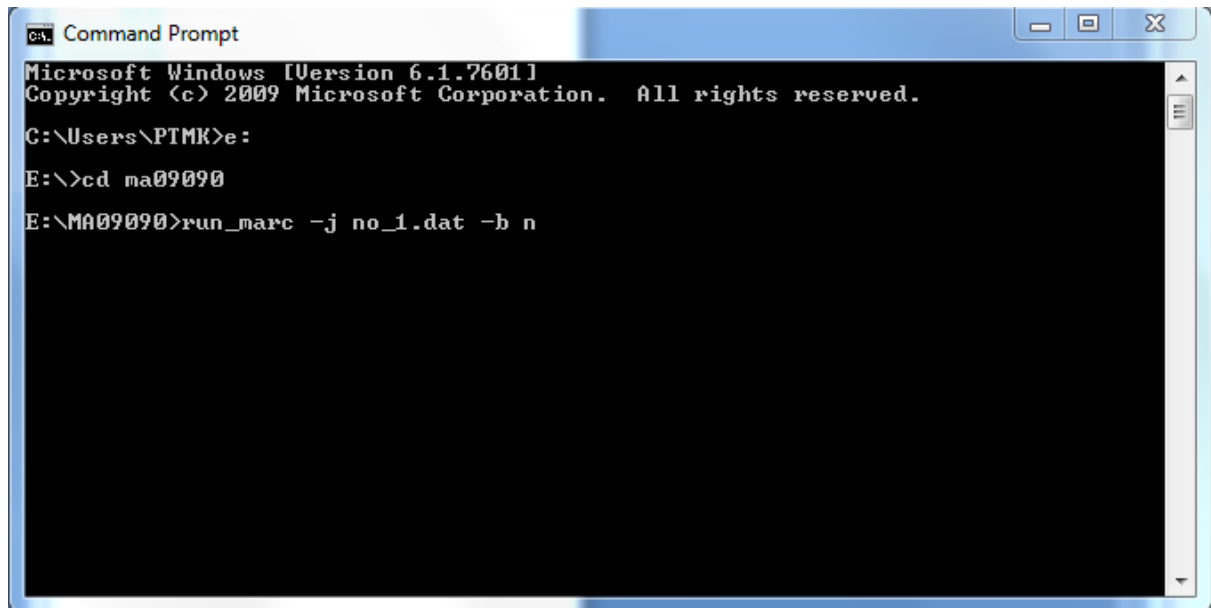


Figure 3.33: Analysis setup a) Follower force, b) Non-positive definite, c) Relative residual force changes.

After all the setup already was done, the analysis part was taken. The apply button was clicked and waited until the analysis can be run. Finally, the analysis using the command prompt, CMD was used. The command was “*run_marc -j filename.dat -b n*”. The command was having no error in the typing. If the file name has a space, so in the

command should replace the space with “_” otherwise there will have an error. Figure 3.34 shows the Command Prompt setup.



```
Microsoft Windows [Version 6.1.7601]
Copyright (c) 2009 Microsoft Corporation. All rights reserved.

C:\Users\PTMK>e:
E:\>cd ma09090
E:\MA09090>run_marc -j no_1.dat -b n
```

Figure 3.34: Command Prompt setup

Result

In order to take and read the result, the result was selected to read and analyze the result after the simulation was completely successful. Firstly, read result was selected then the result file in the analysis part was chose as shown in Figure 3.35. Next, the result icon and quick plot was selected. All result cases and stress global system for fringe result was selected as shown in Figure 3.36. For the deformation result, the displacement and translation was selected then click apply button. For creating the graph data, the x-y plot was selected and the curve data was modified. The option of writing result from the keyboard was selected and the data was saved. The data can be opened in Microsoft excel to make the table or graphical result. Then the result can be taken.

Action:

Object:

Method:

Code:

Type:

Available Jobs

no_12

Job Name

no_12

Job Description

MSC.Marc job created on 21-Mar-13 at 13:15:53

Select Results File...

Translation Parameters...

Apply

Figure 3.35: Result data taken

Action:

Object:

Select Result Cases

Default Static Step, A1:Incr=46,Time=0
 Default Static Step, A1:Incr=47,Time=0
 Default Static Step, A1:Incr=48,Time=0
 Default Static Step, A1:Incr=50,Time=0
 Default Static Step, A1:Incr=52,Time=0
 Default Static Step, A1:Incr=55,Time=0
 Default Static Step, A1:Incr=58,Time=0
 Default Static Step, A1:Incr=61,Time=0
 Default Static Step, A1:Incr=65,Time=1

Select Fringe Result

Force, Nodal External Applied
 Force, Nodal Reaction
 Strain, Total
 Stress, Global System

Quantity:

Select Deformation Result

Displacement, Translation
 Force, Nodal External Applied
 Force, Nodal Reaction

Animate

Apply

Figure 3.36: Quick plot

CHAPTER 4

RESULT AND DISCUSSION

4.1 INTRODUCTION

In this chapter, all the results of the experiment and simulation were presented. The data and results of the experiment and also the finite element analysis will be briefly discussed. For the experimental result, the burst pressure and the interaction between the cracks will be discussed while for the finite element analysis, the stress analysis, displacement, burst pressure and also the interaction between the cracks will be discussed.

The experimental result and finite element analysis result also will be compared to the other assessment method to predict the burst pressure. Though there are various method used for the assessment of the remaining strength of pipe, a few of them only rely on cracks length and depth. Besides, the assessment method is only focused on the single crack. So in the calculation, the length of the crack will become two types which are the summation of both cracks becoming a single crack ($2c_1 + 2c_2$) and the other one is the crack distance between the cracks will be accounted too ($2c_1 + 2c_2 + d$). The analysis will be compared using the method of ASME B31G, Modified B31G and DNV RP-F-101.

4.2 EXPERIMENTAL RESULT

The experimental result is quite important in order to validate the finite element analysis. The expected result is the pipe will be burst up at the cracks area which is the both of the cracks will interact with each other. The maximum pressures were recorded after the pipe burst up. All the result will be discussed briefly.

4.2.1 Burst pressure

The result of the experiment is the burst pressure. This result is taken according to the type of cracks. There are two types of cracks which are both of them have the same crack length, $2c_1 = 2c_2 = 100\text{mm}$. The difference is only at the distance between the cracks which is the first one is $d = 0.5\text{mm}$ and the second one is $d = 2\text{mm}$. The 100mm crack length is used because it will give the lowest burst pressure. So, the experiment will undergo the lowest burst pressure and it will be quite safe and easy. This result will become the minimum benchmark for the burst pressure. Table 4.1 shows the result of the burst pressure of the experiment.

Table 4.1: Burst pressure result from the experiment

Experiment No.	Cracks configuration (mm)			Burst pressure, Pb (MPa)
	$2c_1$	$2c_2$	d	
Experiment 1	100	100	0.5	38.6
Experiment 2	100	100	2.0	40.5

The result of the experiment one and two taken after the pipe was burst up. Then the result of the experiment will be compared to the assessment method which is ASME B31G, Modified B31G and DNV RP-F-101. The comparison was made by taking two cases which is cracks length, L is a summation of both cracks ($2c_1 + 2c_2$) and the other case is L is a summation of both cracks with the distance between the cracks ($2c_1 + 2c_2 + d$). Figure 4.1 shows the cracks configuration and table 4.2 shows the result of the experiment and the assessment method.

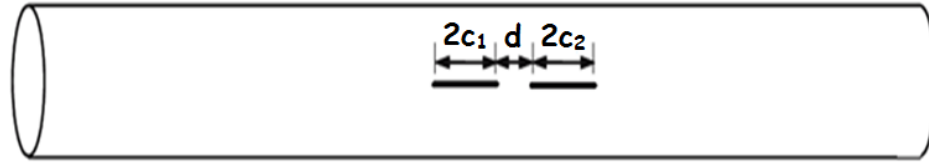


Figure 4.1: Cracks configuration

Table 4.2: Result comparison

Case	Length of cracks, L (mm)	Burst Pressure, P_b (MPa)
Experiment	200.5	38.60
	202	40.50
ASME B31G	200.5	23.71
	202	23.71
Modified ASME B31G	200.5	28.88
	202	28.89
DNV RP-F-101	200.5	35.34
	202	35.36

For the experiment result, the burst pressure for $L = 200.5\text{mm}$ and 202mm is having a larger different compared to the assessment method where the burst pressure is quite the same. This is due to the distance between the cracks, d . For the assessment method, the distance between the cracks, d is neglected and counted as crack itself. Thus, this resulted in the small different of burst pressure. But for the experiment, the distance between the cracks, d is not considered as cracks instead the distance between the cracks is having the metal of the pipe itself. This means that the distance between the cracks is fully metal of the pipe thickness. Thus the burst pressure of the experiment is higher than the assessment method because of the distance between the cracks at the assessment method is acting as cracks while at the experiment, the distance between the cracks have metal that will increase the burst pressure for the experiment.

For the burst pressure with the length of 200.5mm, the experiment result gives the highest burst pressure which is 38.60MPa followed by DNV RP-F-101 assessment method, 35.34MPa. The Modified ASME B31G is the second lowest with 28.88MPa followed by ASME B31G which is 23.71MPa. For the length of 202 mm, the burst pressure of the experiment gives the highest value which is 40.50MPa followed by DNV RP-F-101 with a burst pressure of 35.36MPa. Next is Modified ASME B31G with burst pressure of 28.89MPa and the lowest is ASME B31G which is 23.71MPa. The difference between the assessment methods is because of their formulae in the calculation. For the ASME B31G and modified ASME B31G, their calculation for prediction of burst pressure is more focused on yield strength while for the DNV-RP-F-101 calculation more focused on ultimate tensile strength. Thus the value for the DNV-RP-F-101 is higher than the ASME method due to the different on tensile and yield stress. Figure 4.2 shows the graph of burst pressure for all assessment models and experimental according to the crack length.

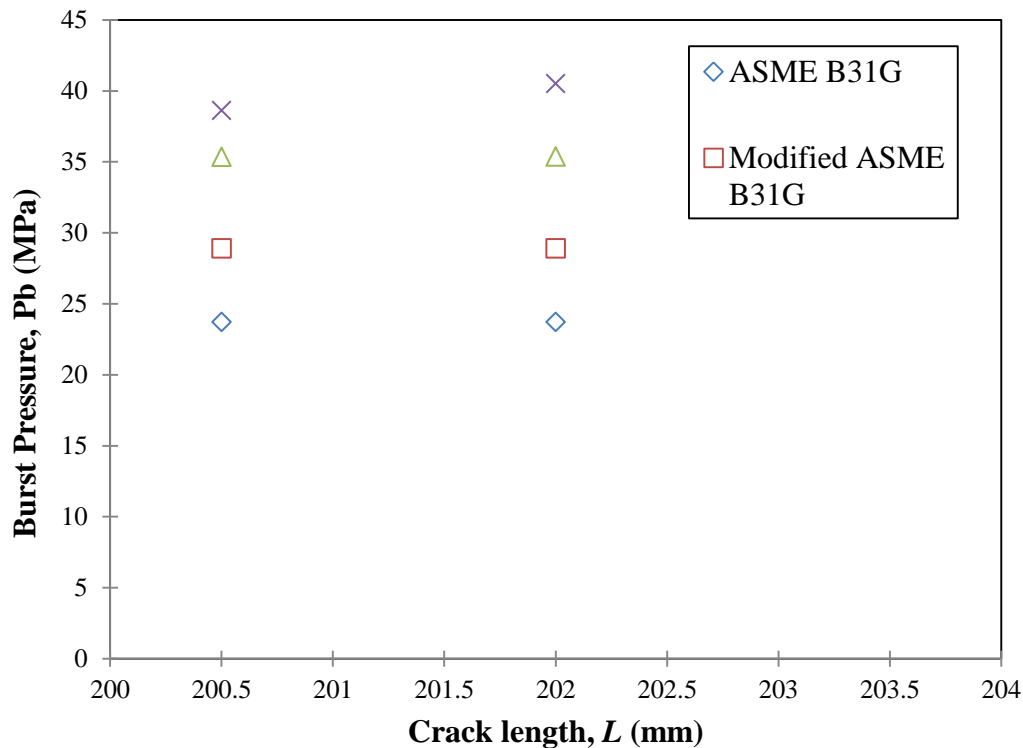


Figure 4.2: Graph of burst pressure against crack length

It can conclude that the distance between the cracks give a small influence to the burst pressure according to the assessment method. Meanwhile, for the experimental result, the distance between the cracks is given quite a huge influence to the burst pressure. Although the calculation is quite far from the experiment, the experiment result is can be considered the best because it consist all the factors such as surrounding factors, pumping flow rate and others. For the calculation, different assessment method to focus on different things such as DNV-RP-F-101 focuses on Ultimate Tensile Stress of the material. As for ASME B31G and Modified ASME B31G, both of them more focus on crack length and yield strength only. But, all of the assessment is only valid for single crack. Thus the multiple aligned cracks can be assumed as one single crack [4].

4.2.2 Cracks Behavior

In this experiment, the behavior of the multiple aligned cracks will be discussed. The pipe will be constantly pumped with hydraulic oil until the pipe burst up. The maximum pressure where the pipe burst is considered the burst pressure. Since the pipe was burst up, the cracks parts of the pipe must be opened. Figure 4.3 shows the cracks area of the pipe after the burst test.



Figure 4.3: Crack part of the pipe after burst test

According to the figure 4.3 where the crack length of 100mm and the distance between the cracks is 0.5mm, at a pressure just before 38.60MPa, both cracks are combining with each other. After the pipe burst, the crack area will bulge or also known as knob. Figure 4.4 shows the characteristic of bulging or knob. Most of the pipes that have the internal pressure will have this kind of defect. The bulging or knob usually occurs in the area of the pipe with the lowest strength. From the experiment, the bulging or knob only occurs in the cracks area.

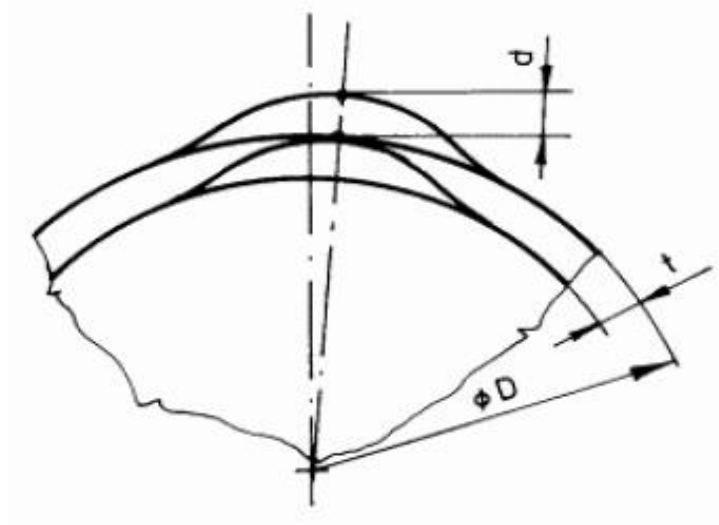


Figure 4.4: Bulging or Knob defect [9]

4.2.3 Cracks Interaction

When the pipe burst up, the crack will be opened at the highest pressure. Some of the phenomena that occur when the cracks opened during the burst process are the interaction between the cracks. The interaction between cracks means that the both of the cracks will interact with each other. These processes are assumed to occur when the pressure is exceeding the yield stress of the pipe. Since the yield stress is the maximum point of the elastic region, the pipe cannot hold the pressure anymore. Thus the pipe will have the defect at the lowest strength area which is in the cracks area.

The depth of the cracks will make the crack become larger. The distance between the cracks will receive higher pressure and stress at the both tips of the cracks. Thus, the cracks will propagate slowly at both tips of the cracks as the pressure increased. When the both side cracks interact, the pipe will be burst up due to the least strength to hold the pressure. Figure 4.5 shows the cracks interaction.

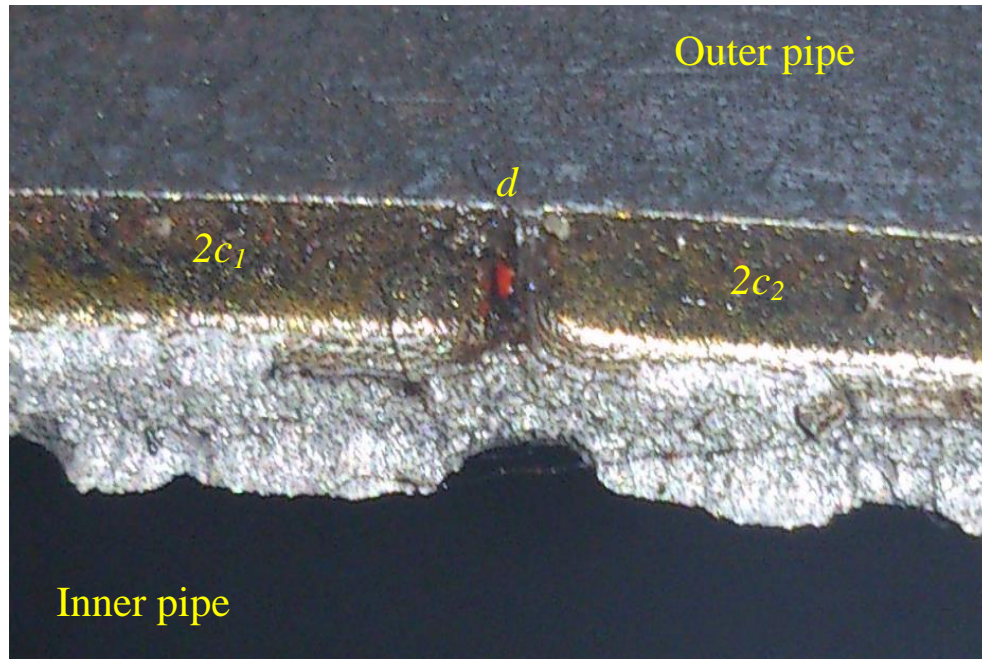


Figure 4.5: Crack interaction.

4.3 FINITE ELEMENT ANALYSIS (FEA) RESULT

The result of Finite Element Analysis (FEA) mainly used to predict the result in the case of the experiment cannot be done. It also used to simplify the working process and reduce the time and cost.

The purpose of the simulation is to research the area of those cannot be done by experiment such as the level of stress according to the pressure. Since it cannot be done by experiment, the simulation will be used to obtain the data. In this simulation, the burst pressure for each of the cases will be determined. Then all the burst pressure will be compared to the assessment method. The stress distribution also will be determined at this chapter and last but not least, the displacement at the distance between the cracks will be analyzed. All of this result will be discussed briefly and scientifically.

4.3.1 Burst pressure

There are 20 simulations that have been simulated using the MSC Marc Patran 2008r1. The data is on the table 4.3. The simulation is arranged according to the cases.

All the simulation has been done and the result obtained is the burst pressure based on the ultimate tensile stress. The data were obtained when the stress on the pipe is completely over the ultimate tensile stress which is 466MPa. The method to determine the value of the stress is by using the average. The area for the data taken is at the distance between the cracks, d . All the stress value in each of nodes along the distance between the cracks will be recorded and then all the data will be divided into how many nodes to get the average. The purpose of take the average result is to get the ideal stress at the point.

Table 4.3: Simulation result

Simulation	defect size (mm)			Burst pressure, P_b (MPa)
	$2c_1$	$2c_2$	d	
Case 1	25	25	0.5	27.3
Case 2	25	25	2.0	41.9
Case 3	25	50	0.5	26.7
Case 4	25	50	2.0	41.3
Case 5	25	75	0.5	26.4
Case 6	25	75	2.0	40.9
Case 7	25	100	0.5	25.2
Case 8	25	100	2.0	40.3
Case 9	50	50	0.5	26.2
Case 10	50	50	2.0	40.7
Case 11	50	75	0.5	25.3
Case 12	50	75	2.0	40.2
Case 13	50	100	0.5	23.8
Case 14	50	100	2.0	39.7
Case 15	75	75	0.5	24.5
Case 16	75	75	2.0	39.6
Case 17	75	100	0.5	22.4
Case 18	75	100	2.0	39.2
Case 19	100	100	0.5	22.1
Case 20	100	100	2.0	38.5

4.3.2 Comparison of burst pressure based on crack length at $d = 0.5\text{mm}$

The result and analysis of burst pressure in case of the crack at $d = 0.5\text{mm}$ is presented. Figure 4.6 shows the comparison of burst pressure and the crack lengths based on the distance between the cracks.

For the crack length of $2c_1 = 25\text{mm}$, the maximum burst pressure is 27.3MPa where the crack length of $2c_1$ and $2c_2$ is equal to 25mm. The minimum burst pressure is 25.2MPa which is at the length of $2c_1$ and $2c_2$ is 25mm and 100mm respectively. For the crack length of $2c_1 = 50\text{mm}$, the maximum burst pressure is 26.7MPa where the crack length of $2c_1$ and $2c_2$ is 50mm and 25mm respectively. The minimum burst pressure is 23.8MPa which is at the length of $2c_1$ and $2c_2$ is 50 mm and 100 mm respectively.

For the crack length of $2c_1 = 75\text{mm}$, the maximum burst pressure is 26.4MPa where the crack length of $2c_1$ and $2c_2$ is 75mm and 25mm respectively. The minimum burst pressure is 22.4MPa which is at the length of $2c_1$ and $2c_2$ is 75mm and 100mm respectively. For the crack length of $2c_1 = 100\text{mm}$, the maximum burst pressure is 25.2MPa where the crack length of $2c_1$ and $2c_2$ is 100mm and 25mm respectively. The minimum burst pressure is 22.1MPa which is at the length of $2c_1$ and $2c_2$ is 100mm and 100mm respectively.

It shows that the crack length of 25mm is having the higher burst pressure than the other length. The length of 100mm having the lowest burst pressure. The burst pressure decrease as the length of crack increased. Therefore, the comparison of those cases shows that the smaller combination of $2c_1$ and $2c_2$, the higher value of burst pressure. It is the opposite where for the lowest burst pressure is taken at the higher combination of $2c_1$ and $2c_2$.

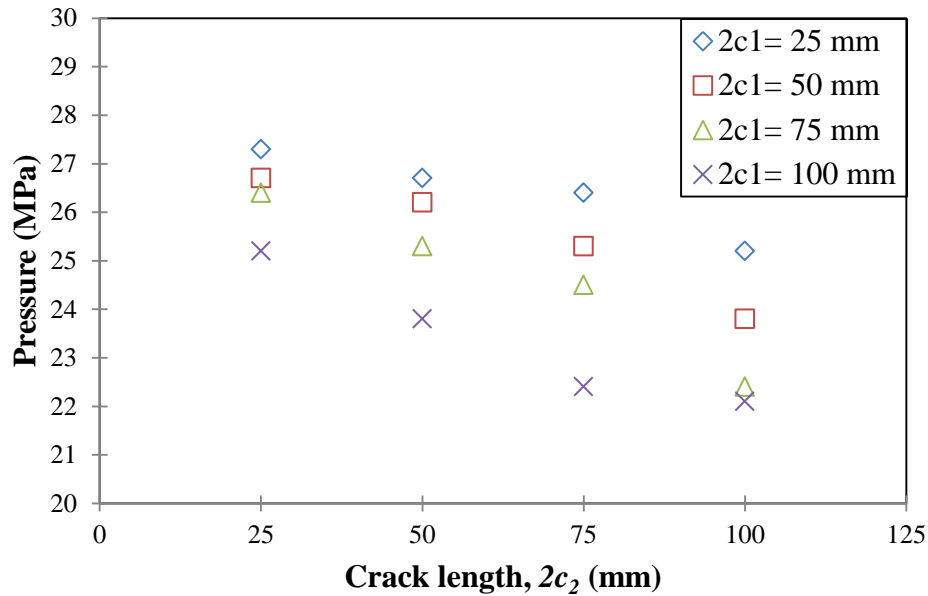


Figure 4.6: Comparison graph of burst pressure versus crack length, $2c_2$ for all value of crack length of $2c_1$

4.3.3 Comparison of burst pressure based on the crack length at $d = 2.0$ mm

The result and analysis of burst pressure in case of the crack at $d = 2.0$ mm is presented. Figure 4.7 shows the comparison of burst pressure and the crack lengths based on the distance between the cracks.

For the crack length of $2c_1 = 25$ mm, the maximum burst pressure is 41.9MPa where the crack length of $2c_1$ and $2c_2$ is equal to 25mm. The minimum burst pressure is 40.3MPa which is at the length of $2c_1$ and $2c_2$ is 25mm and 100mm respectively. For the crack length of $2c_1 = 50$ mm, the maximum burst pressure is 41.3MPa where the crack length of $2c_1$ and $2c_2$ is 50mm and 25mm respectively. The minimum burst pressure is 39.7MPa which is at the length of $2c_1$ and $2c_2$ is 50mm and 100mm respectively.

For the crack length of $2c_1 = 75\text{mm}$, the maximum burst pressure is 40.9MPa where the crack length of $2c_1$ and $2c_2$ is 75mm and 25mm respectively. The minimum burst pressure is 39.2MPa which is at the length of $2c_1$ and $2c_2$ is 75mm and 100mm respectively. For the crack length of $2c_1 = 100\text{mm}$, the maximum burst pressure is 40.3MPa where the crack length of $2c_1$ and $2c_2$ is 100mm and 25mm respectively. The minimum burst pressure is 38.5MPa which is at the length of $2c_1$ and $2c_2$ is 100mm respectively.

It shows that the crack length of 25mm is having the higher burst pressure than the other length. The length of 100mm having the lowest burst pressure. The burst pressure decrease as the crack length increased. Hence, the comparison of all the cases shows that the smaller combination of $2c_1$ and $2c_2$, the higher value of burst pressure. It is the opposite where for the lowest burst pressure is taken at the higher combination of $2c_1$ and $2c_2$.

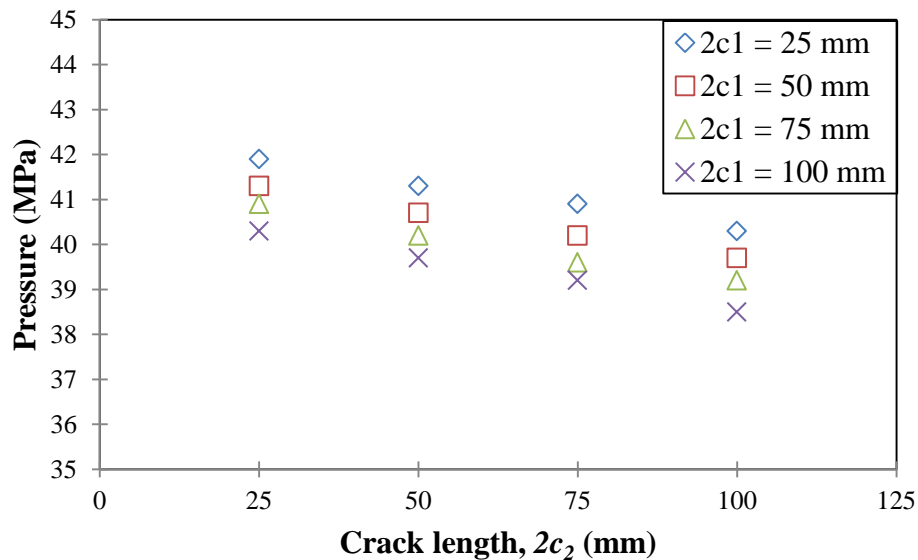


Figure 4.7: Comparison graph of burst pressure versus crack length, $2c_2$ for all value of crack length of $2c_1$

4.3.4 Comparison of burst pressure based on the distance between the cracks

The result and analysis of burst pressure for the case of the distance between the cracks, is presented. For the result of burst pressure based on crack length of $2c_1$, the result is summarized in figure 4.8 to 4.11.

Based on the figure 4.8, the graph shows the burst pressure according to the distance between the crack at the crack length $2c_1 = 25$ mm. Results show that for $d = 0.5$ mm, the burst pressure of 27.3MPa is highest in the combination of $2c_1$ and $2c_2$, which is 25mm each. While for the $d = 2.0$ mm, the highest burst pressure is 41.9MPa at the same point. For the minimum burst pressure, at the $d = 0.5$ mm gives about 25.2MPa and $d = 2.0$ mm burst pressure is 40.3MPa. All of them are at the same point which is $2c_1$ and $2c_2 = 25$ mm and 100mm respectively.

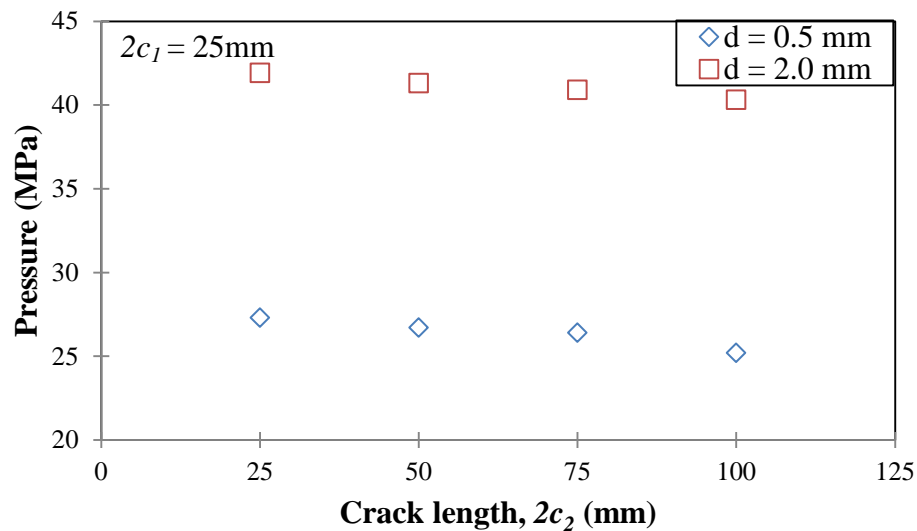


Figure 4.8: Graph of burst pressure according to the distance between the cracks at $2c_1 = 25$ mm

From the figure 4.9, the graph shows the burst pressure according to the distance between the crack at the crack length $2c_1 = 50\text{mm}$. Results show that at the $d = 0.5\text{mm}$, the burst pressure of 26.7MPa is the highest at $2c_1$ and $2c_2$ equal to 50mm and 25mm each. While for the $d = 2.0\text{mm}$, the highest burst pressure is 41.3MPa at the same point. For the minimum burst pressure, at the $d = 0.5\text{mm}$ gives about 25.2MPa and $d = 2.0\text{mm}$ burst pressure is 40.3MPa . All of them are at the same point which is $2c_1$ and $2c_2 = 50\text{mm}$ and 100 mm respectively.

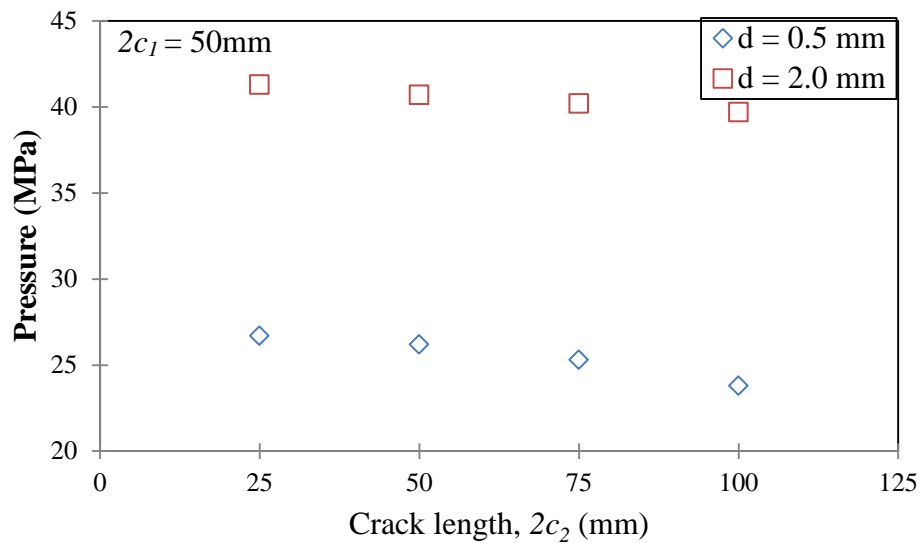


Figure 4.9: Graph of burst pressure according to the distance between the cracks at $2c_1 = 50\text{ mm}$

Based on the figure 4.10, the graph shows the burst pressure according to the distance between the crack at the crack length $2c_1 = 75\text{mm}$. Results show that at the $d = 0.5\text{mm}$, the burst pressure of 26.4MPa is the highest at $2c_1$ and $2c_2$, which are 75mm and 25mm each. While for the $d = 2.0\text{mm}$, the highest burst pressure is 40.9MPa at the same point. For the minimum burst pressure, at the $d = 0.5\text{mm}$ gives about 22.4MPa and $d = 2.0\text{mm}$ burst pressure is 39.2MPa . All of them are at the same point which is $2c_1$ and $2c_2 = 75\text{mm}$ and 100mm respectively.

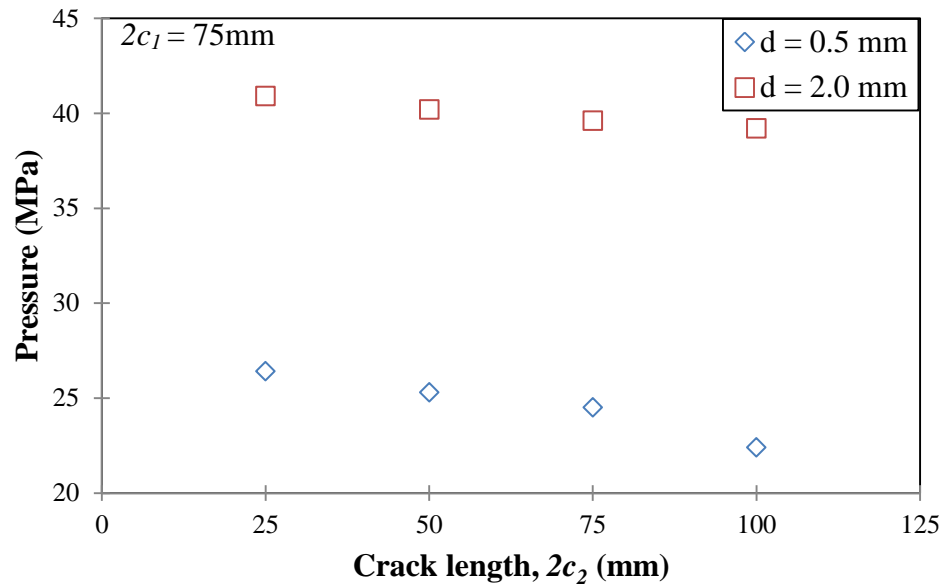


Figure 4.10: Graph of burst pressure according to the distance between the cracks at $2c_1 = 75$ mm

Based on the figure 4.11, the graph shows the burst pressure according to the distance between the crack at the crack length $2c_1 = 100$ mm. Result show that at the $d = 0.5$ mm, the burst pressure of 25.2MPa is the highest at $2c_1$ and $2c_2$, which are 100mm and 25 mm each. While for the $d = 2.0$ mm, the highest burst pressure is 40.3MPa at the same point. For the minimum burst pressure, at the $d = 0.5$ mm gives about 22.1MPa and $d = 2.0$ mm burst pressure is 38.5MPa. All of them are at the same point which is $2c_1$ and $2c_2 = 100$ mm and 100mm respectively.

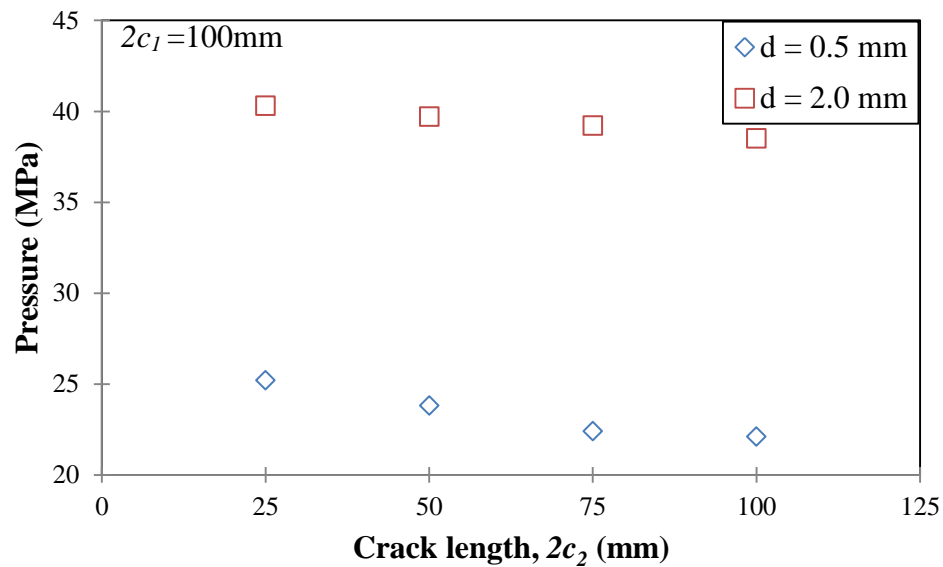


Figure 4.11: Graph of burst pressure according to the distance between the cracks at $2c_1 = 100\text{mm}$

From the graph 4.8 to 4.11, it can conclude that the larger the distance between the cracks, d , the higher burst pressure regarding to the crack length. The smaller crack length with long distance between the cracks will result in higher burst pressure.

4.3.5 Comparison of burst pressure between assessment method and Finite Element analysis of different distance between cracks, $d = 0.5\text{mm}$

There are three major assessment methods that have been used in the comparison for this research which is ASME B31G, Modified ASME B31G and DNV-RP-F-101. The combination of $2c_1 + 2c_2 + d$ will be selected as one single crack. Hence, there are 10 cracks length for $d = 0.5$ and 2mm.

The result and analysis of burst pressure for assessment methods and Finite Element analysis with different distance between the cracks is presented. For the result of burst pressure of assessment method and finite element analysis, the result is summarized in

figure 4.12. Table 4.4 shows the result of burst pressure for both assessment method and the finite element analysis.

Table 4.4: Burst pressure for assessment method and finite element analysis for $d = 0.5\text{mm}$

$2c_1$ (mm)	$2c_2$ (mm)	d (mm)	L (mm)	ASME B31G (MPa)	Modified ASME B31G (MPa)	DNV-RP-F- 101 (MPa)	FEA (MPa)
25	25	0.5	50.5	33.5	28.9	43.4	27.3
25	50	0.5	75.5	23.7	28.7	39.8	26.7
25	75	0.5	100.5	23.7	28.4	38.0	26.4
25	100	0.5	125.5	23.7	28.0	36.9	25.2
50	50	0.5	100.5	23.7	28.4	38.0	26.2
50	75	0.5	125.5	23.7	28.0	36.9	25.3
50	100	0.5	150.5	23.7	27.8	36.2	23.8
75	75	0.5	150.5	23.7	27.8	36.2	24.5
75	100	0.5	175.5	23.7	27.2	35.7	22.4
100	100	0.5	200.5	23.7	25.9	35.4	22.1

The value of the assessment method is calculated based on the L value of the cases. After that, the data will be compared to the finite element analysis. The data for the finite element analysis is taken from the simulation before.

For the assessment method of ASME B31G, the maximum pressure is at the length of 50.5mm which is 33.5MPa while all the remaining length is at the same pressure which is 23.7MPa. This is because for the crack length of lower than 70mm with a fixed outer diameter of 60.5mm and thickness of 4mm will result in different equation for determining the burst pressure. In this case, the length of the crack is 50.5mm, so it will use the different formulae from the crack length of 75.5mm and above. The Modified ASME B31G is quite different from the others. The maximum pressure is at the shortest crack which is 50.5mm with the pressure of 28.9MPa. The minimum pressure is at the longest crack which is

200.5mm with pressure of 25.9MPa. The reading is quite different than the other assessment because of the formulae used for Modified ASME B31G is fixed to the same crack length. This assessment method can be used to determine the burst pressure for the difference of depth of the cracks. Thus, this assessment method is not suitable for determining the burst pressure based on the different crack length.

For the assessment method of DNV-RP-F-101, the maximum pressure is at the length of 50.5mm which is 43.4MPa. While for the minimum pressure is at the length of 200.5mm which is 35.36MPa. The burst pressure is decreasing as the crack length is increasing. This assessment method is given the highest burst pressure as the DNV-RP-F-101 method focuses on the ultimate tensile test of the material. Lastly, for the FEA analysis, the maximum pressure is at the length of 50.5mm which is 27.3MPa. While for the minimum pressure is at the length of 200.5mm which is 22.1MPa. There are some differences from the assessment method where for the analysis, there are metal in the distance between the cracks while for the assessment method is neglecting the metal at the distance between the cracks.

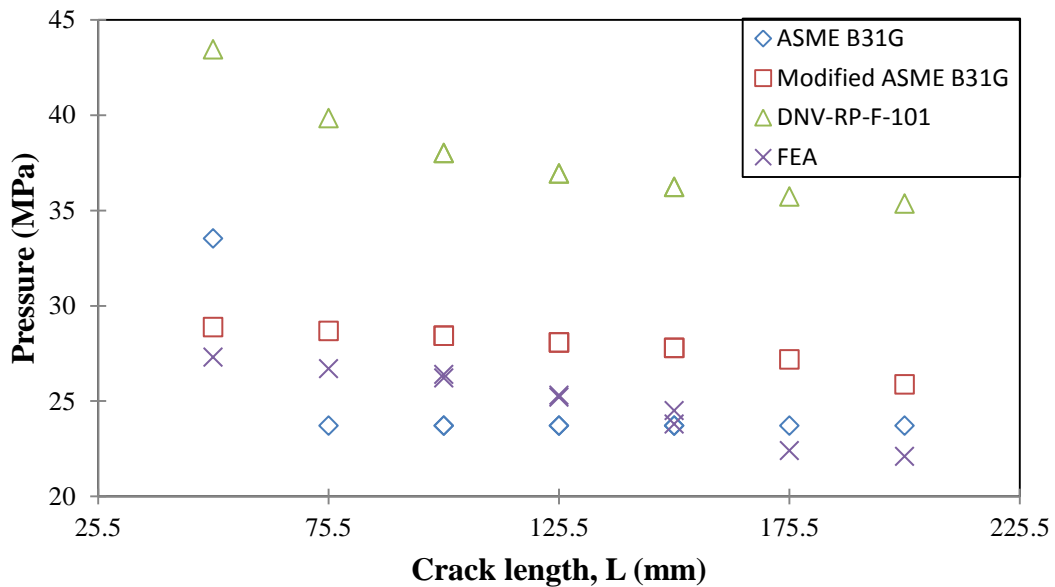


Figure 4.12: Graph of comparison for assessment method and FEA for burst pressure

It can conclude that the longer crack length will result in the lower burst pressure. The FEA result gives the lowest pressure at the longest crack length while the assessment method of DNV-RP-F-101 gives the high pressure at the smallest crack length. It is small differences in the assessment method of Modified ASME B31G where the result of burst pressure is increasing as the length of crack increase.

4.3.6 Comparison of burst pressure between assessment method and Finite Element analysis of different distance between cracks, $d = 2.0$ mm.

The result and analysis of burst pressure for assessment methods and Finite Element analysis with different distance between the cracks is presented. For the result of burst pressure of assessment method and finite element analysis, the result is summarized in figure 4.13.

Table 4.5: Burst pressure for assessment method and finite element analysis for $d = 2.0$ mm

$2c_1$ (mm)	$2c_2$ (mm)	d (mm)	L (mm)	ASME B31G (MPa)	Modified ASME B31G (MPa)	DNV-RP-F- 101 (MPa)	FEA (MPa)
25	25	2.0	52.0	33.5	28.9	43.1	41.9
25	50	2.0	77.0	23.7	28.7	39.7	41.3
25	75	2.0	102.0	23.7	28.4	37.9	40.9
25	100	2.0	127.0	23.7	28.1	36.9	40.3
50	50	2.0	102.0	23.7	28.4	37.9	40.7
50	75	2.0	127.0	23.7	28.1	36.9	40.2
50	100	2.0	152.0	23.7	27.8	36.2	39.7
75	75	2.0	152.0	23.7	27.8	36.2	39.6
75	100	2.0	177.0	23.7	27.2	35.7	39.2
100	100	2.0	202.0	23.7	26.0	35.3	38.5

The value of the assessment method is calculated based on the L value of the cases. After that, the data will be compared to the finite element analysis. The data for the finite element analysis is taken from the simulation before.

For the assessment method of ASME B31G, the maximum pressure is at the length of 52mm which is 33.5MPa while all the remaining length is at the same pressure which is 23.7MPa. This is because for the crack length of lower than 70mm with a fixed outer diameter of 60.5mm and thickness of 4mm will result in different equation for determining the burst pressure. In this case, the length of the crack is 52mm, so it will use the different formulae from the crack length of 77mm and above. The Modified ASME B31G is quite different from the others. The maximum pressure is at the shortest crack which is 52mm with the pressure of 28.9MPa. The minimum pressure is at the longest crack which is 202mm with pressure of 26MPa. The reading is quite different than the other assessment because of the formulae used for Modified ASME B31G is fixed to the same crack length. This assessment method can be used to determine the burst pressure for the difference of depth of the cracks. Thus, this assessment method is not suitable for determining the burst pressure based on the different crack length.

For the assessment method of DNV-RP-F-101, the maximum pressure is at the length of 52mm which is 43.1MPa. While for the minimum pressure is at the length of 202mm which is 35.3MPa. The burst pressure is decreasing as the crack length is increasing. This assessment method is given the highest burst pressure as the DNV-RP-F-101 method focuses on the ultimate tensile test of the material. Lastly, for the FEA analysis, the maximum pressure is at the length of 52mm which is 41.9MPa. While for the minimum pressure is at the length of 202mm which is 38.5MPa. There are some differences from the assessment method where for the analysis, there are metal in the distance between the cracks while for the assessment method is neglecting the metal at the distance between the cracks.

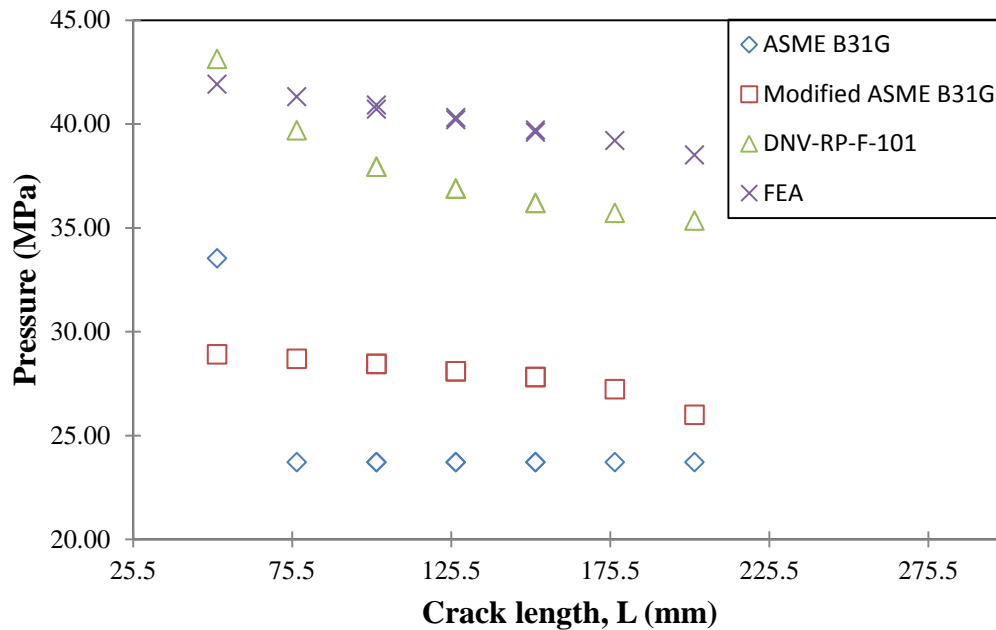


Figure 4.13: Graph of comparison between the assessment method and FEA for burst pressure

From the figure above, the longer the length of crack resulted in the lower burst pressure. The lowest pressure recorded by ASME B31G with 23.7MPa while the high pressure is DNV-RP-F-101 with 43.1MPa. The readings for DNV-RP-F-101 and FEA are the most similar. So, the DNV-RP-F-101 can be stated to be the most accurate assessment method.

4.3.7 Comparison of burst pressure of assessment method based on the distance between the cracks

The result of the burst pressure based on the distance between the cracks according to the analysis method is presented. The analysis includes the assessment method, ASME B31G, Modified ASME B31G, DNV-RP-F-101 and also Finite Element Analysis.

From the figure 4.14, the result of the assessment method of ASME B31G is the same for both distances between the cracks which is 0.5mm and 2.0mm. The highest pressure is at the distance of crack lowest than the others which is 33.5MPa. While the other distance has the same burst pressure of 23.7MPa. This is because the assessment method of ASME B31G is using the similar equations for both conditions.

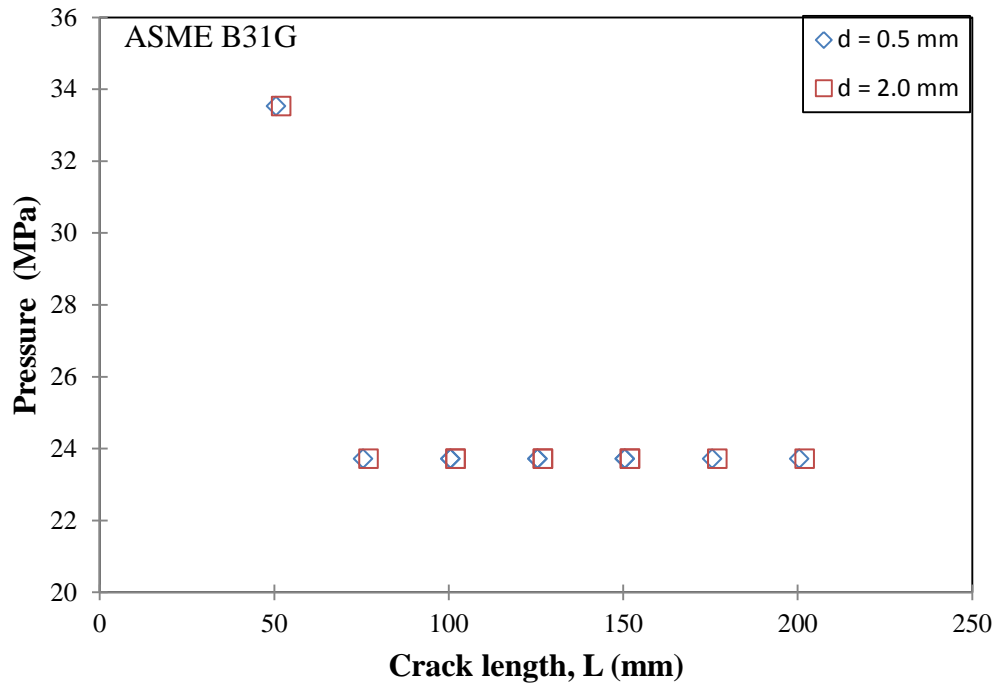


Figure 4.14: Graph of burst pressure for ASME B31G according to the distance between cracks

From figure 4.15, it clearly shows that the result for burst pressure is almost the same for both cases, $d = 0.5\text{mm}$ and 2.0mm . There are only slightly different of the burst pressure between $d = 0.5\text{mm}$ and 2.0mm which is about 0.1MPa . The burst pressure for the $d = 2.0\text{mm}$ is higher than the burst pressure of $d = 0.5\text{mm}$. The graph is different than the others because of the calculation used by Modified ASME B31G is valid for the depth of the cracks only.

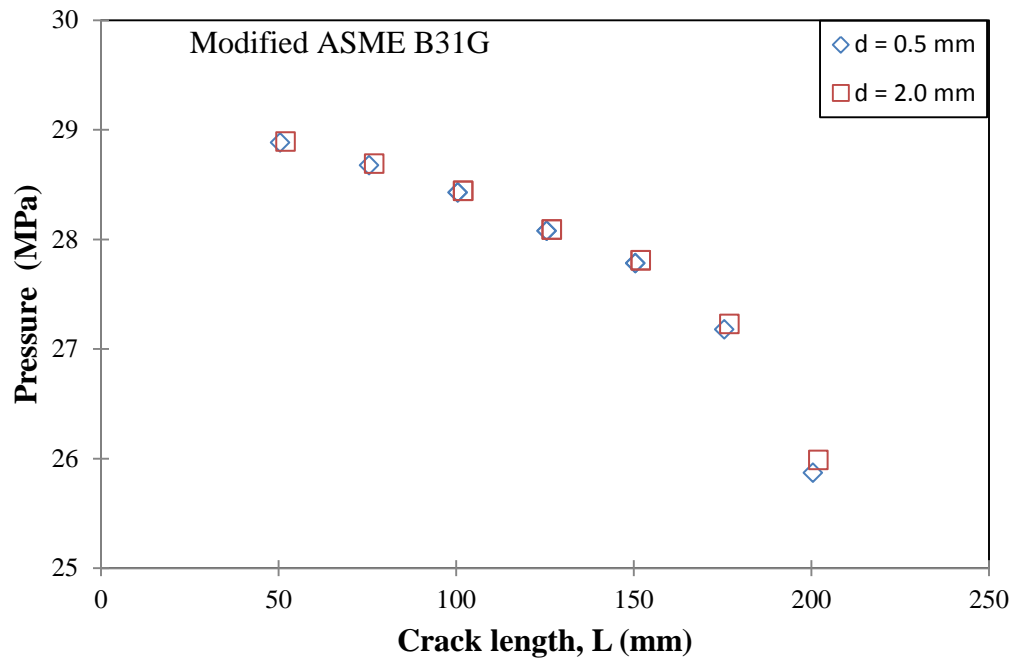


Figure 4.15: Graph of burst pressure for Modified ASME B31G according to the distance between cracks

From figure 4.16, it clearly shows that the result for burst pressure is almost the same for the $d = 0.5\text{mm}$ and 2.0mm . The burst pressure for both cases will decrease as the crack length is increasing. The burst pressure at $d = 0.5\text{mm}$ is higher than the $d = 2.0\text{mm}$ by almost 0.3MPa at each crack length. There is about 7% different from burst pressure at each crack length.

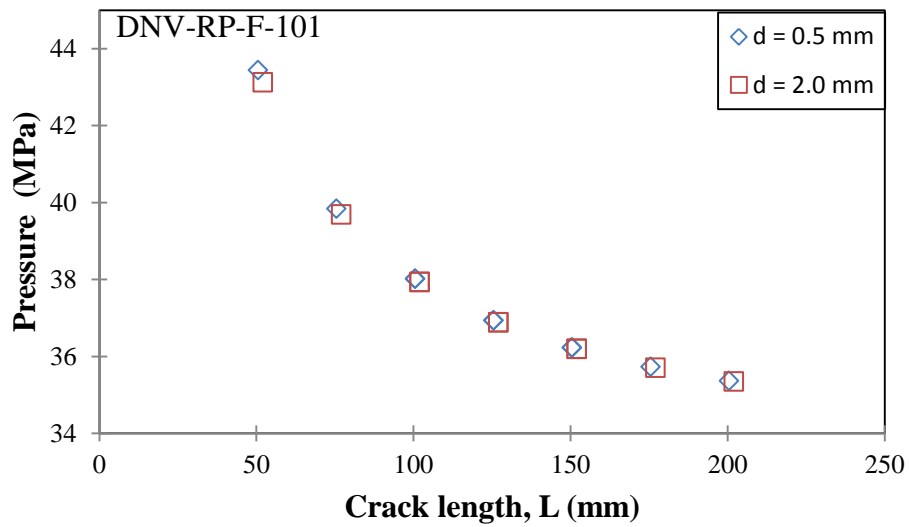


Figure 4.16: Graph of burst pressure for DNV-RP-F-101 according to the distance between cracks

From figure 4.17, the burst pressure for the FEA is different from the other assessment method. The burst pressure is higher in the distance between the cracks, d is 2.0mm compared to the $d = 0.5$ mm.

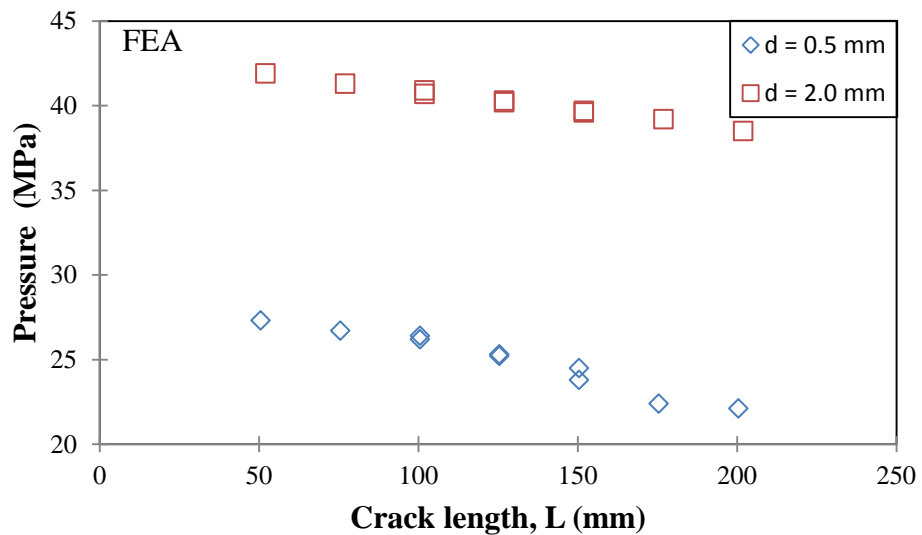


Figure 4.17: Graph of burst pressure for FEA according to the distance between cracks

The difference between the assessment method and the FEA is because of the distance between the cracks. In the assessment method, the calculation is not involving the distance between the cracks. Thus the distance between the cracks is being assumed as single cracks. So that's why the burst pressure of the assessment method is quite the same between the $d = 0.5\text{mm}$ and $d = 2.0\text{mm}$. For the FEA burst pressure, it shows quite big differences between $d = 0.5\text{mm}$ and 2.0mm because of the distance between the cracks, d is not a crack. In the finite element simulation, the distance between the cracks is stated as fully metal. So, the longer distance between the cracks means longer metal between the cracks. That is why the burst pressure for the $d = 0.5\text{mm}$ is lower than the burst pressure for $d = 2.0\text{mm}$.

From all the comparison of burst pressure with the assessment method and FEA result, with the different distance between the cracks and also different length of cracks, it can show that the basically the result for FEA is higher as compared to the other codes which is ASME B31G, Modified ASME B31G and DNV-RP-F-101. This is due to the analysis is stopped when the strain has reached the fracture strain.

The DNV-RP-F101 methods were developed to be mean fits to the experimental and numerical data, and so should be the most accurate methods. The modified B31G method is more accurate than the original ASME B31G method. The methods of DNV-RPF101 were developed and validated through tests on modern, high toughness, line pipe steels. As the development of the DNV-RP-F-101 is more specified, this method is more accurate to predict the burst pressure.

4.3.8 Displacement at the distance between the cracks

The result for comparison of burst pressure between the displacement and the distance between the cracks with a length of cracks is presented. The data taken at the burst pressure for all distances between the cracks and then the displacement at the distance between the cracks will be determined. For the result of displacement result taken in the case 1 which is $2c_1$ and $2c_2$ is 25mm and 50mm. The data also taken for the longest length

of cracks which is $2c_1$ and $2c_2$ is 75mm and 100mm. The data were taken at the shortest and the longest combination of crack length to differentiate the effect of crack length towards the behavior of the displacement.

The result of burst pressure fir displacement and the distance between the cracks is presented. The data is at the $d = 0.5\text{mm}$ and the length is taken at the shortest and the longest cracks length, which is case 1 and case 17. Figure 4.18 is the displacement comparison for both cases.

From the figure 4.18, the graph shows the behavior of the displacement according to the crack length. The highest displacement for case 1 is on the left side which is 0.0077mm while the lowest is on the right side which is 0.0059mm. In case 17, the highest displacement is on the left side which is 0.0074mm and the lowest displacement is on the right side which is 0.0069mm. The behavior of the displacement is higher on the right side.

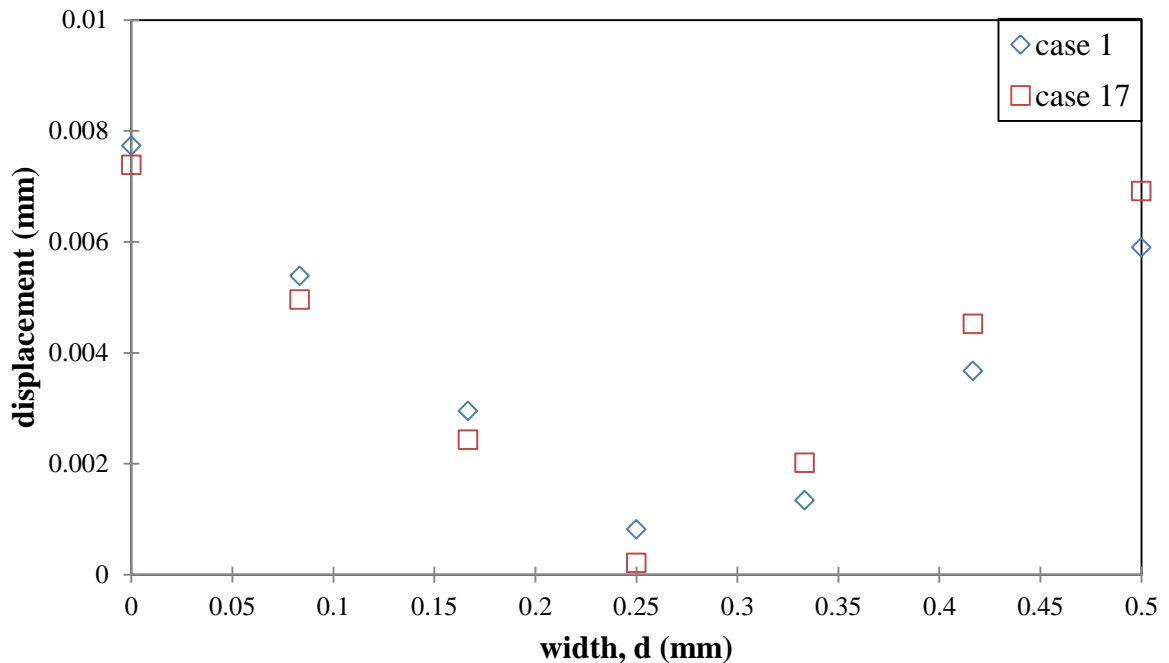


Figure 4.18: Comparison of the displacement by the different combination crack length

From the graph above, it clearly shows that the value of the left side is higher than the right side. This is because the crack on the left side is the longest crack. In case 1 which is 25mm times 50mm, the 50mm is on the left side while the 25mm is on the right side. So the displacement is higher on the left side which is the more crack length. It is the same with the case 17 where 75mm times 100mm. The 100mm is on the left side while the 75mm is on the right side. So the result of displacement is higher on the left side which is situated the longer crack length. It can conclude that the displacement is occurring more on the side which is longer crack length.

The displacement result has been calculated based on the burst pressure. The result will be compared to the actual distance between the cracks to find the percentage of displacement at the burst pressure.

Percentage different calculation:

$$(\sum \text{of displacement} / \text{actual distance between the cracks}) \times 100\%$$

Case 1:

$$= (0.027804/0.5) \times 100 \%$$

$$= 5.560875 \%, \text{ percentage of displacement}$$

$$100 - 5.560875 = 94.43913 \%, \text{ percentage of distance left after the displacement}$$

Case 17:

$$= (0.028442/0.5) \times 100\%$$

$$= 5.688349\%, \text{ percentage of displacement}$$

$$100 - 5.688349 = 94.31165 \%, \text{ percentage of distance left after the displacement}$$

Hence, for case 1:

$$\text{Percentage of displacement} = 5.560875 \%$$

$$\text{Percentage of remaining distance} = 94.43913 \%$$

For case 17:

$$\text{Percentage of displacement} = 5.688349 \%$$

$$\text{Percentage of remaining distance} = 94.31165 \%$$

From the figure 4.19, the result of the displacement for both crack length is quite the same which is about 5 % of displacement. It can tell that the displacement is not dealt a huge influence to the burst pressure. This is because the data are taken at the burst pressure of the pipe but the displacement is only 5 % of the distance between the cracks. This tells that the pipe still burst up when the burst pressure is reached even the displacement of the distance between the cracks is not completely covered to whole distance.

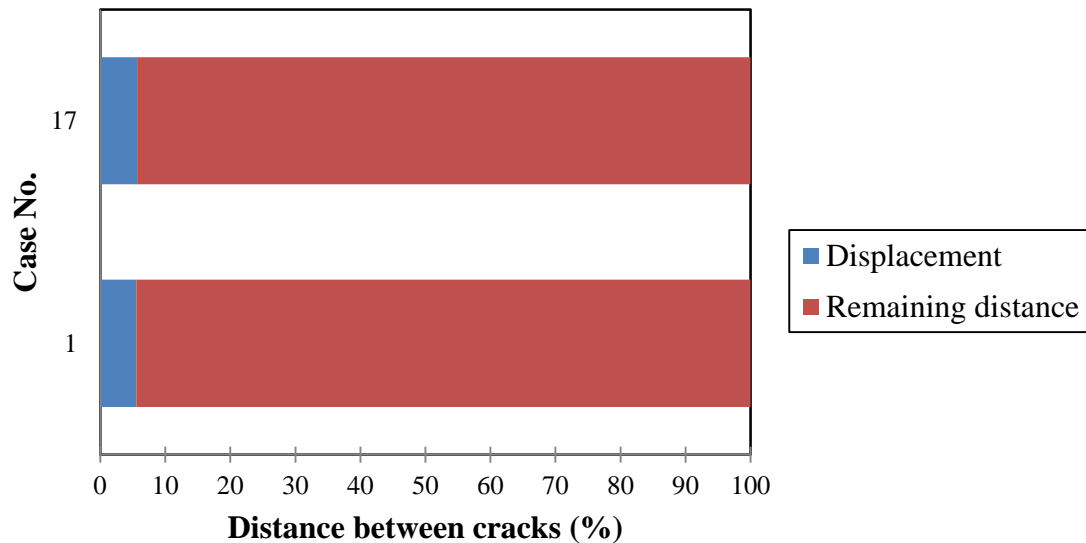


Figure 4.19: Chart for the percentage of displacement and remaining distance

From the whole result and discussion, mostly all the results show that the burst pressure is more affected by the length of the crack and also the longest combination of the cracks. The distance between the cracks does not really affect the burst pressure. It only gives a small increase in the burst pressure. For the displacement, as the same crack length is compared, the displacement is occurring with the same value. But for the different combination of crack length, the displacement is occurring more at the crack with the longer length. Although, the displacement is also not give the huge effect of the burst pressure.

4.3.9 Stress distribution at the distance between the cracks

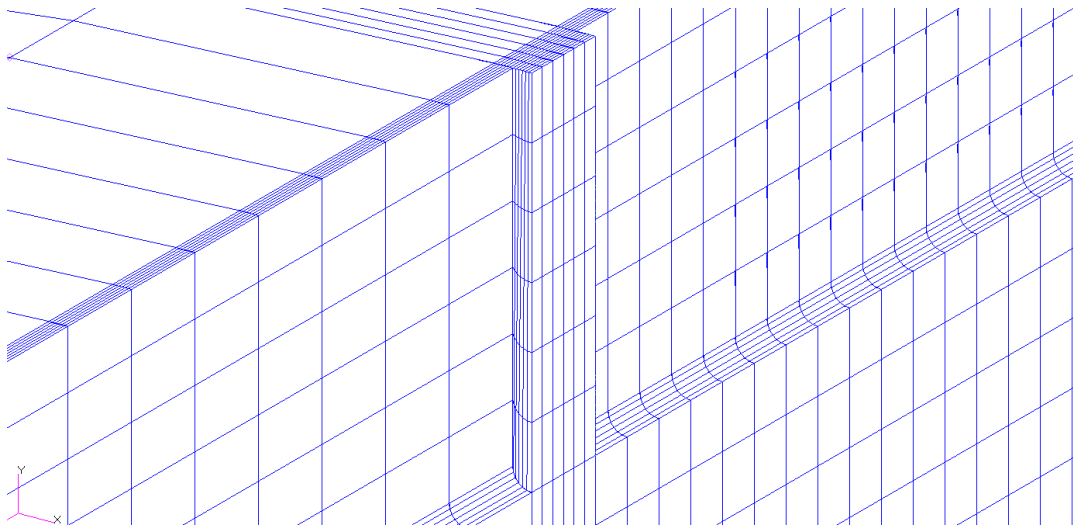
The result of stress distribution at the distance between the cracks of 0.5mm is presented. The stress distribution is taken at the pressure of 0MPa, 10MPa, 20MPa and the burst pressure of the case. The case that been used to taken the result is case of $2c_1$ and $2c_2$ equal to 25mm and 50mm. The other case is at $2c_2 = 75$ mm and 100mm. So, there are 3 cases that will be compared their stress distribution at the pressure of 0MPa, 10MPa, 20MPa and burst pressure. The result is taken in the form of contour of stress distribution. The highest stress is in the red in color while the white color is for the lowest stress. The stress result is based on the Von Misses Stress.

Case 1, $2c_1 = 25$ mm and $2c_2 = 50$ mm

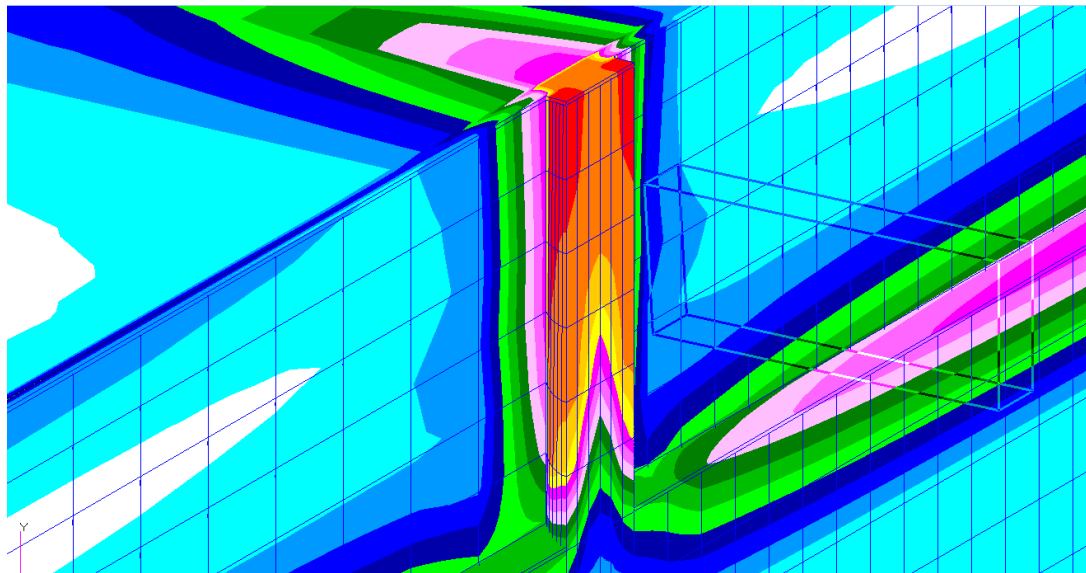
From the figure of 4.20, the picture clearly show about the contour of the stress distribution situated at the distance between the cracks for $d = 0.5$ mm. The pictures show four different contours of stress distribution at different pressure applied. In the first picture, (a) is taken at the pressure is 0MPa. There are no any stress distributions since the pressure is not applied yet. At the pressure of 10MPa, figure (b), the stress distribution is already showing up. The highest stress is located at the center of the distance between the cracks with value of 369MPa. It only occurs at the center which is near to the cracks while the other parts are having the average stress distributions. The stress that interacts with both sides is about 345MPa which is already exceeding the yield stress which is 326MPa. Thus it can be told that the cracks interaction is possibly started at this point.

At the pressure of 20MPa, figure (c), the stress distribution started to change. The maximum stress is moved from the center of the distance between the cracks to the side parts. But it still located near to the cracks. The maximum stress is 494MPa. At this point, it seems that the both cracks are already having the interaction, but it still not burst up yet. This is due to the stress distribution at the distance between the cracks is completely the same at the center of the cracks which is about 431MPa. For the burst pressure, figure (d), the pressure is at 27.3MPa. The stress distribution is quite the same with pressure of

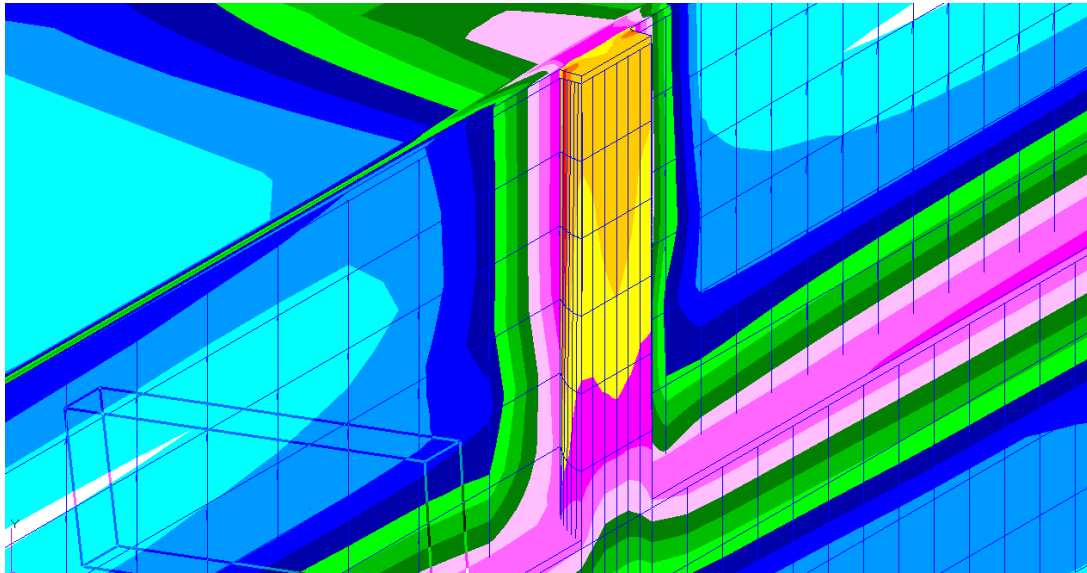
20MPa, but the value of stress is higher. The maximum stress is about 569MPa. This is also located at the side parts of the distance between the cracks. Since the stress of 534MPa covers all the distance between the cracks is already exceeding the Ultimate Tensile Stress, which is 465MPa, the pipe is burst up. From the figures, the stress distribution can be told that started from the center of the distance between the cracks and move to the side of the distance between the cracks. It's also located near to the area of the cracks happened.



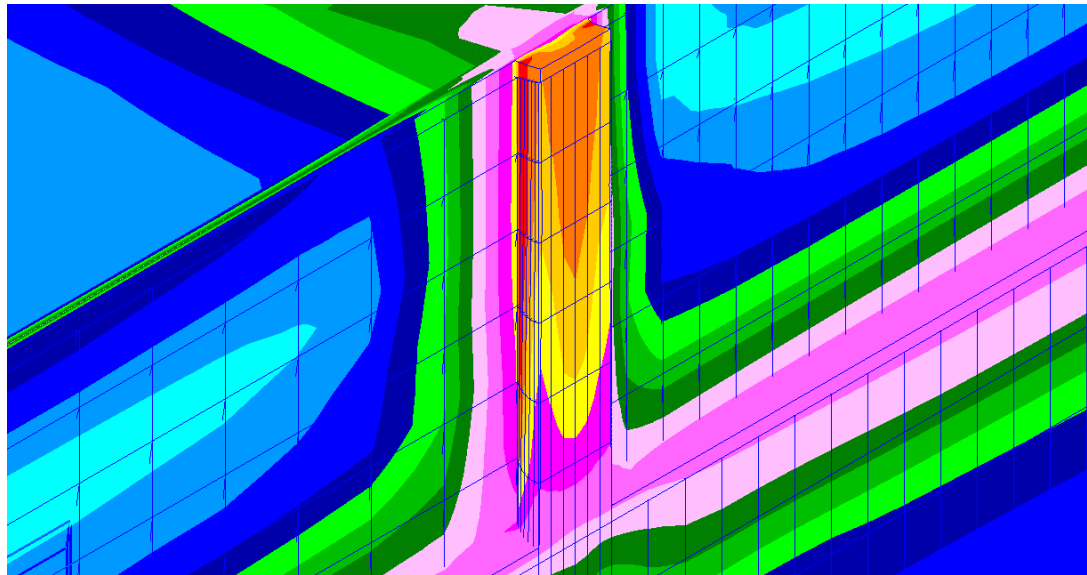
(a) $P = 0\text{MPa}$, Max Stress = 0MPa



(b) $P = 10\text{MPa}$, Max Stress = 369MPa



(c) $P = 20\text{MPa}$, Max Stress = 494MPa



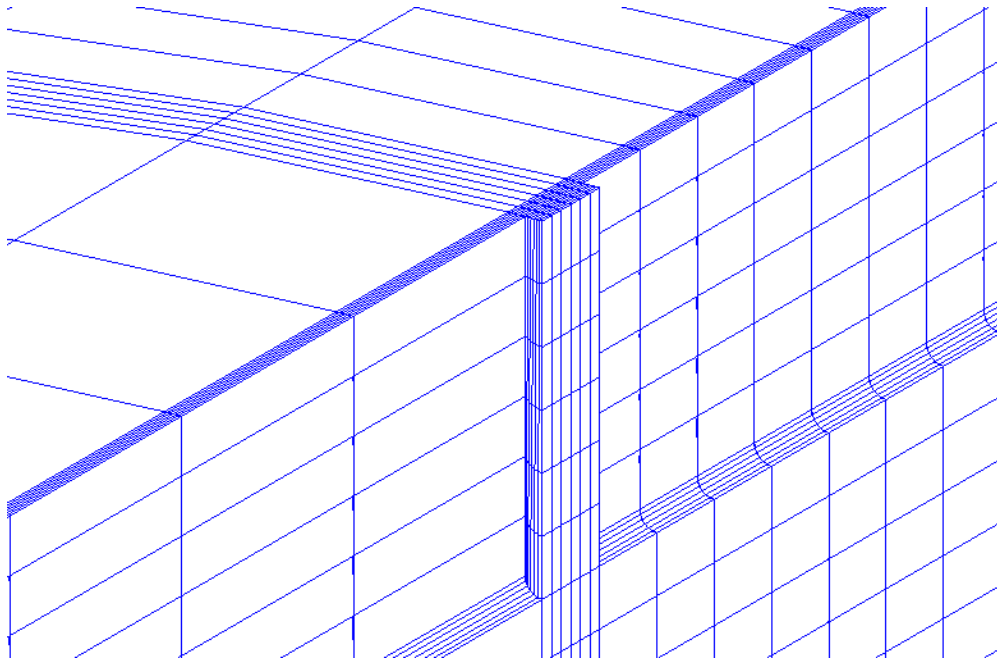
(d) $P = 27.3\text{MPa}$, Max Stress = 569MPa

Figure 4.20: (a-d) Von Misses Stress contour for $2c_1 = 25\text{mm}$ and $2c_2 = 50\text{mm}$

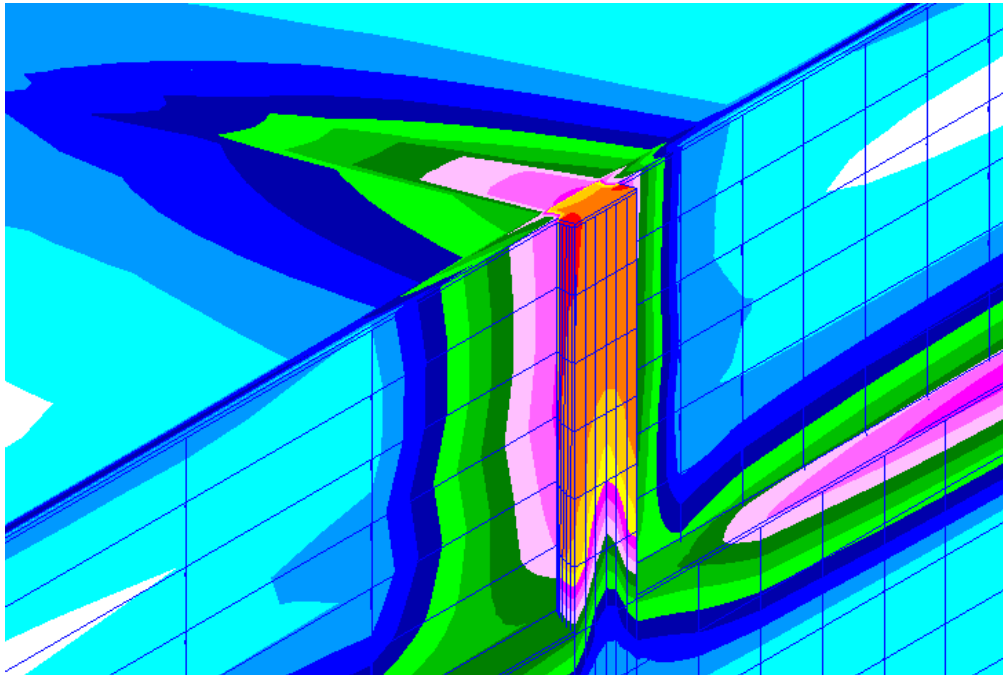
Case 2, $2c_1 = 25\text{mm}$ and $2c_2 = 75\text{mm}$

From the figure of 4.21, the picture clearly show about the contour of the stress distribution situated at the distance between the cracks for $d = 0.5\text{mm}$. The pictures show four different contours of stress distribution at different pressure applied. In the first picture, (a) is taken at the pressure is 0MPa . There are no any stress distributions since the pressure is not applied yet. At the pressure of 10MPa , figure (b), the stress distribution is already showing up. The highest stress is located at the center of the distance between the cracks with value of 383MPa . However, it concentrated on the area which is near to the longest cracks, 75mm . The stress that interacts with both sides is about 358MPa which is already exceeding the yield stress which is 326MPa . Thus it can be told that the cracks interaction is possibly started at this point.

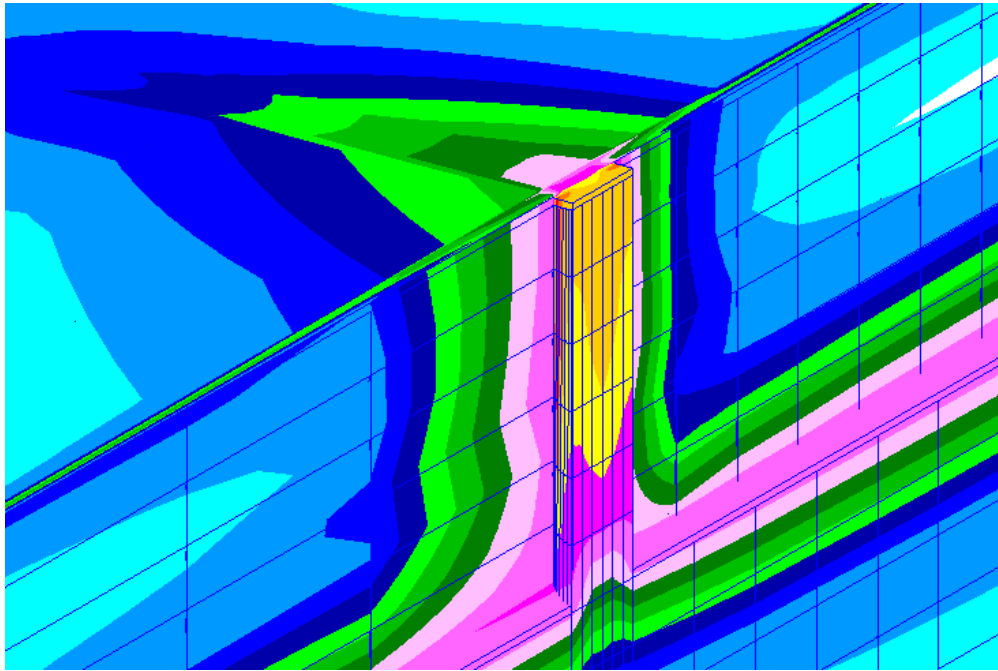
At the pressure of 20MPa , figure (c), the stress distribution started to change. The maximum stress is moved from the center of the distance between the cracks to the side parts. But it still located near to the cracks. The maximum stress is 503MPa . At this point, it seems that the both cracks are already having the interaction, but it still not burst up yet. This is due to the stress distribution at the distance between the cracks is completely the same at the center of the cracks which is about 440MPa . For the burst pressure, figure (d), the pressure is at 26.4MPa . The stress distribution is quite the same with pressure of 20MPa , but the value of stress is higher. The maximum stress is about 566MPa . This is also located at the side parts of the distance between the cracks. Since the stress of 531MPa covers all the distance between the cracks is already exceeding the Ultimate Tensile Stress, which is 465MPa , the pipe is burst up. From the figures, the stress distribution can be told that started from the center of the distance between the cracks and move to the side of the distance between the cracks. It's also located near to the area of the cracks happened.



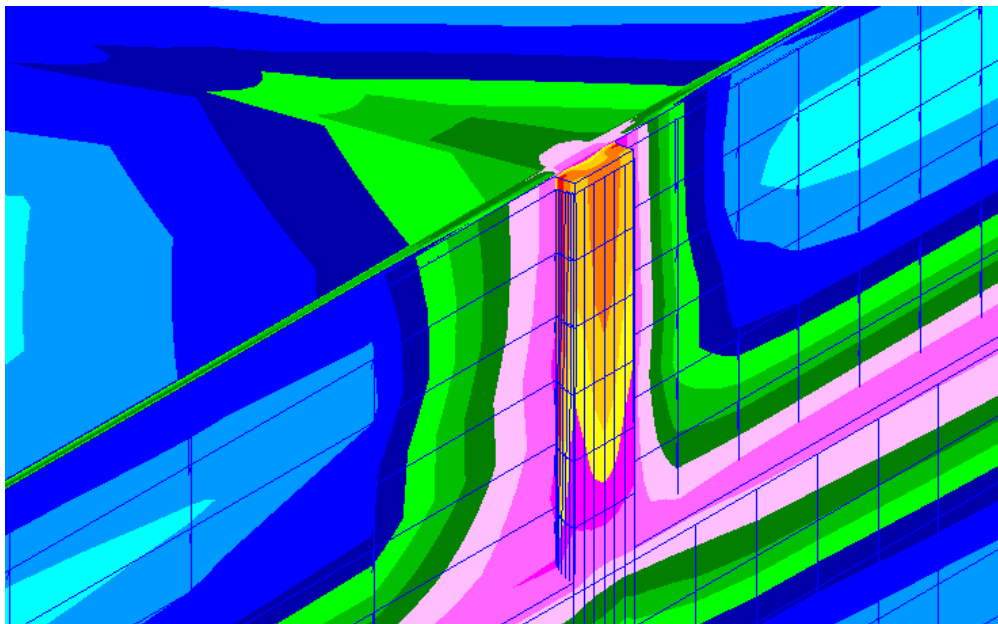
(a) $P = 0$, Max Stress = 0Mpa



(b) $P = 10\text{MPa}$, Max Stress = 383MPa



(c) $P = 20\text{MPa}$, Max Stress = 503MPa



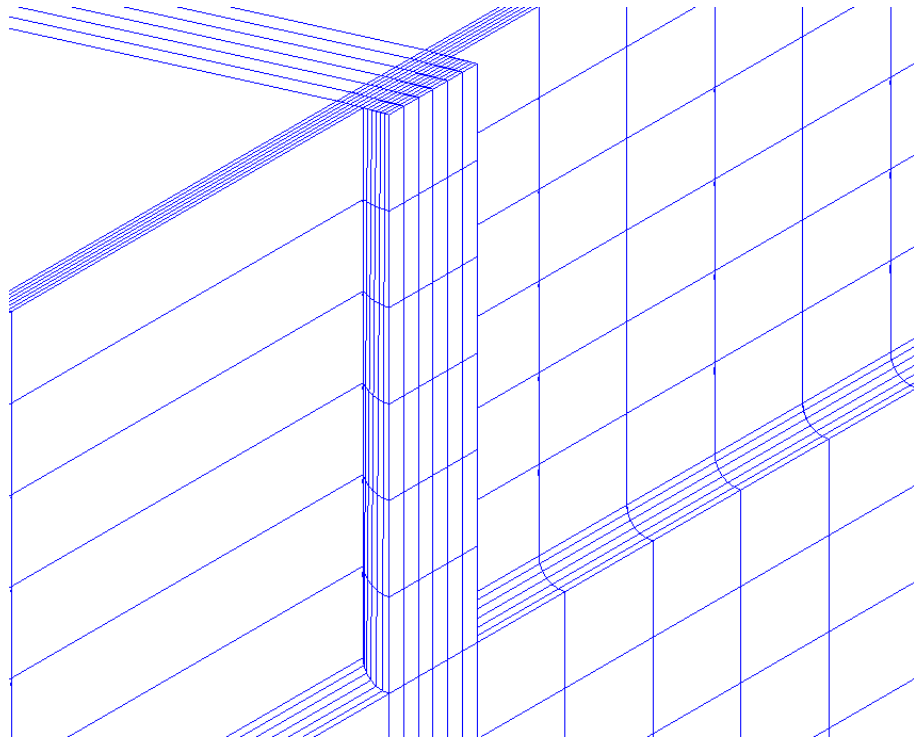
(d) $P = 26.4\text{MPa}$, Max Stress = 566MPa

Figure 4.21: (a-d) Von Mises Stress contour for $2c_1 = 25\text{mm}$ and $2c_2 = 75\text{mm}$

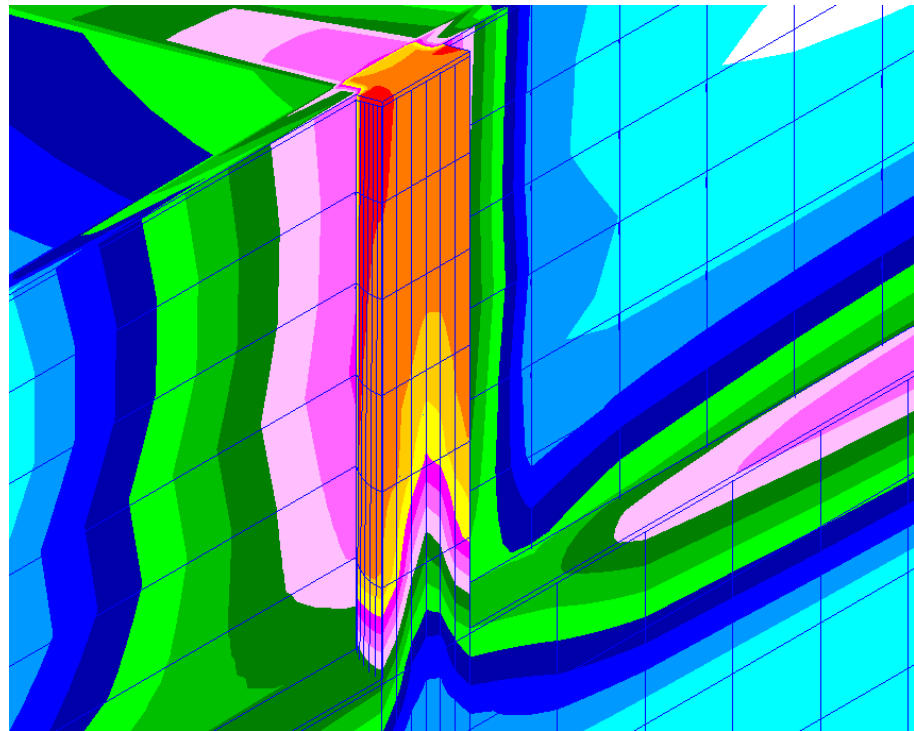
Case 3, $2c_1 = 25\text{mm}$ and $2c_2 = 100\text{mm}$

From the figure of 4.22, the picture clearly show about the contour of the stress distribution situated at the distance between the cracks for $d = 0.5\text{mm}$. The pictures show four different contours of stress distribution at different pressure applied. In the first picture, (a) is taken at the pressure is 0MPa . There are no any stress distributions since the pressure is not applied yet. At the pressure of 10MPa , figure (b), the stress distribution is already showing up. The highest stress is located at the center of the distance between the cracks with value of 380MPa . However, it concentrated on the area which is near to the longest cracks, 100mm . The stress that interacts with both sides is about 356MPa which is already exceeding the yield stress which is 326MPa . Thus it can be told that the cracks interaction is possibly started at this point.

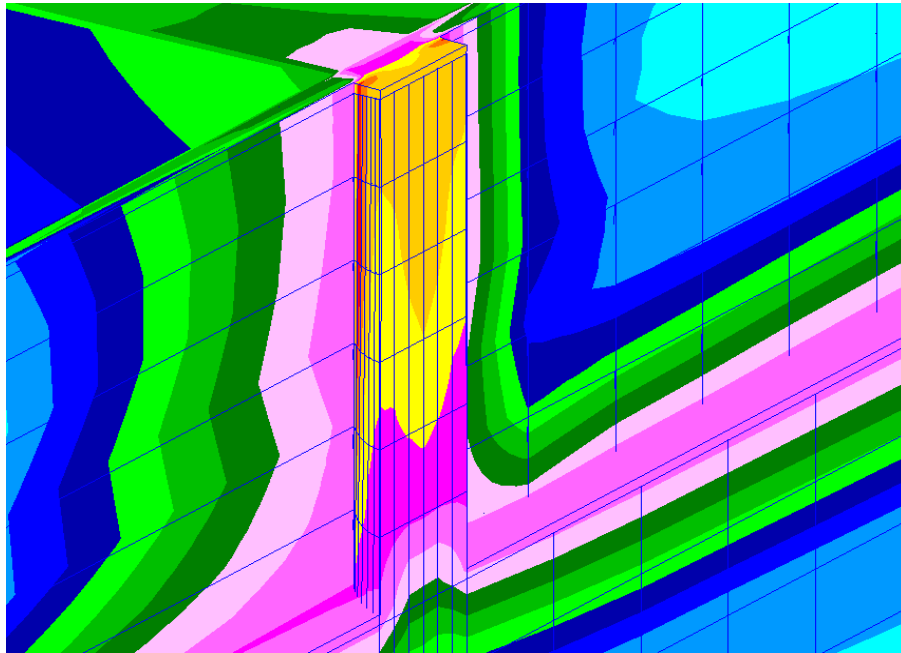
At the pressure of 20MPa , figure (c), the stress distribution started to change. The maximum stress is moved from the center of the distance between the cracks to the side parts. But it still located near to the cracks. The maximum stress is 504MPa . At this point, it seems that the both cracks are already having the interaction, but it still not burst up yet. This is due to the stress distribution at the distance between the cracks is completely the same at the center of the cracks which is about 440MPa . For the burst pressure, figure (d), the pressure is at 25.2MPa . The stress distribution is quite the same with pressure of 20MPa , but the value of stress is higher. The maximum stress is about 568MPa . This is also located at the side parts of the distance between the cracks. Since the stress of 533MPa covers all the distance between the cracks is already exceeding the Ultimate Tensile Stress, which is 465MPa , the pipe is burst up. From the figures, the stress distribution can be told that started from the center of the distance between the cracks and move to the side of the distance between the cracks. It's also located near to the area of the cracks happened.



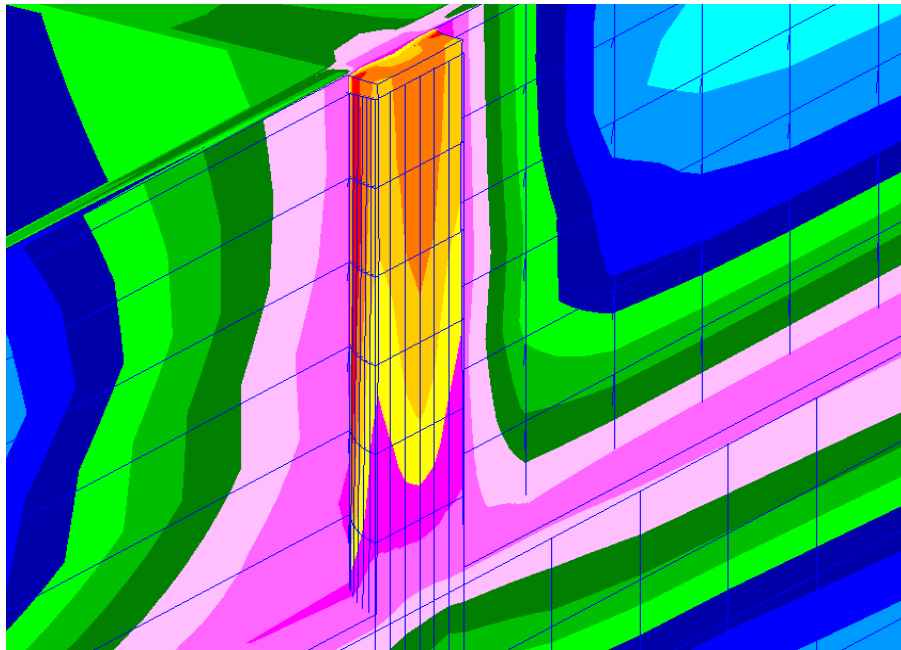
(a) $P = 0\text{MPa}$, Max Stress = 0MPa



(b) $P = 10\text{MPa}$, Max Stress = 380MPa



(c) $P = 20\text{MPa}$, Max Stress = 504MPa



(d) $P = 25.2\text{MPa}$, Max Stress = 568MPa

Figure 4.22: (a-d) Von Mises Stress contour for $2c_1 = 25\text{mm}$ and $2c_2 = 100\text{mm}$

CHAPTER 5

CONCLUSION AND RECOMMENDATION

5.1 INTRODUCTION

This chapter will present the conclusion of this research based on the result and discussion from the experiment, simulation and also calculation process. The findings will be evaluated with the objectives of the research whether it is complete as a conclusion and the recommendation is suggested to improve the research in the further study.

5.2 CONCLUSION

Pipelines are the highest capacity and the safest ways for the oil and gas transmission. But with the increasing in their age, the pipe will probably have a leakage and also could be burst up. It can cause quite fatal destruction. Failures due to the multiple cracks become a major concern in these problems and also in maintaining the pipeline integrity. Hence, the researches of multiple cracks have been done.

In this research, experiments on burst test of multiple cracks have been performed. The finite element analysis models also been made to search and collect useful data of the multiple cracks. Using an assessment method of predicting the burst pressure such as ASME B31G, Modified ASME B31G and DNV-RP-F-101, the result of the experiment and the simulation can be validated, thus the effect of the different cracks length, different length of distance between the cracks towards the burst pressure already can be studied and obtained the result.

- 1) For multiple axial cracks, when the amount of cracks increases, the burst pressure of the pipe will decrease. This is proven by the increasing of number of cracks will result in increasing the length of cracks. As the length of cracks increase, the burst pressure will decrease.
- 2) The burst pressure is not greatly affected by the distance between the cracks. This is proven by the calculation of assessment method for predicting of burst pressure. The distance between the cracks can be neglected if it is too small because it will only give small effect of the burst pressure.
- 3) For the multiple axial cracks, the interaction at the distance between the cracks is more concentrated at the longer cracks length. This is proven from the FEA analysis for the various combinations of different length of cracks. The interaction is more concentrated at the side with longer cracks length.

5.3 RECOMMENDATION

Even the researches have done, there are some recommendations and all of these suggestions are crucial and very important to make the result of the further study is better and accurate.

For the further study, other material such API and AISI based material can be used instead of material grade B, which is API 5L L242. This is because of in the real life, the oil and gas industries used lots of material type for the pipelines. Different material properties will give different result of analysis.

Then, the experiment of the burst pressure is needed to be done in more quantity. Since in this research, there are only two experiments of burst pressure, it is crucial to have more experiment on the different type of case. This can help to predict the burst pressure of the other case more accurately since the experiment result is more reliable than the finite element analysis or the assessment methods.

REFERENCES

- [1] Havard Devold. (2009). An introduction to an oil and gas production, Oil and gas production book. Edition 2.0 Oslo.
- [2] Joint UNDP/World Bank Energy Sector Management Assistance Programme (ESMAP). Cross-Border Oil and Gas Pipelines. Problems and Prospects.
- [3] S.I. Moon, Y.S. Chang, Y.J. kim, J.H. Lee, M.H.Song, Y.H. Choi. (2007). Determination of failure pressure for tubes with two non-aligned axial through-wall cracks.
- [4] Y.K. Lee, Y.P. Kim, M.W. Moon, W.H. Bang, K.H. Oh, W.S. Kim. (2005). The prediction of failure pressure of gas pipeline with multi corroded region.
- [5] Pure Technologies Ltd., Types of pressure pipe.
http://www.puretechltd.com/types_of_pipe/
- [6] Donald R. Prestly. (2012). How to recognize different type of pipe.
<http://www.dummies.com/how-to/content/how-to-recognize-different-types-of-pipes.html>
- [7] LY. XU, Y.F Cheng. (2012). Reliability and Failure Pressure Prediction of Various Grades of Pipelines Steel in the Presence of Corrosion Defects and Pre Strain, International Journal of Pressure Vessels and Piping, Vol.89.
- [8] RB. Francini, B N Leis, Charles R Miele. Updated Study on the Joining of Materials with Unequal Wall Thickness, European Pipeline Research Group, 13th Biennial Joint Technical Meeting.
- [9] H.Adib-Ramezani, Jeong, J., G. Pluvillage. (2006). Structural integrity evaluation of X52 gas pipes subjected to external corrosion defects using the SINTAP procedure.

- [10] Dr. A. Hashem El-Sayed. Oil and Gas Pipeline Design, Maintenance and Repair, Petroleum Engineering Mining, Petroleum and Metallurgical Eng. Dept. Faculty of Engineering, Cairo University notes.
- [11] Corrosion Prevention Association, Internet Web Site, http://www.corrosionprevention.org.uk/what_is_corrosion_prevention.php.
- [12] A. Arnold, J. Freund, W. Hater, V. Ender and M. Schweinsberg. (2009). Accelerated Development of Corrosion Inhibitor Formulations by Electrochemical Method and Short-Time Corrosion Test.
- [13] Micheal Prendsil. (2001). Volatile Corrosion Inhibitor Coatings, Supplement in Material Performance.
- [14] Introduction to Materials Selection, Internet Web Site, <http://corrosiondoctors.org/MatSelect/Introduction.htm>.
- [15] Cathodic Protection (CP), Internet Web Site, <http://corrosiondoctors.org/CP/Introduction.htm>
- [16] API 5L Specification for ERW Steel Pipes, Internet Web sites, http://www.htgrp.com.my/images/pdf/steel_pipes_hollow_sections/API%205L.pdf.

